UNIVERSITY OF CALIFORNIA
SANTA CRUZ

Mechanisms of translational reading frame maintenance

A dissertation submitted in partial satisfaction
of the requirements for the degree of

DOCTOR OF PHILOSOPHY

in

Molecular, cellular and developmental biology

by

Dustin Niblett

June 2025

The Dissertation of Dustin Niblett is
approved:

_____
Professor Harry F. Noller, chair

_____
Professor Manuel Ares, Jr.

_____
Professor William G. Scott

_____
Assistant Professor Sarah Loerch

_____
Peter Biehl
Vice Provost and Dean of Graduate Studies

TABLE OF CONTENTS

LIST OF TABLES AND FIGURES

Chapter 3. Implications of nucleotides near the 3' end of 16S rRNA in guarding the translational reading frame

Chapter 4. Translational reading frame maintenance by a universally conserved nucleotide in 16S rRNA

ABSTRACT

Mechanisms of translational reading frame maintenance

Dustin Niblett

The nature of the genetic code, where mRNA is decoded as a series of non-overlapping triplets, is inherently prone to frameshifting errors that occur when the mRNA register is shifted into one of two improper reading frames. While a typical protein is several hundred amino acids in length, a single frameshifting error can produce a product that is not only non-functional, but that is also toxic to the cell. Frameshifting errors can occur through multiple potential routes, either by tRNA binding out-of-frame, mis-translocation, or by spontaneous slippage of the ribosome along the mRNA. The mechanisms by which cells achieve such remarkable accuracy throughout the dynamic process of protein synthesis are still not well understood. The work within this thesis aims to elucidate the mechanisms of translational reading frame maintenance and the pathways that result in frameshifting in the context of programmed frameshifting sequences. We measure frameshifting efficiency on these sequences using an *in vitro* protein synthesis assay reconstituted with mutant components. We first show that domain IV of elongation factor EF-G, a translational GTPase that catalyzes ribosomal translocation, protects against -1 frameshifting. We suggest domain IV of EF-G stabilizes the codon-anticodon duplex on its transit from the A site to the P site and restricts the duplex from moving too far. We then demonstrate that two of the few residues in 16S rRNA that contact the mRNA, A1503 and G926, help to prevent frameshifting, likely by restricting unregulated movement of the mRNA. We also compare two different types of programmed frameshifting motifs: ‘simultaneous slippage’ using the dnaX gene and ‘hungry frameshifting’ using the prfB gene. We demonstrate that the former stimulates frameshifting during translocation, while the latter proceeds via a different pathway. These results are consistent with the popular model for the prfB +1 frameshifting mechanism, which presumes that the frameshifting occurs on ribosomes with a vacant A site.

ACKNOWLEDGEMENTS

I would like to thank the Noller lab and the UC Santa Cruz PBSE program for the wonderful opportunity to be a part of this great community of scientists. Under the mentorship of Professor Harry Noller and Dr. Laura Lancaster I have received superb training, had many thought-provoking conversations, and have consistently been encouraged to grow as a scientist. Much of this work would not have been possible without the efforts of other members of the Noller lab, both past and present. I would especially like to thank Gillian Rexroad, Alexandria Smart, and Jake Cozy for their contributions to this thesis and for helpful discussions, and John Paul Donohue for excellent computational support and training. I am additionally incredibly grateful to members of the UCSC RNA center, including my thesis committee members Manuel Ares Jr., Sarah Loerch, and William G. Scott, as well as Professor Joshua Arribere, for their lessons and encouragement. Finally, I would like to thank my colleagues, friends, and family, who have made my life more fulfilling and given me a shoulder to lean on, especially my parents Jan and Michael, who have fostered my curiosity since I was young and who continue to be my biggest supporters.

PUBLISHED MATERIAL INCLUDED

The text of this dissertation includes reprints of the following previously published material:

Chapter 2: Niblett D, Nelson C, Leung CS, Rexroad G, Cozy J, Zhou J, Lancaster L, Noller HF. Mutations in domain IV of elongation factor EF-G confer -1 frameshifting. RNA. 2021 Jan;27(1):40-53. doi: 10.1261/rna.077339.120. Epub 2020 Oct 2. PMID: 33008838; PMCID: PMC7749637.

Candidate contributions: D.N., L.L., and H.F.N. designed experiments. D.N. conducted the experiments with the exception of the primer extension assays (L.L., Figure 2 and Figure S3), the manual mRNA quenching measurements (G.R., Fig. 3 C/D,) and the 30S head rotation FRET (G.R., Figure 5C/D). D.N. and H.F.N. analyzed the data and D.N., L.L., and H.F.N wrote the paper.

Chapter 3: Smart A, Lancaster L, Donohue JP, Niblett D, Noller HF. Implication of nucleotides near the 3' end of 16S rRNA in guarding the translational reading frame. Nucleic Acids Res. 2024 Jun 10;52(10):5950-5958. doi: 10.1093/nar/gkae143. PMID: 38452198; PMCID: PMC11162774.

Candidate contributions: D.N. designed the -1 frameshifting assays. A.S., H.F.N, L.L, and D.N. wrote the paper.

Chapter 4: Niblett D, Lancaster L, Cozy J, Noller HF. Translational reading frame maintenance by a universally conserved nucleotide in 16S rRNA. In preparation.

]

Chapter 1. Introduction

Protein synthesis takes place on the ribosome

In all organisms, genetic information in the form of DNA is used to encode polypeptides that perform the bulk of the tasks necessary to sustain life. During protein synthesis, messenger RNA (mRNA) copies of protein-coding genes are decoded in three-nucleotide segments called codons on the ribosome, a massive molecular complex (2.5 MDa in bacteria) consisting of three large ribosomal RNAs (rRNA) and ~50 proteins. The rules by which 64 possible mRNA trinucleotides are mapped to 20 different amino acids in addition to protein start and stop signals are known as the genetic code. Amino acids arrive at the ribosome covalently attached to the 3' end of transfer RNAs (tRNA), which recognize their corresponding codon via base-pairing by a complementary anti-codon. The three stop codons are instead recognized by release factors, which catalyze the release of the growing peptide chain and terminate protein synthesis. A single start codon, AUG, simultaneously marks where protein synthesis begins and encodes the amino acid methionine.

Protein synthesis can be divided into three phases: initiation, elongation, and termination. During initiation, the proper start codon is selected with the help of initiation factors and the first amino acid is brought to the ribosome by initiator-methionyl tRNA. During elongation, the ribosome undergoes repetitive cycles of codon-decoding and amino acid incorporation followed by translocation, where the ribosome advances along the mRNA by one codon. Termination occurs when a stop codon is recognized and the polypeptide is released from the ribosome.

Anatomy of the bacterial ribosome

The bacterial ribosome is composed of one large subunit (the 50S subunit) and one small subunit (the 30S subunit) (Fig. 1A). In the model bacterium *Escherichia coli,* the 50S

subunit is a complex of 5S rRNA (120 nucleotides), 23S rRNA (2904 nucleotides), and 34 ribosomal proteins while the 30S subunit consists of 16S rRNA (1542 nucleotides) and 21 ribosomal proteins. The 30S subunit can be further subdivided into two domains termed the head and body domains, with the cleft between them where the mRNA binds being referred to as the neck (Fig. 1B). Both subunits come together to form the 70S ribosome. The core features of the ribosome are extremely conserved across all three domains of life, with over 130 universally conserved nucleotides in the 16S rRNA alone (Noller et al 2022).

The ribosome has three separate binding sites for tRNA (Fig. 1C). Translation initiation begins with initiator methionyl-tRNA in the peptidyl (P) site. During the elongation cycle, aminoacyl-tRNAs enter the ribosome at the aminoacyl site (A site), where the growing polypeptide chain is transferred from the P site to the incoming amino acid in the A site in a process known as the peptidyl transfer reaction. The peptidyl-tRNA is then translocated from the A site to the P site to make room for the next incoming aminoacyl-tRNA at the A site. At the same time, the deacyl-tRNA is translocated from the P site to the exit site (E site) where it can dissociate from the ribosome into solution.

The elongation cycle

After the initiation phase of protein synthesis, where the AUG start codon is recognized and the first amino acid is brought to the ribosome by initiator-methionyl tRNA, the ribosome then enters the elongation phase of protein synthesis. During this phase, repetitive cycles of tRNA binding, amino acid incorporation, and translocation occur. The events of the elongation cycle are coupled with several large-scale conformational rearrangements of the ribosome that result in gradual movement of the A- and P-site tRNAs towards their next binding site (Fig. 2A).

Inter-subunit rotation (Fig. 2B), where the 30S subunit rotates ~5-10° relative to the 50S subunit, can occur spontaneously and reversibly (Frank and Agrawal, 2001; Valle et al,

2003, Agirrezabala et al, 2008; Cornish et al, 2008). The equilibrium between the rotated and non-rotated conformations is dynamic, with the frequency of forward and reverse inter-subunit rotation being dependent on the nature of the tRNAs bound to the ribosome. Ribosomes bound with a single peptidyl-tRNA in the P site exist predominantly in the 'classical' conformation, where the two subunits are by convention said to be non-rotated relative to each other (Ermolenko et al, 2007; Cornish et al, 2008). Upon binding of A-site tRNA and transfer of the peptide from the P-site tRNA to the A-site tRNA, the rotated state becomes much more favorable (Ermolenko et al, 2007; Cornish et al, 2008). Inter-subunit rotation is coupled to the movement of the acceptor ends of the A- and P-site tRNAs to the P and E sites on the 50S subunit, while their anticodons stay in place on the 30S subunit (Moazed and Noller, 1989; Agirrezabala et al, 2008; Dunkle et al, 2011) (Fig. 2C). For this reason, ribosomes in this state are referred to as 'hybrid'-state ribosomes. The nomenclature A/P and P/E is used to describe the positions of the tRNA where the first letter signifies the 30S binding site and the second letter signifies the 50S binding site for each tRNA.

While inter-subunit rotation occurs both spontaneously and rapidly, completion of translocation on the 30S subunit is extremely slow in the absence of factors, occurring at rate of approximately 4×10^{-4}/min (Fredrick and Noller, 2003). Addition of the translation elongation factor EF-G results in stimulation of the rate of translocation by 4-5 orders of magnitude (Gavrilova et al, 1971; Gavrilova et al, 1976; Rodnina et al, 1997; Fredrick and Noller, 2003). EF-G is a 5-domain translational GTPase that binds to ribosomes containing peptidyl-tRNA in the A site and deacyl-tRNA in the P site, hydrolyzes GTP, and catalyzes translocation. During EF-G-catalyzed translocation, the head domain of the 30S subunit undergoes ~20° rotation relative to the 30S body (Fig. 2D), moving the mRNA and the anticodon ends of the A/P and P/E tRNAs to ap/P and pe/E positions (Zhou et al, 2013; Zhou et al, 2014) (Fig. 2E). This nomenclature is used to describe a state where the anticodon end of the A-tRNA contacts A site features on the 30S head domain and P site features on the

30S body domain, while the acceptor end has been fully translocated to the P site. The P-tRNA has undergone an analogous change in position. Ribosomes in this conformation are termed ‘chimeric-hybrid’ to describe the mixed binding sites of the tRNA anticodon ends on the 30S subunit. Forward rotation of the 30S head domain is accompanied by reverse inter-subunit rotation (Guo and Noller, 2012). Upon EF-G dissociation and reverse head rotation, the deacyl-tRNA can dissociate from the ribosome and the elongation cycle can begin its next round.

Translational reading frame maintenance

The nature of the genetic code, where each trinucleotide encodes one amino acid, gives rise to three different possible ways a protein-coding gene can be decoded known as translational reading frames (Fig. 3). The proper reading frame is selected at translation initiation by recognition of the correct AUG start codon. Maintaining the proper reading frame from this point forward entails ensuring that movement of tRNA and mRNA remain coupled and occur in three-nucleotide increments. Transition to one of the two incorrect reading frames during translation is known as a translational frameshift and is much more problematic than a simple substitution error. While a substitution error results in a single amino acid change, which is generally well tolerated by proteins (Kurland, 1992), frameshifting errors result in a continuous series of incorrect amino acids as each codon is shifted forward or back by one nucleotide. Additionally, there is no evolutionary pressure to avoid stop codons in an incorrect reading frame and high frequencies of out-of-frame stop codons may even be positively selected for (Tse et al, 2010). As such, most frameshifting errors result in termination shortly after the frameshifting site. Frameshifting events lead to the generation of mis-folded and truncated proteins, which have dominant-toxic effects on the cell (Drummond and Wilke, 2008). Attempts to approximate the level of frameshifting errors during protein synthesis suggest an upper-bound of $3x10^{-5}$ frameshifts per codon, with the actual error rate likely being lower (Kurland, 1992). In contrast, substitution errors are estimated to be on the

order of 10^{-4}-10^{-3} per codon, reflecting the lower cost of accumulating such errors (Kurland, 1992).

Programmed translational frameshifting

While a translational frameshift is typically an error that renders the protein product non-functional, there are some examples of genes which have evolved to exploit frameshifting as a feature. These are known as programmed frameshifting sequences. The mRNAs for these genes contain frameshift stimulatory elements, which in combination can stimulate frameshifting to efficiencies as high as 80% (Tsuchihashi and Kornberg, 1990). One advantage of programmed frameshifting is the ability to encode two different protein isoforms in a single mRNA, which vary at their C-termini as the result of a frameshifting event. A well-studied example of this is the dnaX gene from *E. coli* (Fig. 4), which encodes two different subunits of DNA polymerase III, where one is a truncated variant of the other (Blinkowa and Walker, 1990; Flower and McHenry, 1990; Tsuchihashi and Kornberg, 1990). This results in the coupled expression of both isoforms at a fixed ratio from a single mRNA.

Frameshifting can also be used as a way of regulating gene expression, which is seen in the prfB gene from many species of bacteria (Craigen et al, 1985; Craigen and Caskey, 1986; Baranov, 2002) (Fig. 4) and in the ODC antizyme gene from mammals (Matsufuji et al, 1995). The programmed frameshifting event within both genes is regulated by the gene product itself (Donly et al, 1990; Matsufuji et al, 1995). High concentrations of product result in an inhibition of frameshifting, which leads to synthesis of a non-functional truncated product. When the concentration of product becomes too low, frameshifting is stimulated and synthesis of the functional product is resumed. The result is an autoregulatory feedback loop that maintains a stable level of expression,

Finally, frameshifting is very common among viruses as a method for coupling the expression of neighboring genes at a fixed ratio while maintaining a compact genome. The

first example of this was discovered in Rous sarcoma virus, where the gag and pol genes, encoding structural proteins and enzymes required for viral replication respectively, were fused as a polyprotein via a frameshift in ~5% of gag translation products (Jacks and Varmus, 1985). Many similar examples have since been discovered across diverse families of viruses (Atkins et al, 2016).

Programmed frameshift stimulatory elements

While examples of programmed frameshifting are diverse, common features are found among the stimulatory elements within (Fig. 4). The vast majority of programmed frameshifting events take place at a 'slippery sequence,' or an mRNA sequence where the tRNAs can form stable codon-anticodon interactions in both the 0-frame and an alternative frame upon slippage by one nucleotide. For example, the -1 frameshifting sequence from the dnaX gene of *E. coli* utilizes an *A AAA AAG* slippery sequence. In *E. coli,* both AAA and AAG are read by the same lysyl-tRNA, which has a strong preference for AAA (Lustig et al, 1981; Tsuchihashi and Brown, 1992). This means that the A-site tRNA, which reads AAG in the 0-frame, favors the -1 frame thermodynamically, which reads AAA.

In bacteria, programmed frameshifting sequences may additionally utilize an internal Shine-Dalgarno (SD) sequence upstream of the slippery sequence. SD sequences are canonically used in translation initiation to help position the ribosome at the proper start codon via base-pairing to the anti-SD on 16S rRNA (Shine and Dalgarno, 1975). Examples of internal SD usage in programmed frameshifting differ between -1 and +1 frameshifting in the spacing between the SD sequence and the slippery sequence. Within the -1 dnaX gene for example, the internal SD is located 11 nucleotides upstream of the first nucleotide of the P site (position +1), a spacing which is unusually large when compared to the optimal 7-nucleotide spacing seen in translation initiation (Larsen et al, 1994). In contrast, the SD in the prfB +1 frameshifting sequence is just 3 nucleotides upstream of the +1 position, making it shorter than seen in translation initiation (Weiss et al, 1988). It has been suggested that the

stretching or compaction of the SD:anti-SD helix biases the re-alignment of the ribosome along the mRNA in the minus or positive direction respectively by inducing mechanical force (Choi et al, 2020). Additionally, increasing the spacing between the upstream SD and the P site has been shown to slow down the ribosome, likely causing the ribosomes on the dnaX sequence to spend additional time over the slippery sequence and increasing the probability of a frameshift (Wakabayashi et al, 2020). Short spacing on the other hand, as in prfB, has been suggested to destabilize codon-anticodon interactions, favoring the tRNA-mRNA unpairing that precedes their realignment (Devaraj and Fredrick, 2010; Tinoco et al, 2013).

Most examples of programmed -1 frameshifting, such as in dnaX or in viral gag-pol genes, make use of an mRNA secondary structure located downstream of the slippery sequence (Farabaugh, 1996a/b). As is the case for the internal SD sequences, these have also been shown to slow down the ribosome and cause it to spend more time over the slippery sequence (Chen et al, 2014; Kim et al, 2014; Bao et al; 2020). Additionally, these secondary structures have been shown to bias the conformational dynamics of the ribosome. Using smFRET to measure inter-subunit rotation, the stem-loops located downstream of the slippery sequence in both dnaX and HIV-1 programmed -1 frameshifting sequences were shown to stall the ribosome in the non-rotated conformation (Kim et al, 2014; Bao et al, 2020). It was also demonstrated that the presence of the downstream stem-loop inhibited binding of A-site tRNA, which was explained by a cryo-EM analysis that showed the stem-loop docking into the A site and blocking binding of incoming tRNA (Bao et al, 2020).

Unlike the large majority of -1 frameshifting sequences, the +1 frameshifting sequence located on the prfB gene encoding RF2 lacks any downstream secondary structure to stall the ribosome. Instead, it utilizes a slowly decoded UGA stop codon, which is decoded by RF2 itself. The stop codon is followed by a CUA trinucleotide, which is known to provide a poor termination context that impairs stop codon recognition (Major et al, 1996; Poole et al, 1998). When RF2 levels in the cell are limiting, the ribosome stalls on the slippery sequence

for enough time to allow for slippage in the +1 direction, leading to synthesis of the completed RF2 product (Donly et al, 1990; Adamski et al, 1993). When RF2 concentrations in the cell rise, termination out-competes frameshifting, giving rise to a truncated and non-functional product that is likely targeted for degradation. The +1 shift-site in the mammalian ODC antizyme gene is similar to prfB in that it also consists of a 4-nucleotide slippery sequence overlapping with an in-frame stop codon (Matusfuji et al, 1995). Frameshifting during ODC antizyme synthesis is believed to form a similar feedback loop in response to polyamine levels, with polyamines likely affecting translation termination efficiency (Petros et al, 2005).

+1 prfB frameshifting versus -1 dnaX frameshifting

The four-nucleotide slippery sequences found in examples of programmed +1 frameshifting contrast the seven-nucleotide slippery sequences usually seen in -1 frameshifting, suggesting that the two types of frameshifting occur with one tRNA bound and two tRNAs bound respectively. The requirement for a slowly-decoded codon in the A site among known +1 sequences, which would result in prolonged time spent with a vacant A site, provides additional support for this idea. This mechanism for +1 frameshifting appears similar to 'hungry frameshifting' stimulated *in vitro* by leaving out in-frame aminoacyl-tRNAs from the reaction (Caliskan et al, 2017; Korniy et al, 2019; Poulis et al, 2023). In fact, the slowly-decoded stop codon in the prfB sequence can also be substituted for sense codons, with the resulting frameshifting efficiency being inversely correlated with the rate at which that codon is decoded (Curran and Yarus, 1989). On the other hand, -1 frameshifting has most commonly been described using a 'simultaneous slippage' model, where two tRNAs undergo slippage along the mRNA in tandem (Jacks et al, 1988; Weiss et al, 1989). The downstream secondary structure seen in the dnaX gene has additionally been suggested by several studies to predominantly affect the translocation step of the elongation cycle, which occurs after A-site tRNA binding and peptidyl transfer (Caliskan et al, 2014; Kim et al, 2014; Kim and Tinoco, 2017). Despite this, the -1 programmed frameshifting pathway is still poorly

characterized. In fact, peptide sequencing and mass spectrometry of frameshifting products indicate the possibility that ribosomes translating dnaX and other -1 frameshifting sequences can undergo frameshifting through more than one distinct pathway (Yelverton et al, 1994; Yan et al, 2015).

Mechanisms of translational reading frame maintenance

As seen above, the majority of programmed frameshifting sequences stimulate frameshifting on a slippery sequence, which allows the tRNA to re-pair with the mRNA in a new alternative frame. For this to occur, the tRNA(s) must un-pair with the mRNA in the original reading frame, re-position themselves along the mRNA, and finally re-pair with the mRNA in the new reading frame. Frameshifting of this variety can thus be inhibited by stabilizing the proper 0-frame codon-anticodon interactions or by preventing unregulated movement of the tRNA relative to the mRNA.

Consisting of only three base-pair interactions, codon-anticodon interactions are relatively fragile on their own in solution. These weak interactions are stabilized by the translational machinery during protein synthesis, ensuring that proper codon-anticodon interactions are protected on the relatively long timescales of protein synthesis. In between rounds of translocation, the codon-anticodon duplexes are held within their binding pockets at the A, P, and E sites on the ribosome (Fig. 5). The A-site for example is formed from a network of universally conserved nucleotides in 16S rRNA that clamp down on the A-site codon-anticodon, stabilizing the duplex and restricting the movement and conformational space of the mRNA and tRNA (Fig. 5A).

During translocation, the A-site codon-anticodon must leave the relative safety of this binding site and make its way to the P site. In structures of ribosomes trapped in pre-translocation, mid-translocation, and post-translocation states, residues within loops I and II at the tip of domain IV of EF-G can be seen in contact with the A-site codon-anticodon

duplex, suggesting that the tip of domain IV remains in contact with the duplex throughout the entirety of its trajectory to the P site (Gao et al, 2009; Zhou et al, 2014; Brilot et al, 2013; Carbone et al 2021; Petrychenko et al 2021; Rundlet et al; 2021) (Fig. 5C). In this manner, the A-site codon-anticodon is passed from 16S rRNA to EF-G at the start of translocation, ensuring that the duplex is never left unguarded. Consistent with EF-G having a role in translational reading frame maintenance, a structure of a ribosome undergoing spontaneous translocation in the absence of EF-G captured disruption of the translational reading frame resulting in a frameshift (Zhou et al, 2019). Chapter 2 of this thesis will focus on the role of domain IV of EF-G in maintaining the translational reading frame.

In addition to stabilization of codon-anticodon interactions, frameshifting can also be prevented by restricting the movement of the mRNA and tRNA such that spontaneous un-pairing of the two due to thermal fluctuations does not result in a productive frameshifting event. While the positions of the tRNAs are largely fixed within their specific three-dimensional binding sites on the ribosome, the mRNA has significantly more freedom to slide within the channel. Outside of the decoding center described above, there are relatively few interactions between ribosomal rRNA and the mRNA. A universally conserved residue in the P site, G926, protrudes into the mRNA tunnel and contacts the mRNA (Fig. 5B/D). This residue is within hydrogen bonding distance to phosphates within the P site codon at every step of the elongation cycle. G926 also stacks between the -1 base and G1505 of 16S rRNA in most classical and hybrid-state structures (Fig. 5B), while the mRNA wraps around G926 in chimeric-hybrid structures (Fig. 5D), In both cases, the placement of G926 presents a barrier to mRNA movement. In the E site, A1503 intermittently intercalates and retracts between bases -1/-2 throughout the elongation cycle and must be displaced before the mRNA can move (Fig. 5D). Chapters 3 and 4 will focus on A1503 and G926 respectively.

FIGURES

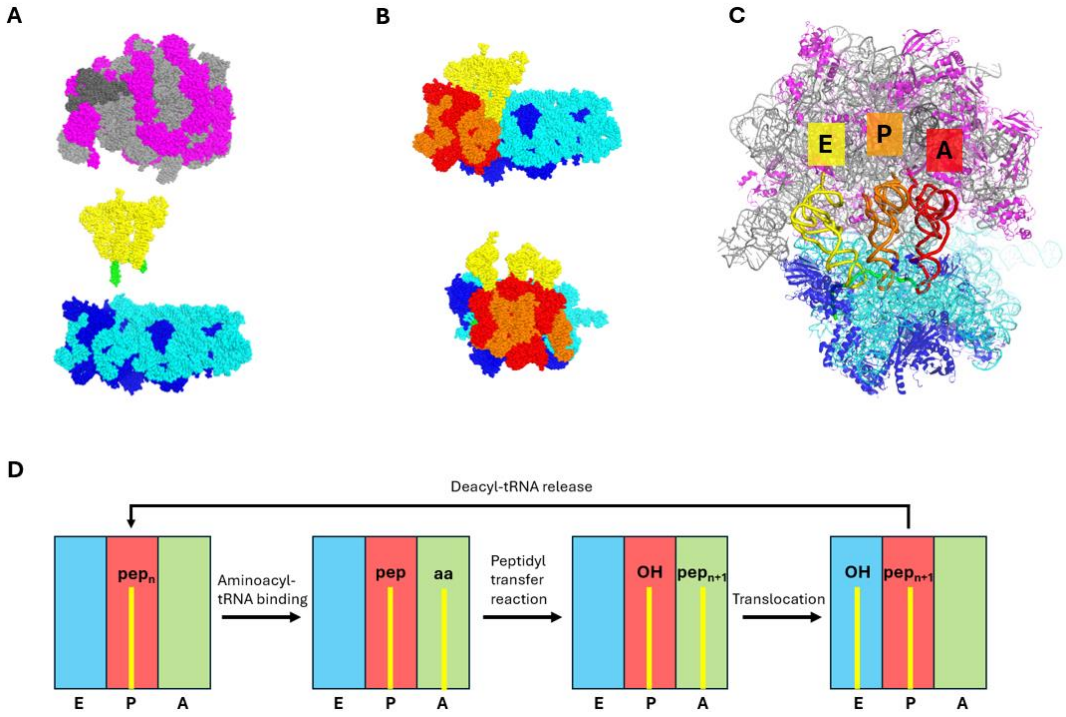

Figure 1. Anatomy of bacterial ribosome. (A) The 70S ribosome is formed from a 50S large subunit composed of 5S rRNA (dark grey), 23S rRNA (light grey), and ~30 ribosomal proteins (magenta) and a 30S small subunit composed of 16S rRNA (cyan) and ~20 ribosomal proteins (blue). The ribosome contains binding sites for mRNA (green) and three tRNAs (yellow). (B) The 30S subunit can be subdivided into a head (rRNA in orange and ribosomal proteins in red) and body domain. The mRNA and anticodon ends of the tRNAs bind along the neck, a cleft between the head and body domains. (C) There are three binding sites for tRNA on the ribosome: the aminoacyl site (red), the peptidyl site (orange), and the exit site (yellow). (D) Schematic overview of protein synthesis and movement of tRNA through the ribosome. The cycle begins with peptidyl-tRNA (pep) of length n occupying the P site. Aminoacyl-tRNA (aa) then binds to the A site. The peptidyl transfer reaction attaches the growing peptide to the incoming amino acid, resulting in a deacyl-tRNA (OH) in the P site and an elongated peptide of length n+1 in the A site. Translocation brings the peptidyl- and

deacyl-tRNA to the P and E sites respectively, allowing for deacyl-tRNA to dissociate and for the cycle to restart.

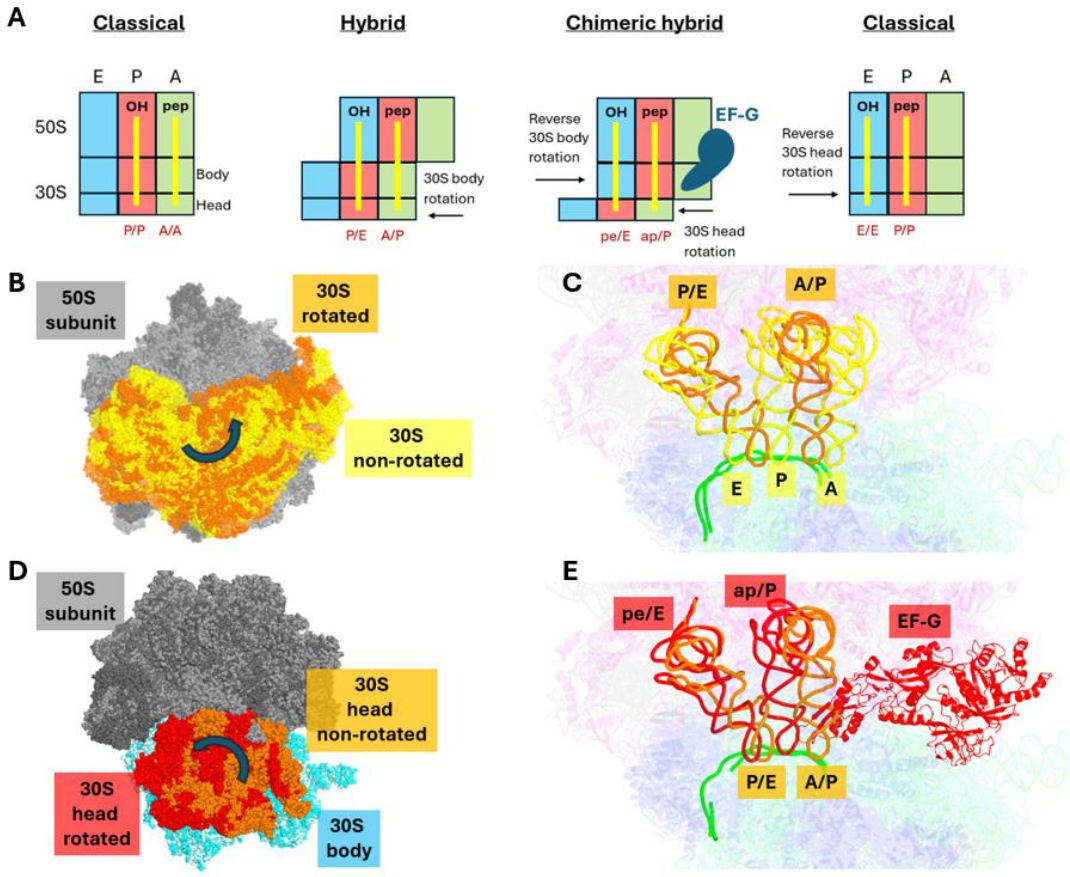

Figure 2. Large scale ribosomal rearrangements and tRNA movement during the elongation cycle. (A) Schematic representation of translocation. After the peptidyl transfer reaction, inter-subunit (30S body) rotation becomes favorable, resulting in the hybrid-state conformation where the acceptor ends of the A- and P-site tRNAs have moved to the P and E sites respectively. Binding of EF-G results in reverse inter-subunit rotation and forward 30S head rotation, moving the tRNA on the 30S body and forming the chimeric-hybrid state conformation. Translocation is completed upon dissociation of EF-G and reverse 30S head rotation. (B, D) Atomic resolution structures (Carbone et al, 2021) of classical-, hybrid-, and

chimeric-hybrid-state ribosomes were aligned on 23S rRNA (B) or on the 16S body domain (D). Inter-subunit (yellow to orange) and 30S head (orange to red) rotation are depicted. (C, E) Positions of the tRNAs in B and D are shown.

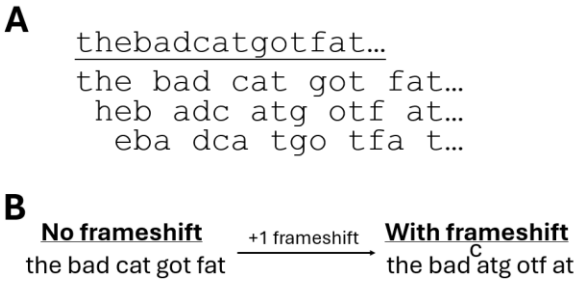

Figure 3. Translational reading frames (A) The set of codons translated from an mRNA depends on which reading frame is selected. Translation in an incorrect reading frame results in an erroneous product. (B) A translational frameshift occurs when the ribosome shifts from one reading frame to another during translation, resulting in a series of incorrect codons.

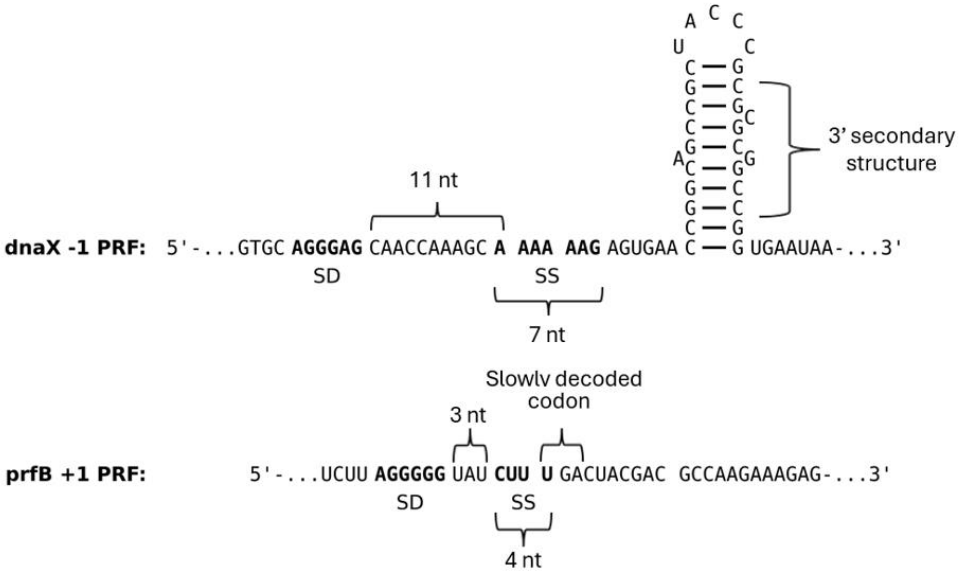

Figure 4. Examples of stimulatory elements found within programmed frameshifting sequences. The stimulatory elements for the dnaX -1 (top) and prfB +1 (bottom) frameshifting sequences are shown. (SS) The slippery sequence is the most important element for most programmed frameshifting sequences. It allows the tRNA to slip by one nucleotide and still maintain favorable base-pairing with the mRNA. (SD) A Shine-Dalgarno sequence that pairs with the anti-SD on the ribosome. A large spacing between the SD and the SS promotes -1 frameshifting and a small spacing promotes +1 frameshifting. (3' secondary structure) An impediment to forward movement by the ribosome that alters the rate of translocation and ribosomal conformational dynamics. (Slowly-decoded codon) A codon that stalls the ribosome with a vacant A site.

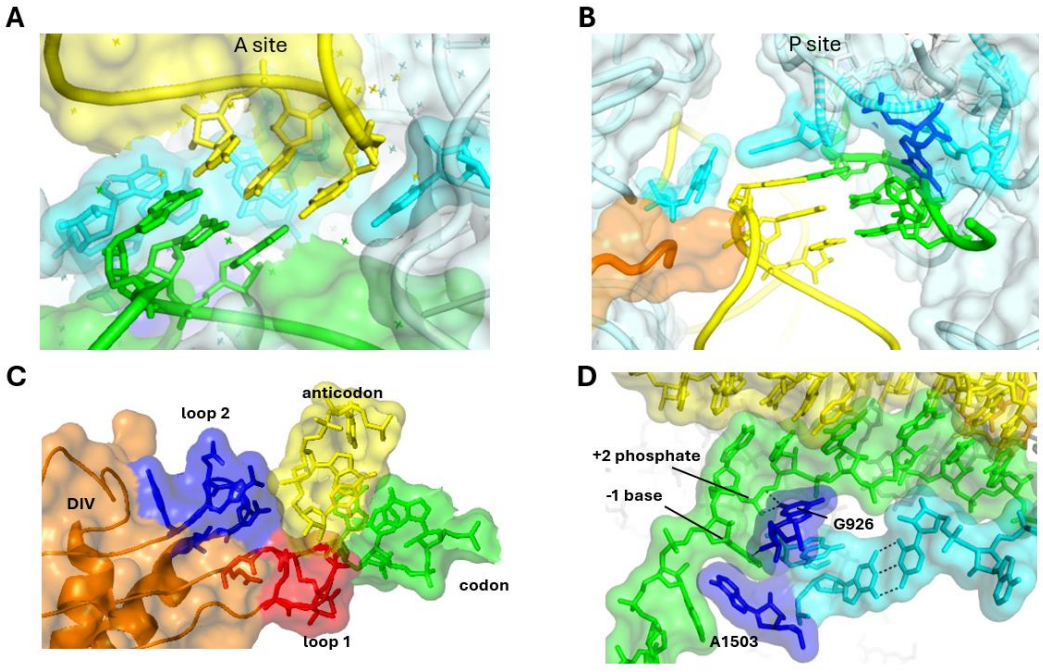

Figure 5. rRNA and EF-G residues that contact the codon-anticodon duplex and contribute to reading frame maintenance. (A) The nucleotides that make up the ribosomal decoding center (cyan) surround the A-site codon-anticodon (green-yellow) duplex on three sides, forming a network that is significantly more stable than the codon-anticodon

interactions alone (B) P-site interactions are less extensive. Among them, G926 (blue) forms two hydrogen bonds to the +1 phosphate and stacks on the -1 base. Ribosomal protein S9 (orange) contacts the tRNA anticodon stem-loop at positions 33-34. (C) In partially-translocated chimeric-hybrid ribosomes, the tip of domain IV of EF-G (orange) reaches into the ribosomal A site where loops I (red) and II (blue) contact both the codon and anticodon. (D) In chimeric-hybrid state ribosomes, the mRNA wraps around G926, which continues to form two hydrogen-bonds with the mRNA backbone. Meanwhile, A1503 intercalates between the -1 and -2 bases in the E site. Structures used came from Watson et al, 2020 (A,B) and Zhou et al, 2014 (C,D).

REFERENCES

Adamski, F. M., Donly, B. C., & Tate, W. P. (1993). Competition between frameshifting, termination and suppression at the frameshift site in the Escherichia coli release factor-2 mRNA. *Nucleic acids research*, *21*(22), 5074–5078. https://doi.org/10.1093/nar/21.22.5074

Agirrezabala X, Lei J, Brunelle JL, Ortiz-Meoz RF, Green R, Frank J. Visualization of the hybrid state of tRNA binding promoted by spontaneous ratcheting of the ribosome. Mol Cell. 2008 Oct 24;32(2):190-7. doi: 10.1016/j.molcel.2008.10.001. PMID: 18951087; PMCID: PMC2614368.

Atkins JF, Loughran G, Bhatt PR, Firth AE, Baranov PV. Ribosomal frameshifting and transcriptional slippage: From genetic steganography and cryptography to adventitious use. Nucleic Acids Res. 2016 Sep 6;44(15):7007-78. doi: 10.1093/nar/gkw530. Epub 2016 Jul 19. PMID: 27436286; PMCID: PMC5009743.

Baranov PV, Gesteland RF, Atkins JF. Release factor 2 frameshifting sites in different bacteria. EMBO Rep. 2002 Apr;3(4):373-7. doi: 10.1093/embo-reports/kvf065. Epub 2002 Mar 15. PMID: 11897659; PMCID: PMC1084053.

Bao C, Loerch S, Ling C, Korostelev AA, Grigorieff N, Ermolenko DN. mRNA stem-loops can pause the ribosome by hindering A-site tRNA binding. Elife. 2020 May 19;9:e55799. doi: 10.7554/eLife.55799. PMID: 32427100; PMCID: PMC7282821.

Blinkowa AL, Walker JR. Programmed ribosomal frameshifting generates the Escherichia coli DNA polymerase III gamma subunit from within the tau subunit reading frame. Nucleic Acids Res. 1990 Apr 11;18(7):1725-9. doi: 10.1093/nar/18.7.1725. PMID: 2186364; PMCID: PMC330589.

Brilot AF, Korostelev AA, Ermolenko DN, Grigorieff N. Structure of the ribosome with elongation factor G trapped in the pretranslocation state. Proc Natl Acad Sci U S A. 2013 Dec 24;110(52):20994-9. doi: 10.1073/pnas.1311423110. Epub 2013 Dec 9. PMID: 24324137; PMCID: PMC3876248.

Caliskan N, Katunin VI, Belardinelli R, Peske F, Rodnina MV. Programmed -1 frameshifting by kinetic partitioning during impeded translocation. Cell. 2014 Jun 19;157(7):1619-31. doi: 10.1016/j.cell.2014.04.041. PMID: 24949973; PMCID: PMC7112342.

Caliskan N, Wohlgemuth I, Korniy N, Pearson M, Peske F, Rodnina MV. Conditional Switch between Frameshifting Regimes upon Translation of dnaX mRNA. Mol Cell. 2017 May 18;66(4):558-567.e4. doi: 10.1016/j.molcel.2017.04.023. PMID: 28525745.

Carbone CE, Loveland AB, Gamper HB Jr, Hou YM, Demo G, Korostelev AA. Time-resolved cryo-EM visualizes ribosomal translocation with EF-G and GTP. Nat Commun. 2021 Dec 13;12(1):7236. doi: 10.1038/s41467-021-27415-0. PMID: 34903725; PMCID: PMC8668904.

Chen J, Petrov A, Johansson M, Tsai A, O'Leary SE, Puglisi JD. Dynamic pathways of -1 translational frameshifting. Nature. 2014 Aug 21;512(7514):328-32. doi: 10.1038/nature13428. Epub 2014 Jun 11. PMID: 24919156; PMCID: PMC4472451.

Choi J, O'Loughlin S, Atkins JF, Puglisi JD. The energy landscape of -1 ribosomal frameshifting. Sci Adv. 2020 Jan 1;6(1):eaax6969. doi: 10.1126/sciadv.aax6969. PMID: 31911945; PMCID: PMC6938710.

Cornish PV, Ermolenko DN, Noller HF, Ha T. Spontaneous intersubunit rotation in single ribosomes. Mol Cell. 2008 Jun 6;30(5):578-88. doi: 10.1016/j.molcel.2008.05.004. PMID: 18538656; PMCID: PMC2491453.

Craigen WJ, Caskey CT. Expression of peptide chain release factor 2 requires high-efficiency frameshift. Nature. 1986 Jul 17-23;322(6076):273-5. doi: 10.1038/322273a0. PMID: 3736654.

Craigen WJ, Cook RG, Tate WP, Caskey CT. Bacterial peptide chain release factors: conserved primary structure and possible frameshift regulation of release factor 2. Proc Natl Acad Sci U S A. 1985 Jun;82(11):3616-20. doi: 10.1073/pnas.82.11.3616. PMID: 3889910; PMCID: PMC397836.

Curran JF, Yarus M. Rates of aminoacyl-tRNA selection at 29 sense codons in vivo. J Mol Biol. 1989 Sep 5;209(1):65-77. doi: 10.1016/0022-2836(89)90170-8. PMID: 2478714.

Devaraj A, Fredrick K. Short spacing between the Shine-Dalgarno sequence and P codon destabilizes codon-anticodon pairing in the P site to promote +1 programmed frameshifting. Mol Microbiol. 2010 Dec;78(6):1500-9. doi: 10.1111/j.1365-2958.2010.07421.x. Epub 2010 Oct 14. PMID: 21143320; PMCID: PMC3071715.

Donly BC, Edgar CD, Adamski FM, Tate WP. Frameshift autoregulation in the gene for Escherichia coli release factor 2: partly functional mutants result in frameshift enhancement. Nucleic Acids Res. 1990 Nov 25;18(22):6517-22. doi: 10.1093/nar/18.22.6517. PMID: 2251114; PMCID: PMC332604.

Dunkle JA, Wang L, Feldman MB, Pulk A, Chen VB, Kapral GJ, Noeske J, Richardson JS, Blanchard SC, Cate JH. Structures of the bacterial ribosome in classical and hybrid states of tRNA binding. Science. 2011 May 20;332(6032):981-4. doi: 10.1126/science.1202692. PMID: 21596992; PMCID: PMC3176341.

Ermolenko DN, Majumdar ZK, Hickerson RP, Spiegel PC, Clegg RM, Noller HF. Observation of intersubunit movement of the ribosome in solution using FRET. J Mol Biol. 2007 Jul 13;370(3):530-40. doi: 10.1016/j.jmb.2007.04.042. Epub 2007 Apr 20. PMID: 17512008.

Farabaugh PJ. Programmed translational frameshifting. Annu Rev Genet. 1996a;30:507-28. doi: 10.1146/annurev.genet.30.1.507. PMID: 8982463.

Farabaugh PJ. Programmed translational frameshifting. Microbiol Rev. 1996b Mar;60(1):103-34. doi: 10.1128/mr.60.1.103-134.1996. PMID: 8852897; PMCID: PMC239420.

Flower AM, McHenry CS. The gamma subunit of DNA polymerase III holoenzyme of Escherichia coli is produced by ribosomal frameshifting. Proc Natl Acad Sci U S A. 1990 May;87(10):3713-7. doi: 10.1073/pnas.87.10.3713. PMID: 2187190; PMCID: PMC53973.

Frank J, Agrawal RK. Ratchet-like movements between the two ribosomal subunits: their implications in elongation factor recognition and tRNA translocation. Cold Spring Harb Symp Quant Biol. 2001;66:67-75. doi: 10.1101/sqb.2001.66.67. PMID: 12762009.

Fredrick K, Noller HF. Catalysis of ribosomal translocation by sparsomycin. Science. 2003 May 16;300(5622):1159-62. doi: 10.1126/science.1084571. PMID: 12750524.

Gao YG, Selmer M, Dunham CM, Weixlbaumer A, Kelley AC, Ramakrishnan V. The structure of the ribosome with elongation factor G trapped in the posttranslocational state. Science. 2009 Oct 30;326(5953):694-9. doi: 10.1126/science.1179709. PMID: 19833919; PMCID: PMC3763468.

Gavrilova LP, Spirin AS. Stimulation of "non-enzymic" translocation in ribosomes by p-chloromercuribenzoate. FEBS Lett. 1971 Oct 1;17(2):324-326. doi: 10.1016/0014-5793(71)80177-1. PMID: 11946059.

Gavrilova LP, Kostiashkina OE, Koteliansky VE, Rutkevitch NM, Spirin AS. Factor-free ("non-enzymic") and factor-dependent systems of translation of polyuridylic acid by Escherichia coli ribosomes. J Mol Biol. 1976 Mar 15;101(4):537-52. doi: 10.1016/0022-2836(76)90243-6. PMID: 772221.

Guo Z, Noller HF. Rotation of the head of the 30S ribosomal subunit during mRNA translocation. Proc Natl Acad Sci U S A. 2012 Dec 11;109(50):20391-4. doi: 10.1073/pnas.1218999109. Epub 2012 Nov 27. PMID: 23188795; PMCID: PMC3528506.

Jacks T, Varmus HE. Expression of the Rous sarcoma virus pol gene by ribosomal frameshifting. Science. 1985 Dec 13;230(4731):1237-42. doi: 10.1126/science.2416054. PMID: 2416054.Kurland CG. Translational accuracy and the fitness of bacteria. Annu Rev Genet. 1992;26:29-50. doi: 10.1146/annurev.ge.26.120192.000333. PMID: 1482115.

Jacks, T., H. D. Madhani, F. R. Masiarz, and H. E. Varmus. 1988. Signals for ribosomal frameshifting in the Rous sarcoma virus gag-pol region. Cell 55:447–458.

Kim HK, Liu F, Fei J, Bustamante C, Gonzalez RL Jr, Tinoco I Jr. A frameshifting stimulatory stem loop destabilizes the hybrid state and impedes ribosomal translocation. Proc Natl Acad Sci U S A. 2014 Apr 15;111(15):5538-43. doi: 10.1073/pnas.1403457111. Epub 2014 Mar 31. PMID: 24706807; PMCID: PMC3992627.

Kim HK, Tinoco I Jr. EF-G catalyzed translocation dynamics in the presence of ribosomal frameshifting stimulatory signals. Nucleic Acids Res. 2017 Mar 17;45(5):2865-2874. doi: 10.1093/nar/gkw1020. PMID: 27799473; PMCID: PMC5389563.

Korniy N, Goyal A, Hoffmann M, Samatova E, Peske F, Pöhlmann S, Rodnina MV. Modulation of HIV-1 Gag/Gag-Pol frameshifting by tRNA abundance. Nucleic Acids Res. 2019 Jun 4;47(10):5210-5222. doi: 10.1093/nar/gkz202. PMID: 30968122; PMCID: PMC6547452.

Kurland CG. Translational accuracy and the fitness of bacteria. Annu Rev Genet. 1992;26:29-50. doi: 10.1146/annurev.ge.26.120192.000333. PMID: 1482115.

Larsen, B., Wills, N. M., Gesteland, R. F., & Atkins, J. F. (1994). rRNA-mRNA base pairing stimulates a programmed -1 ribosomal frameshift. *Journal of bacteriology*, *176*(22), 6842–6851.

Lustig F, Elias P, Axberg T, Samuelsson T, Tittawella I, Lagerkvist U. Codon reading and translational error. Reading of the glutamine and lysine codons during protein synthesis in vitro. J Biol Chem. 1981 Mar 25;256(6):2635-43. PMID: 6782093.

Major LL, Poole ES, Dalphin ME, Mannering SA, Tate WP. Is the in-frame termination signal of the Escherichia coli release factor-2 frameshift site weakened by a particularly poor context? Nucleic Acids Res. 1996 Jul 15;24(14):2673-8. doi: 10.1093/nar/24.14.2673. PMID: 8758994; PMCID: PMC145990.

Matsufuji S, Matsufuji T, Miyazaki Y, Murakami Y, Atkins JF, Gesteland RF, Hayashi S. Autoregulatory frameshifting in decoding mammalian ornithine decarboxylase antizyme. Cell. 1995 Jan 13;80(1):51-60. doi: 10.1016/0092-8674(95)90450-6. PMID: 7813017; PMCID: PMC7133313.

Moazed D, Noller HF. Intermediate states in the movement of transfer RNA in the ribosome. Nature. 1989 Nov 9;342(6246):142-8. doi: 10.1038/342142a0. PMID: 2682263.

Noller HF, Donohue JP, Gutell RR. The universally conserved nucleotides of the small subunit ribosomal RNAs. RNA. 2022 May;28(5):623-644. doi: 10.1261/rna.079019.121. Epub 2022 Feb 3. PMID: 35115361; PMCID: PMC9014874.

Petros LM, Howard MT, Gesteland RF, Atkins JF. Polyamine sensing during antizyme mRNA programmed frameshifting. Biochem Biophys Res Commun. 2005 Dec 23;338(3):1478-89. doi: 10.1016/j.bbrc.2005.10.115. Epub 2005 Oct 27. PMID: 16269132.

Petrychenko V, Peng BZ, de A P Schwarzer AC, Peske F, Rodnina MV, Fischer N. Structural mechanism of GTPase-powered ribosome-tRNA movement. Nat Commun. 2021 Oct 11;12(1):5933. doi: 10.1038/s41467-021-26133-x. PMID: 34635670; PMCID: PMC8505512.

Poole ES, Major LL, Mannering SA, Tate WP. Translational termination in Escherichia coli: three bases following the stop codon crosslink to release factor 2 and affect the decoding efficiency of UGA-containing signals. Nucleic Acids Res. 1998 Feb 15;26(4):954-60. doi: 10.1093/nar/26.4.954. PMID: 9461453; PMCID: PMC147352.

Poulis P, Peske F, Rodnina MV. The many faces of ribosome translocation along the mRNA: reading frame maintenance, ribosome frameshifting and translational bypassing. Biol Chem. 2023 Apr 21;404(8-9):755-767. doi: 10.1515/hsz-2023-0142. PMID: 37077160.

Rodnina MV, Savelsbergh A, Katunin VI, Wintermeyer W. Hydrolysis of GTP by elongation factor G drives tRNA movement on the ribosome. Nature. 1997 Jan 2;385(6611):37-41. doi: 10.1038/385037a0. PMID: 8985244.

Rundlet EJ, Holm M, Schacherl M, Natchiar SK, Altman RB, Spahn CMT, Myasnikov AG, Blanchard SC. Structural basis of early translocation events on the ribosome. Nature. 2021 Jul;595(7869):741-745. doi: 10.1038/s41586-021-03713-x. Epub 2021 Jul 7. PMID: 34234344; PMCID: PMC8318882.

Shine J, Dalgarno L. Determinant of cistron specificity in bacterial ribosomes. Nature. 1975 Mar 6;254(5495):34-8. doi: 10.1038/254034a0. PMID: 803646.

Tinoco I Jr, Kim HK, Yan S. Frameshifting dynamics. Biopolymers. 2013 Dec;99(12):1147-66. doi: 10.1002/bip.22293. Erratum in: Biopolymers. 2014 Mar;101(3):306. PMID: 23722586; PMCID: PMC4011568.

Tse H, Cai JJ, Tsoi HW, Lam EP, Yuen KY. Natural selection retains overrepresented out-of-frame stop codons against frameshift peptides in prokaryotes. BMC Genomics. 2010 Sep 9;11:491. doi: 10.1186/1471-2164-11-491. PMID: 20828396; PMCID: PMC2996987.

Tsuchihashi Z, Brown PO. Sequence requirements for efficient translational frameshifting in the Escherichia coli dnaX gene and the role of an unstable interaction between tRNA(Lys) and an AAG lysine codon. Genes Dev. 1992 Mar;6(3):511-9. doi: 10.1101/gad.6.3.511. PMID: 1547945.

Tsuchihashi Z, Kornberg A. Translational frameshifting generates the gamma subunit of DNA polymerase III holoenzyme. Proc Natl Acad Sci U S A. 1990 Apr;87(7):2516-20. doi: 10.1073/pnas.87.7.2516. PMID: 2181440; PMCID: PMC53720.

Valle M, Zavialov A, Sengupta J, Rawat U, Ehrenberg M, Frank J. Locking and unlocking of ribosomal motions. Cell. 2003 Jul 11;114(1):123-34. doi: 10.1016/s0092-8674(03)00476-8. PMID: 12859903.

Wakabayashi H, Warnasooriya C, Ermolenko DN. Extending the Spacing between the Shine-Dalgarno Sequence and P-Site Codon Reduces the Rate of mRNA Translocation. J Mol Biol. 2020 Jul 24;432(16):4612-4622. doi: 10.1016/j.jmb.2020.06.008. Epub 2020 Jun 13. PMID: 32544497; PMCID: PMC7387212.

Watson ZL, Ward FR, Méheust R, Ad O, Schepartz A, Banfield JF, Cate JH. Structure of the bacterial ribosome at 2 Å resolution. Elife. 2020 Sep 14;9:e60482. doi: 10.7554/eLife.60482. PMID: 32924932; PMCID: PMC7550191.

Weiss RB, Dunn DM, Dahlberg AE, Atkins JF, Gesteland RF. Reading frame switch caused by base-pair formation between the 3' end of 16S rRNA and the mRNA during elongation of protein synthesis in Escherichia coli. EMBO J. 1988 May;7(5):1503-7. doi: 10.1002/j.1460-2075.1988.tb02969.x. PMID: 2457498; PMCID: PMC458402.

Weiss, R. B., D. M. Dunn, M. Shuh, J. F. Atkins, and R. F. Gesteland. 1989. E. coli ribosomes re-phase on retroviral frameshift signals at rates ranging from 2 to 50 percent.

Yan S, Wen JD, Bustamante C, Tinoco I Jr. Ribosome excursions during mRNA translocation mediate broad branching of frameshift pathways. Cell. 2015 Feb 26;160(5):870-881. doi: 10.1016/j.cell.2015.02.003. Epub 2015 Feb 19. PMID: 25703095; PMCID: PMC4344849.

Yelverton E, Lindsley D, Yamauchi P, Gallant JA. The function of a ribosomal frameshifting signal from human immunodeficiency virus-1 in Escherichia coli. Mol Microbiol. 1994 Jan;11(2):303-13. doi: 10.1111/j.1365-2958.1994.tb00310.x. PMID: 8170392; PMCID: PMC7192232.

Zhou J, Lancaster L, Donohue JP, Noller HF. Crystal structures of EF-G-ribosome complexes trapped in intermediate states of translocation. Science. 2013 Jun 28;340(6140):1236086. doi: 10.1126/science.1236086. PMID: 23812722; PMCID: PMC3979973.

Zhou J, Lancaster L, Donohue JP, Noller HF. How the ribosome hands the A-site tRNA to the P site during EF-G-catalyzed translocation. Science. 2014 Sep 5;345(6201):1188-91. doi: 10.1126/science.1255030. PMID: 25190797; PMCID: PMC4242719.

Zhou J, Lancaster L, Donohue JP, Noller HF. Spontaneous ribosomal translocation of mRNA and tRNAs into a chimeric hybrid state. Proc Natl Acad Sci U S A. 2019 Apr 16;116(16):7813-7818. doi: 10.1073/pnas.1901310116. Epub 2019 Apr 1. PMID: 30936299; PMCID: PMC6475402.

Chapter 2. Mutations in domain IV of elongation factor EF-G confer -1 frameshifting

ABSTRACT

A recent crystal structure of a ribosome complex undergoing partial translocation in the absence of elongation factor EF-G showed disruption of codon–anticodon pairing and slippage of the reading frame by −1, directly implicating EF-G in preservation of the translational reading frame. Among mutations identified in a random screen for dominant-lethal mutations of EF-G were a cluster of six that map to the tip of domain IV, which has been shown to contact the codon–anticodon duplex in trapped translocation intermediates. In vitro synthesis of a full-length protein using these mutant EF-Gs revealed dramatically increased −1 frameshifting, providing new evidence for a role for domain IV of EF-G in maintaining the reading frame. These mutations also caused decreased rates of mRNA translocation and rotational movement of the head and body domains of the 30S ribosomal subunit during translocation. Our results are in general agreement with recent findings from Rodnina and coworkers based on in vitro translation of an oligopeptide using EF-Gs containing mutations at two positions in domain IV, who found an inverse correlation between the degree of frameshifting and rates of translocation. Four of our six mutations are substitutions at positions that interact with the translocating tRNA, in each case contacting the RNA backbone of the anticodon loop. We suggest that EF-G helps to preserve the translational reading frame by preventing uncoupled movement of the tRNA through these contacts; a further possibility is that these interactions may stabilize a conformation of the anticodon that favors base-pairing with its codon.

INTRODUCTION

Errors in maintenance of the translational reading frame are much more dangerous than missense errors. While most proteins can tolerate substitutions at many different positions (Kurland 1992), shifting of the reading frame not only results in incorporation of a

continuous series of incorrect amino acids, but soon leads to premature termination at an out-of-frame stop codon. The resulting incomplete polypeptides are often toxic, caused by dominant-lethal effects (Drummond and Wilke 2008). The importance of maintaining the reading frame is reflected in the high fidelity of translocation, with frameshifting error rates less than 10^{-5} (Kurland 1992). In spite of decades of study, the mechanisms by which the translational reading frame is preserved during the coupled translocation of the mRNA and tRNAs are still only poorly understood. We know that tRNAs can be translocated in the absence of mRNA in an elongation factor EF-G-catalyzed reaction (Tnalina et al. 1982; Yusupova et al. 1986), showing that the translocation mechanism indeed acts on the tRNA; however, there is no convincing evidence that the mRNA can be actively translocated in the absence of tRNA. This suggests that the mRNA is moved only passively, by virtue of its base-pairing to tRNA. Coupled movement of mRNA and A-tRNA would thus appear to rely strongly, if not completely, on maintaining correct codon–anticodon pairing during translocation. Although these weak triplet duplexes are stabilized by their interactions with the ribosome, they immediately become vulnerable to disruption as they move out of their binding sites during translocation. How, then, is mRNA movement strictly coupled to tRNA movement?

A clue to the mechanism of reading-frame maintenance comes from cryo-EM and X-ray structures of ribosome-EF-G complexes trapped in various states of translocation. One key structure is that of the chimeric hybrid-state intermediate, in which the head domain of the 30S subunit is rotated by ~20°, and the A- and P-site tRNAs are bound in ap/P (or ap/ap) and pe/E states, respectively (Ramrath et al. 2013; Zhou et al. 2014). In this state, the anticodon stem–loop (ASL) of the A-tRNA is held approximately between the A site of the head domain and the P site of the body domain of the 30S subunit, while the ASL of the P-tRNA is positioned between the P site of the head domain and the E site of the body domain, hence the term “chimeric.” Their acceptor ends have moved fully into the 50S P site (or in the

ap/ap state, shared between the 50S A and P sites) and the 50S E site, respectively. In these structures, the tip of the long, flexible domain IV of EF-G contacts the codon–anticodon duplex (Ramrath et al. 2013; Zhou et al. 2014). An X-ray structure of a posttranslocation EF-G-ribosome complex (Gao et al. 2009) and a cryo-EM structure of a pretranslocation complex (Brilot et al. 2013) both found domain IV in contact with their respective P-site and A/P-state codon–anticodon duplexes. Taken together, these three structures suggest that domain IV maintains contact with the duplex during its trajectory from the A site to the P site, consistent with a smFRET study that directly observed rearrangement of domain IV in pre and posttranslocation complexes in solution (Salsi et al. 2014b). Finally, in a recent crystal structure of a ribosome complex containing tRNAs that translocated spontaneously into chimeric hybrid states in the absence of EF-G, codon–anticodon pairing was disrupted, resulting in a −1 shift of the reading frame, providing direct evidence for a role for EF-G in coupling of mRNA and tRNA movement (Zhou et al. 2019). Interestingly, the A-tRNA had moved further in this complex than in the corresponding EF-G-containing complex, suggesting that EF-G may actually restrict movement of the tRNA during translocation.

In an effort to further understand the role of EF-G in translocation, we have undertaken a global screen for dominant-lethal mutations in EF-G of *E. coli* (Nelson C, Leung CS, Noller HF, et al., in prep.). Among these, we identified a cluster of six dominant-lethal mutations mapping to the tip of domain IV (Fig. 1). Prompted by the structural evidence described above, we tested whether any of these mutant forms of EF-G influence the translational reading frame. Using a system based on in vitro translation of a full-length protein containing a “slippery sequence,” we find that the presence of each of these six mutant EF-Gs greatly stimulates shifting into the −1 reading frame in our in vitro system. All but one of these mutations also confer reduced rates of mRNA translocation and rotation of the head and body domains of the 30S ribosomal subunit. Our frameshifting results are in agreement with recent studies by Peng et al. (2019) showing −1 frameshifting during in vitro

translation of an oligopeptide with mutant forms of EF-G carrying several mutations at two positions in domain IV. In the structure of the chimeric hybrid-state intermediate (Zhou et al. 2014), all of the contacts between domain IV and the codon–anticodon duplex are formed with ribose or phosphate moieties in the RNA backbone of the anticodon loop. We propose that these contacts between domain IV and the anticodon loop help to preserve the translational reading frame by preventing uncoupled movement of the tRNA during translocation; a further possibility is that these contacts may also help to stabilize an anticodon conformation that favors base-pairing with its codon.

RESULTS

EF-G mutants were isolated from an unbiased global screen, using random PCR mutagenesis (Materials and Methods), from which dominant-lethal mutations were mapped to all five structural domains of EF-G (Nelson C, Leung CS, Noller HF, et al., in prep.). Here, we focus on a cluster of mutations in loops I (positions 507–513) and II (positions 579–589) at the tip of domain IV (Fig. 1). These include mutant Q507H in loop I and H583R, D586V, S587Y, S587P, and S588P in loop II (Table 1), all of which are highly conserved, with the exception of S588. In addition, Q507D, which was found by Peng et al. (2019) to induce strong frameshifting, was created by directed mutagenesis and included in our studies. The numbering of EF-G residues refers to EF-G from the *fusA* gene of *E. coli* throughout, excluding its amino-terminal methionine residue.

In vitro translocation activities of domain IV mutants

The seven domain IV mutant EF-Gs were tested for their ability to undergo multiple rounds of translocation using a toe-printing assay (Fig. 2; Hartz et al. 1988; Fredrick and Noller 2003). Pretranslocation complexes bound to an mRNA coding for MVVV were prepared by binding N-Ac-Met-tRNA^{Met} to the P site, followed by introducing excess Val-tRNA·EF-Tu·GTP ternary complex and EF-G·GTP. A DNA primer annealed to the 3′ end of

the mRNA was then extended by reverse transcriptase. The register of the ribosome on the mRNA can be determined from the length of the resulting extended DNA. All seven mutants were capable of translocating through all 3 Val codons during the 5 min incubation (followed by an additional 5 min during primer extension; see Materials and Methods) (Fig. 2). EF-G mutant H91L, a dominant-lethal mutation at a position known to be critical for GTP hydrolysis (Cunha et al. 2013; Holtkamp et al. 2014; Salsi et al. 2014a), which was included as a negative control, showed only a single round of translocation, as expected (Fig. 2).

Rates of mRNA translocation were measured by a fluorescence quenching assay using a mRNA with pyrene attached to position +9, which is quenched by contact with the ribosome upon translocation by one codon (Studer et al. 2003). At t = 0, EF-G·GTP was rapidly mixed with a pretranslocation complex containing N-Ac-Met-Val-tRNA^{Val} in the ribosomal A site and tRNA^{Met} in the P site in a stopped-flow fluorimeter. Two of the mutants, S587P and S588P, have severe rate defects, more than 100-fold slower than wild-type EF-G (Table 1; Fig. 3A,B). The other mutants show moderate defects, having rates three- to 10-fold down from wild-type, except for Q507H, whose kinetics are nearly indistinguishable from those of wild-type (Fig. 3B). Interestingly, although nearly all of the mutants show mRNA quenching rate behaviors that are clearly biphasic, as has consistently been reported for wild-type EF-G (Peske et al. 2004; Shi et al. 2009; Munro et al. 2010; Ermolenko and Noller 2011), D586V can be fitted well to a pure single-exponential curve (Fig. 3A). The quenching curves are dominated by the fast phase (Qk_1), except for Q507D, where Qk_2 is predominant (Table 1). Due to their very low activities, the rates of mRNA quenching by S587P and S588P were measured manually (Materials and Methods) (Fig. 3C,D). Thus, all mutant EF-Gs can support multiple rounds of translocation but show a considerable range of rate defects.

Domain IV mutants were then tested for their ability to carry out synthesis of the full-length 27 kDa ribosomal protein S2, which contains seven internal methionines, in an in vitro translation reaction using [^{35}S]-methionine to label the polypeptide products. In initial

experiments, each mutant EF-G was added in an approximately twofold molar excess over the wild-type EF-G present in the S100 extract in the in vitro system (Supplemental Fig. S1). The amount of full-length protein synthesized by mutant EF-Gs in the presence of wild-type EF-G was comparable to the amount synthesized by wild-type EF-G alone, except for the S588P mutant, whose presence caused a strong dominant inhibitory effect (Fig. 4A). We next asked if the domain IV mutants can support synthesis of a full-length protein in the absence of wild-type EF-G. To do this, we constructed a strain in which the genomic copy of wild-type EF-G was replaced with EF-G containing an amino-terminal 6-His sequence. We then prepared S100 extract from the strain, removing the 6-His-EF-G with Ni^{++} resin (Materials and Methods). In the absence of wild-type EF-G, all mutant EF-Gs had robust activity, catalyzing synthesis of full-length protein in amounts comparable to that of wild-type EF-G, with the exception of S587P and S588P, which were unable to produce full-length protein above background amounts (Fig. 4B). In addition to the full-length S2 protein, a shorter ~23 kDa product is consistently produced at a reduced level in both S100 extracts (Fig. 4). The 23 kDa product is likely the result of translation of a ~100-nt 3′-truncated version of the S2 mRNA. We observed that incubation of the S2 mRNA with S100 extract results in an RNA product whose size is consistent with the loss of ~100 nt from the mRNA caused by a nuclease activity present in the extract (Supplemental Fig. S2). This conclusion is supported by quantification of these products across all mutants in independent experiments, which shows that the relative proportions of the full-length and 23 kDa products remain constant for a given mutant across multiple experiments, independent of the amount of full-length S2 protein synthesized (Supplemental Table SI).

Rates of rotation of 30S subunit body and head domains

Rates of intersubunit (30S body domain) rotation, which is coupled to movement of tRNAs from their classical states to hybrid states (Ermolenko et al. 2007), were measured by FRET changes using doubly labeled ribosomes containing a Cy5–S6 acceptor on the 30S

subunit and a Cy3–L9 donor on the 50S subunit, in a stopped-flow fluorimeter (Ermolenko et al. 2007). Starting with a pretranslocation complex in the rotated, hybrid state containing mRNA, N-Ac-Met-Val-tRNA^{Val} in the ribosomal A site and tRNA^{Met} in the P site, we followed reverse intersubunit rotation to the nonrotated classical state by an increase in FRET efficiency upon rapid mixing with EF-G·GTP (Fig. 5A,B; Ermolenko et al. 2007). Reverse intersubunit rotation rates for the mutant EF-Gs paralleled the order of their rates of mRNA translocation: Q507H has virtually no defect, but the rates for H583R and S587Y are approximately twofold down, Q507D and D586V slower, and S587P and S588P barely detectable (Table 1; Fig. 5A,B). All intersubunit rotation kinetics followed single-exponential behavior.

Forward and reverse rotation of the 30S subunit head domain were also measured using a FRET-based assay, with protein S12 in the 30S body domain labeled with the donor Alexa 488 and protein S19 in the head domain with the acceptor Alexa 568 (Guo and Noller 2012). All mutants except Q507D showed forward and reverse head rotation rates that paralleled their respective rates of 30S body rotation, including barely detectable rates for S587P and S588P (Table 1; Fig. 5C,D). The rates of mRNA quenching were most similar to the rates of reverse 30S head rotation, in keeping with our previous conclusion that mRNA quenching is the result of contact by the 30S head domain with the 3′-pyrene fluor during its return to the nonrotated state (Guo and Noller 2012). An apparent anomaly is seen for Q507D, whose rate of reverse head rotation is several-fold slower than its rate of mRNA quenching. However, the mRNA quenching kinetics for Q507D, unlike the other EF-G mutants and wild-type EF-G, are dominated by the slow phase (Qk_2) (Table 1). Its reverse head rotation rate (0.37 sec^{-1}) in fact bears similarity to the slow phase of its mRNA quenching kinetics (0.32 sec^{-1}), suggesting that Q507D has an interesting atypical defect involving reverse head rotation (Table 1). The overall relative rates of translocation-related events for most of the mutant EF-Gs are generally in the order of forward head rotation >

reverse head rotation ≈ mRNA quenching > reverse body rotation, as previously reported for wild-type EF-G (Guo and Noller 2012).

Although the activities of S587P and S588P mutants were only barely detectable in our stopped-flow kinetic measurements (Fig. 5), they were nevertheless fully capable of supporting multiple rounds of translocation in a toe-printing assay, likely due to the longer incubation times in the latter assay (Fig. 2). To further clarify this point, we retested S588P in a toe-printing time-course experiment at room temperature, quenching the translocation reaction with viomycin at different time points prior to primer extension (Supplemental Fig. S3; Fredrick and Noller 2003). It can be seen that an extent of translocation comparable to that of wild-type EF-G at 30 sec is only reached by S588P after 4 min (Supplemental Fig. S3).

Mutations in domain IV cause increased levels of −1 frameshifting

We based our frameshifting assay on the *dnaX* gene, which contains three elements that promote −1 frameshifting: an internal Shine–Dalgarno (SD) sequence, a slippery sequence, and a downstream 11 bp hairpin (Tsuchihashi and Brown 1992; Larsen et al. 1994). We excluded the downstream hairpin from our construct, but introduced the internal SD (AGGGAG) and the slippery sequence (AA AAA AAG) into the S2 protein mRNA sequence at positions 365–370 and 381–388, respectively (see Materials and Methods). This construct is predicted to stimulate frameshifting to the −1 reading frame, which would result in translation termination at an out-of-frame UGA stop codon at position 417, creating a truncated 16 kDa polypeptide product. In vitro translation of this modified mRNA with wild-type EF-G resulted in synthesis of the predicted 16 kDa frameshift product at 23% frameshifting efficiency (Table 2; Fig. 6A). This is consistent with results that show ~9%–27% frameshifting with *dna X* in the absence of downstream secondary structure (Tsuchihashi and Kornberg 1990; Larsen et al. 1994, 1997; Chen et al. 2014; Kim and Tinoco 2017). All seven domain IV mutant EF-Gs, even in the presence of endogenous wild-type EF-G in our S100 extract (Supplemental Fig. S1), increased the synthesis of frameshifted product to 50%–67%.

This corresponds to a 3.4- to 6.8-fold increase in the relative abundance of frameshifted product to zero-frame product over that of wild-type EF-G, with H583R, S587Y, and S588P showing the highest rates of frameshifting (Fig. 6A,B). This result demonstrates the dominant properties of these mutant forms of EF-G.

We next measured frameshifting in the absence of endogenous wild-type EF-G. For the mutants that show robust translational activity (Q507D, Q507H, H583R, D586V, and S587Y), the relative abundance of frameshifted product induced by the mutant EF-Gs increased to 3.7- to 7.2-fold over that of wild-type EF-G (Table 2; Fig. 6C,D). The most dramatic increase was seen for Q507D, suggesting that this mutant does not compete as well with wild-type EF-G (Table 2). For mutants S587P and S588P, there is a clear increase in the amount of frameshifted protein product compared to S100 extract alone (Fig. 6D), but we could not quantify the level of frameshifting for these mutants because they do not produce a full-length protein (Fig. 4B). The increase in frameshifting caused by the domain IV mutants (55%–70% vs. 24% for wild-type EF-G) is comparable to frameshift stimulation by the downstream secondary structure element in the *dna X* system that is absent in our mRNA construct (Tsuchihashi and Kornberg 1990; Tsuchihashi and Brown 1992; Larsen et al. 1994, 1997; Chen et al. 2014; Kim and Tinoco 2017). Frameshifting efficiencies showed a roughly inverse correlation with rates of translocation, intersubunit rotation and 30S head rotation (Fig. 7).

In order to confirm that these mutations are indeed causing −1 frameshifting, we created mRNAs with UGA to GGA read-through mutations in the −1 and +1 frames at the first out-of-frame stop codon following the slippery sequence (Fig. 8A). The resulting read-throughs would be predicted to create products with a ∼3 kDa increase in size over the frameshift product from the nonmutated mRNA. When the mutated mRNAs were tested, only the mRNA containing the UGA to GGA substitution in the −1 reading frame generated a product of the predicted size, along with disappearance of the original frameshift product (Fig.

8B). This result was observed for translation with both wild-type EF-G and all seven domain IV mutants.

For mutants with the highest degrees of frameshifting, an additional band is seen corresponding to the predicted size for a +1 frameshift product (Fig. 8). The intensity of this band is greatest in the presence of EF-G mutants with the highest degrees of frameshifting and is absent in the translation products from the +1 bypass mRNA (Fig. 8B). Given that the slippery sequence is compatible with a −2 frameshift, but does not allow cognate tRNA-mRNA pairing with a +1 frameshift, we infer that this product is likely generated from a −2 slip caused by two −1 slips, rather than an authentic +1 frameshifting event.

DISCUSSION

Our study was prompted by a recent crystal structure of a ribosome-tRNA-mRNA complex that had undergone spontaneous partial translocation in the absence of EF-G or antibiotics (Zhou et al. 2019). The resulting translocation intermediate is similar to a previous EF-G-containing chimeric hybrid-state complex that had been trapped with fusidic acid (Zhou et al. 2014), providing an opportunity to compare in detail the influence of EF-G on the movements of tRNA and mRNA during translocation. In both complexes, the tRNAs were trapped in intermediate states between their pre- and posttranslocation positions. The anticodon ends of the A-site tRNAs had both moved into chimeric a/p states, positioned between A site features of the 30S head domain and P site features of the 30S body. Most unexpected was the finding that, in the absence of EF-G, base-pairing of the A-tRNA codon–anticodon duplex was disrupted, and the anticodon end of the tRNA had actually moved *further* than in the corresponding EF-G-containing complex. Examination of the relative positions of the codon and anticodon in the EF-G-deficient complex showed that the anticodon register had slipped by one position, into the −1 reading frame, providing direct evidence that EF-G plays a role in maintaining the reading frame. Meanwhile, in a screen for dominant-lethal mutations in EF-G (Nelson C, Leung CS, Noller HF, et al., in prep.), we

identified a cluster of six mutations that map to the tip of domain IV, which was found to contact the codon–anticodon duplex in the trapped chimeric hybrid-state intermediate (Ramrath et al. 2013; Zhou et al. 2014), a pretranslocation complex (Brilot et al. 2013), and a posttranslocation complex (Gao et al. 2009). Our results show that all six mutations in domain IV cause an increase in −1 frameshifting as well as a range of defects in translocation itself. These mutations have escaped detection in previous searches for mutations in the genomic copy of the *fusA* gene (Dahlfors and Kurland 1990; Hou et al. 1994), possibly because of their dominant-lethal phenotypes.

Domain IV of EF-G has long been implicated in catalysis of translocation (Rodnina et al. 1997; Martemyanov and Gudkov 1999; Savelsbergh et al. 2000; Gao et al. 2009; Khade and Joseph 2011; Ramrath et al. 2013; Liu et al. 2014; Peng et al. 2019). Indeed, for the seven mutant forms of EF-G tested in our studies, all of them, with the exception of Q507H, conferred diminished rates of translocation-associated processes, including defects in mRNA translocation, intersubunit rotation and rotation of the head domain of the 30S subunit (Table 1). Their rates of translocation-associated processes were in the order WT ≈ Q507H > H583R ≈ S587Y > Q507D > D586V >>> S587P ≈ S588P. It has been shown that complete deletion of domain IV results in a ∼1000-fold decrease in the rate of translocation without impairing binding of EF-G to the ribosome, single-round GTP hydrolysis, or Pi release (Rodnina et al. 1997; Martemyanov and Gudkov 1999). Site-directed mutations at four positions at the tip of domain IV have been found in several previous studies to cause decreased rates of translocation, including defects for H583K, H583R (Savelsbergh et al. 2000); Q507L, H583K, S588P, and E589A (Liu et al. 2014); and Q507D, Q507E, and H583K (Peng et al. 2019). Three of these four positions were found among the mutations from our dominant-lethal screen (Q507H, H583R, and S588P), which also identified mutations (S587Y, S587P, and D586V) at two additional positions.

While it is clear that these mutations in domain IV confer translocation defects, what are their effects on frameshifting? We used an in vitro assay to monitor stimulation of frameshifting, based on translation of full-length ribosomal protein S2 using a mRNA containing a “slippery sequence” with an upstream Shine–Dalgarno-like sequence. To exclude the possible effects of downstream structured mRNA elements, which are known to strongly increase frameshifting efficiency (Atkins et al. 2016; Choi et al. 2020), our construct lacks any such downstream hairpin or pseudoknot elements (Materials and Methods). All six of the domain IV mutants identified in our screen, plus an additional Q507D mutant (Peng et al. 2019) dramatically stimulate frameshifting into the −1 reading frame by approximately four- to sevenfold over that of wild-type EF-G (Table 2; Fig. 6). Even experiments done with mutant EF-Gs in the presence of wild-type EF-G showed strong increases in frameshifting (Table 2; Fig. 6A,B). Thus, the observed stimulation of −1 frameshifting is dominant in vitro, although we cannot distinguish whether or not this frameshifting defect is responsible for the observed in vivo dominant-lethal phenotypes of the domain IV mutations. While our studies were in progress, Rodnina and coworkers (Peng et al. 2019) reported stimulation of frameshifting by their mutations at positions 507 in loop I and 583 in loop II, using an assay based on in vitro translation of oligopeptides through three different slippery sequences, analyzed by incorporation of radioactively labeled amino acids. All of their mutations conferred −1 frameshifting, with efficiencies ranging from 30% to 80%, in good overall agreement with our findings, in spite of the very different methodologies used in the two studies. In addition to residues Q507 and H583, we find that mutations at D586, S587, and S588 in loop II also stimulate frameshifting (Table 2).

How do mutations in domain IV promote frameshifting? Structures of complexes representing three different states of the translocation process (Gao et al. 2009; Brilot et al. 2013; Zhou et al. 2014) suggest that domain IV remains in contact with the codon–anticodon duplex throughout its trajectory between the A and P sites. Contacts made by domain IV in

the chimeric hybrid state (Fig. 9A–D; Zhou et al. 2014) overlap, but are not identical with those seen in the posttranslocation state (Fig. 9E; Gao et al. 2009), indicating some shifting of their positions. In the pretranslocation state (Brilot et al. 2013), the corresponding segments of the domain IV and tRNA backbones are similarly juxtaposed, although the 7.6 Å cryo-EM structure is not of sufficient resolution to conclude whether any of the same contacts occur.

We propose that contact between domain IV and the RNA backbone of the anticodon loop helps to preserve the reading frame by restraining the tRNA from uncoupled movement during translocation. Frameshifting efficiency would then be expected to be increased by mutations in the tip of domain IV that disrupt these interactions. Q507 (loop I), H583 and D586 (loop II), which have strong frameshifting phenotypes, all contact the backbone of the anticodon loop of the transiting A-site tRNA in the chimeric-hybrid state (Fig. 9; Zhou et al. 2014). Although S587P and S588P show frameshifting effects, neither S587 nor S588 actually contact the translocating tRNA or mRNA. However, proline substitutions at these positions likely cause misfolding of the loop II region, creating both translocation and frameshifting defects. The S587Y mutation does not affect translocation as dramatically as the S587P mutation, but strongly stimulates frameshifting, presumably because the bulky tyrosine side chain interferes with normal interaction of domain IV with the anticodon loop. Interestingly, contacts between domain IV and the anticodon loop are centered around nucleotides that interact with the crucial first and second codon positions, suggesting the further possibility that these interactions may stabilize a conformation of the anticodon that favors base-pairing with its codon.

Rodnina and coworkers (Peng et al. 2019) have pointed out that the increased frameshifting efficiencies of domain IV EF-G mutants appear to be correlated with slow rates of translocation-associated processes. Our findings are in general agreement with this (Fig. 7); for example, S588P, which is extremely slow at translocation, shows one of the strongest

frameshifting efficiencies. Peng et al. (2019) have proposed that during fast translocation, the ribosome remains committed to the 0 frame before it can slip into the −1 frame, whereas long pauses can allow equilibrium that favors the −1 frame, depending on the mRNA sequence. However, a counterexample from our results is Q507H, which has virtually wild-type translocation rates (Table 1), yet causes a strong increase in frameshifting efficiency (Table 2). This result shows that increased frameshifting cannot be explained solely by the effects of slow translocation.

How would slow translocation promote frameshifting? Structures (Ramrath et al. 2013; Zhou et al. 2014, 2019) suggest that the chimeric hybrid state is the state most vulnerable to reading frame disruption, so any mutation that prolongs this state would likely induce higher levels of frameshifting. This idea is supported by the Q507D mutant, which has an unusually strong defect in its rate of reverse 30S head rotation relative to forward head rotation (Table 1). This implies that Q507D, which is one of the most efficient frameshifters of the mutants that show robust translational activity, must spend more time in the rotated, chimeric-hybrid state. The P-site tRNA ASL, bound tightly to the 30S head, moves with forward head rotation toward the 30S E site, whereas the A-site tRNA, lacking strong contact with the head, can move freely into the space vacated by the transiting P-tRNA, which can result in disruption of its codon–anticodon interaction, as seen in the absence of EF-G (Zhou et al. 2019). Thus, the more time spent in this state, especially with a weakened domain IV contact, the more likely a frameshift event will occur. Peng et al. (2019) also observed a significantly delayed reverse head rotation for the Q507D mutant, although they report a several 100-fold defect, whereas we observe a ninefold rate decrease compared to wild-type EF-G. One difference between the two studies is that Peng et al. monitored head rotation via fluorescence quenching between probes on S13 in the 30S head and L33 on the 50S subunit, thus requiring deconvolution of the rates of 30S head and body rotation, whereas our FRET probes, on S12 in the 30S body and S19 in the 30S head, allow direct measurement of

forward and reverse head rotation. Nevertheless, our findings are in agreement in that for Q507D, reverse head rotation is the most defective step. Quite independently, the strong stimulatory effects of downstream secondary structure elements on frameshifting have been attributed to inhibition of reverse head rotation (Caliskan et al. 2014; Yan et al. 2015), providing further support for this possibility.

Interestingly, early searches for EF-G mutations affecting frameshifting identified mutants that decrease the rate of frameshifting. One of these, a G502D mutation (Hou et al. 1994), which introduces a negatively charged side chain into loop I, is consistent with a role in reading frame maintenance for domain IV. It is less obvious how another mutation, Q121R (Dahlfors and Kurland 1990), would affect frameshifting, raising the possibility of a connection between the GTPase and reading-frame maintenance functions of EF-G.

The effects of domain IV mutations on translocation rates are not well understood. It has been proposed that domain IV is involved in initiating translocation by disrupting contacts between the codon–anticodon duplex and the decoding center, which is believed to be the rate-limiting step of translocation (Gao et al. 2009; Khade and Joseph 2011; Ramrath et al. 2013; Liu et al. 2014). Our results, together with the aforementioned previous mutational studies, implicate the two conserved loops I and II at the tip of domain IV in catalysis. Initial contact between domain IV and the pretranslocation complex must somehow trigger release of the codon–anticodon duplex from the 30S A site, possibly by inducing a conformational change in the decoding center around nucleotides G530, A1492, and A1493 of 16S rRNA. Our sole view of EF-G bound to a pretranslocation complex is a 7.6 Å resolution cryo-EM structure, which reveals the positions of the protein and RNA backbones of EF-G, the tRNAs, mRNA, ribosomal proteins and rRNA (Brilot et al. 2013). This structure shows loop I of domain IV within contact distance of the anticodon loop of the A/P tRNA; together with the chimeric hybrid-state and posttranslocation structures (Gao et al. 2009; Ramrath et al. 2013; Zhou et al. 2014), this observation shows that loop I remains in contact with the tRNA

anticodon loop during its entire excursion from the A site to the P site. Most interesting is that loop II of domain IV is within contact distance of the 530 loop of 16S rRNA around positions 517 and 530 (Brilot et al. 2013) (PDB 4V7D), raising the intriguing possibility that contact between loop II and the 530 loop might trigger release of the codon–anticodon duplex from the 30S A site. Earlier studies showing that mutations at positions 517 and 529 of 16S rRNA confer frameshifting phenotypes (O'Connor et al. 1992, 1997; Santer et al. 1995) could be explained by weakening of the contacts between loop II and the 530 loop, and are consistent with the finding that many of the same EF-G mutations that increase frameshifting also cause defects in translocation. It should be noted that these mutants also have miscoding phenotypes, so their increased frameshifting could derive from effects on near-cognate tRNA binding, in addition to any potential effects on EF-G function. Merging both the translocation and reading-frame functions in domain IV would ensure that upon release of the codon–anticodon duplex from the decoding site, movement of the tRNA is immediately restrained to prevent its uncoupled translocation.

MATERIALS AND METHODS

Screening for dominant-lethal mutations in EF-G and purification of mutant EF-G proteins

PCR mutagenesis (Cadwell and Joyce 1992) was used to generate random mutations in the *E. coli* MRE600 gene coding for EF-G, modified to contain a carboxy-terminal 6-His tag, which was then ligated into the expression vector pBAD-18 (Guzman et al. 1995). To screen for dominant-lethal mutants, DH10B transformants were replica-plated on plates containing 0.5 mM arabinose or 0.2% glucose, to turn expression on or off, respectively. Transformants that grew on glucose but not on arabinose were scored as dominant-lethal candidates, as will be described in detail elsewhere (Nelson C, Leung CS, Noller HF, et al., in prep.). Following DNA sequencing, candidate mutants were recreated by site-directed mutagenesis (Kunkel 1985) and retested for their resulting phenotypes. Mutant

EF-G proteins were expressed in strain DH10B by induction with 2 mM arabinose for 3 h at 37°C, and purified using Ni-NTA resin (Qiagen) as described (Guo and Noller 2012).

Materials

Tight-couple 70S ribosomes were purified as described (Lancaster et al. 2002). IF1, IF2, and IF3 were prepared as described (Lancaster and Noller 2005), as was wild-type EF-G (Ramrath et al. 2013). To prepare in vitro-transcribed $tRNA^{Met}$, the gene from *E. coli* strain MRE600 was cloned into plasmid pRZ (Walker et al. 2003), which is designed to produce RNA transcripts with homogeneous 3′ ends via catalytic HDV ribozyme cleavage of the transcript. Following transcription and gel purification, 2′,3′-cyclic phosphate was removed from the 3′ end of $tRNA^{Met}$ by incubation with T4 polynucleotide kinase (NEB) (Schurer et al. 2002). Aminoacylation (Moazed and Noller 1989) of transcribed $tRNA^{Met}$ was shown to be >95% as monitored by acid gel electrophoresis (Varshney et al. 1991). fMet-$tRNA^{fMet}$ (Sigma), Val-$tRNA^{Val1}$ (Subriden) and NAcMet-$tRNA^{Met}$ (transcribed) were prepared as described (Moazed and Noller 1989; Lancaster and Noller 2005).

Toeprint analysis

mRNA MVVV_100

(5′GGAAAGGAAAUAAAA**AUGGUAGUAGUA**GAUAGAAAAUAAUAGAAGAAUCGGAUAAG AGAACACAGGAUCCAGCUGGCGUAAUAGCGAAGAGGCCCGCACC), coding for MVVV, was preannealed to 5′-[^{32}P]-labeled DNA primer (5′GGTGCGGGCCTCTTCGC), then used to form P-site tRNA complexes containing 0.4 μM 70S ribosomes, 0.8 μM N-Ac-Met-tRNA, and 1.2 μM mRNA MVVV_100/primer, in 25 mM Tris·HCl (pH 7.5), 100 mM NH_4Cl, 15 mM $MgCl_2$ and 1 mM DTT, that was incubated for 20 min at 37°C. Ternary complex was formed with 7.5 μM EF-Tu, 1.5 μM Val-$tRNA^{Val1}$, and 2 mM GTP in 25 mM Tris·HCl (pH 7.5), 100 mM NH_4Cl and 1 mM DTT and incubated for 5 min at 37°C. Translocation was initiated by adding 6 pmol ternary complex and 10 pmol EF-G to 2 pmol of P-site complex in a final condition of

25 mM Tris·HCl (pH 7.5), 100 mM NH_4Cl, 7.5 mM $MgCl_2$, 1 mM DTT, and 1 mM GTP, in a total volume of 10 µL. After 5 min incubation at 37°C, primer extension was initiated by adding 1 µL of extension mix containing 0.55 mM of each dNTP and 0.05 µL of AMV reverse transcriptase (Seikagaku) in the same buffer, and incubation was continued for 5 min at 37°C. Reactions were ethanol precipitated, run on an 8 M urea, 7.5% polyacrylamide gel and autoradiographed. For the toe-printing time-course reactions (Fredrick and Noller 2003), the P-site complex was cooled to room temperature prior to addition of ternary complex and EF-G, and incubation was at room temperature. To stop translocation at each time point, 9 µL of the reaction were added to 1 µL of 10 mM viomycin. Primer extension was initiated and incubated at 37°C as above.

Gemonic replacement of wild-type EF-G with 6His-EF-G

The DNA sequence containing 475 nt upstream and 1000 nt downstream from the amino terminus of the *fusA* gene was PCR-amplified from *E. coli* MRE600 genomic DNA, then cloned into the Bam HI site of plasmid pKC. The synthetic oligonucleotide 5′GCGATGGGTGTTGTACGAGCGTGGTGGTGGTGGTGGTGCATTTGTTTCCTCGTTTATC was used to add a 6-His sequence to the amino terminus of the EF-G gene (Kunkel 1985). The DNA was then subcloned into the Bam HI site of plasmid pKO3 (Link et al. 1997). Strain 6His_EF-G was generated by genomic replacement of the EF-G gene with 6-His-EF-G in *E. coli* strain CSH142 as described (Link et al. 1997). The mutation was confirmed by sequencing genomic DNA that was PCR-amplified using primers flanking the cloned region.

Preparation of S100 extracts

S100 extract was prepared from 10 g of *E. coli* MRE600 cells, or 4 L of strain 6His_EFG, and purified over DEAE resin according to previously published protocols (Traub et al. 1981). To deplete EF-G, S100 extract from strain 6His_EF-G was mixed with 1 mL Ni-NTA agarose resin (Qiagen; 50% slurry) for 1 h at 4°C. The mixture was packed in a column

and the flow-through was collected and filtered through a 0.8 μ syringe filter (Corning). The absence of EF-G in the flow-through was confirmed by SDS gel electrophoresis of the S100 extract before and after the column, with purified EF-G used as a marker.

Construction of frameshift mRNAs

Site-directed mutagenesis (Kunkel 1985) of pET24b::S2 (Culver and Noller 1999) was used to generate frameshifting mRNAs by modifying the S2 gene to obtain an internal Shine–Dalgarno sequence (AGGGAG) at positions 365–370, and a slippery sequence (AAAAAAG) at positions 381–388 (Tsuchihashi and Brown 1992; Farabaugh 1996; Tinoco et al. 2013), as shown in Table 3. In addition, the plus-one frame stop codon (TGA) at positions 404–406 and the minus-one stop codon (TGA) at positions 417–419 were mutated to GGA in +1RT and −1RT, respectively, to create read-through of the first out-of-frame stop codons. The mRNAs were transcribed from plasmid linearized with Xho I (NEB).

***In vitro* translation**

Initiation complexes were formed with a 1:2:3:3 molar ratio of 70S ribosomes (0.5–1.0 μM), fMet-tRNA^{fMet}, mRNA, and initiation factors IF1, IF2, and IF3 in a buffer containing 50 mM Tris·HCl (pH 7.5), 60 mM NH_4Cl, 8 mM $MgCl_2$, 2 mM DTT, 1 mM GTP, and incubated at 37°C for 30 min. Total *E. coli* MRE600 tRNA (Roche) was aminoacylated with 1.0–1.3 μL S100 per 0.1 A260 Unit of tRNA in the same buffer with the addition of 1 mM ATP, 0.2 mM amino acids minus methionine, 6.75 μM methionine, and 0.07 to 0.14 μM [^{35}S]-methionine (1175 Ci/mMol, PerkinElmer) at 37°C for 15 min. Both reactions were added to a translation mix containing 100 pmol EF-Tu and 37.5 pmol wild-type or mutant EF-G per pmol of ribosomes. The final combined mixture contained 0.2 mM total amino acids (except for methionine), 1 mM ATP and GTP, 5 mM phosphoenolpyruvate, 100 nM ribosomes, 0.0075 A260 units/μL tRNA, and 0.75-1.0 μL of S100 per pmol of ribosomes. The combined mixture

was incubated for 30 min at 37°C. After incubation, the mixture was analyzed on a 15% (29:1 polyacrylamide:bis) gel and visualized by autoradiography.

Quantification of frameshifting

The amounts of 0, −1, and −2-frame product produced from in vitro translation were quantified using ImageLab (BioRad). Background subtraction was adjusted to isolate individual peaks corresponding to protein products from the three reading frames and the peaks were integrated and normalized according to the number of [^{35}S]-methionines in the predicted sequence of each product: S2 full-length (S2FL) = 7 Met; 23 kDa (23 kDa) = 7 Met; −1 frameshift (−1 FS) = 5 Met; and −2 frameshift (−2 FS) = 5 Met. Percent frameshifting (%FS) was calculated as (−1 FS + −2 FS)/(−1 FS + −2 FS + S2FL + 23 kDa) × 100. Ratio of frameshifted product (FS/0-F) was calculated as (−1 FS + −2 FS)/(S2 FL + 23 kDa). FS/0-F was normalized to wild-type EF-G by dividing the FS/0-F ratio of each mutant by the EF-G wild-type FS/0-F ratio to determine the fold-increase in the frameshift ratio for each mutant.

Fluorescent labeling of ribosomal proteins

Ribosomal proteins S6–D41C and L9–N11C were labeled with Cy5 and Cy3 (Amersham GE) respectively, and S12–K108C and S19–Q56C were labeled with Alexa488 and Alexa568 (Invitrogen), respectively, essentially as described previously (Cornish et al. 2008; Guo and Noller 2012), except that excess dye was removed from labeled S6 and L9 by size exclusion chromatography on a Superdex 75 column (Pharmacia Biotech), in a buffer containing 1 M NH_4Cl, 6 mM βME, and 20 mM Tris-HCl (pH 7.5). The same procedure was followed for S12 and S19, except that the buffer was supplemented with 0.0025% Nikkol and 1 M urea.

Preparation of double labeled ribosomes

A total of 30S subunits lacking S6, and 50S subunits lacking L9, were isolated from S6 deletion (Keio collection; CGSC #10995), and L9 deletion (Lieberman et al. 2000) strains,

respectively, essentially as described (Moazed and Noller 1989; Hickerson et al. 2005), and reconstituted with S6–D41C–Cy5 and L9–N11C–Cy3 as described for L9 (Ermolenko et al. 2007) with the following modifications. Subunits were incubated with a 2.5 molar excess of protein for 1 h in 200 mM NH_4Cl, 20 mM $MgCl_2$, 5 mM βME, and 25 mM Tris·HCl (pH 7.5) prior to reassociating and isolating as 70S subunits as described (Hickerson et al. 2005). Doubly labeled S12–Alx488/S19–Alx568 70S ribosomes were reconstituted as described (Guo and Noller 2012) and stored in 20 mM Tris·HCl (pH 7.5), 100 mM NH_4Cl, 15 mM $MgCl_2$, 5 mM βME, and 0.01% Nikkol.

Stopped-flow mRNA quenching and intersubunit and 30S head rotation kinetics

Fluorescence changes due to mRNA quenching, intersubunit rotation, and 30S head rotation were measured using an Applied Photophysics SX-20 stopped-flow apparatus by rapidly mixing pretranslocation complex with EF-G·GTP, as described (Guo and Noller 2012). All stopped-flow experiments were conducted in 100 mM NH_4Cl, 10 mM $MgCl_2$, 1 mM DTT, 0.01% Nikkol, and 25 mM Tris·HCl (pH 7.5) at 22°–23°C, with final concentrations of 37.5 nM 70S ribosomes, 375 nM EF-G, and 0.5 mM GTP after mixing. Pretranslocation complexes contained 3′-pyrene labeled mv24 mRNA (or unlabeled mv39 mRNA), deacylated elongator $tRNA^{Met}$ bound to the P site and N-acetyl-Met-Val-$tRNA^{Val}$ bound to the A site. For intersubunit rotation experiments, Cy3 was excited at 550 nm and emission from Cy5 was collected using a 645 nm long-pass filter. For 30S head rotation experiments, fluorescence readings were collected as described previously (Guo and Noller 2012), with the exception that Alexa488 was excited at 496 nm. Rates were obtained by fitting individual mRNA quenching and head rotation traces to double exponentials and intersubunit rotation traces to single exponentials using a standard R package nlsLM, which is the R interface to the Levenberg-Marquardt Nonlinear Least-Squares algorithm included in package minpack.lm (http://CRAN.R-project.org/package=minpack.lm). Kinetic values from traces that were collected after the

effects of mixing within the stopped-flow had dissipated and had exponential fits that converged were averaged.

Manual recording of mRNA quenching rates

For the two mutants S587P and S588P, manual measurements of mRNA fluorescence quenching were done using a Cary Varian Eclipse Fluorescence Spectrophotometer with excitation at 343 nm. Pretranslocation complexes and EF-G·GTP mixes were formed essentially as described above except that the concentrations of 70S ribosomes and EF-G were 800 nM and 8 pmol/μL, respectively. After combining pretranslocation complexes with EF-G·GTP, fluorescence emission at 380 nm was recorded over 5 min at 22°C. Final concentrations were 400 nM 70S ribosomes, 4 μM EF-G, 0.5 mM GTP, 100 mM NH_4Cl, 10 mM $MgCl_2$, 1 mM DTT, 0.01% Nikkol, and 25 mM Tris·HCl (pH 7.5). Data for both mutants could be fit to a single exponential.

FIGURES AND TABLES

Table I. Effects of mutations in domain IV of EF-G on rates of translocation events.[a]

Mutant	Qk_1	Qk_2	fk_1	RBR	FHR	RHR
WT	4.12	0.26	0.78	2.60	15.38	3.37
Q507D	1.38	0.32	0.35	0.51	5.96	0.37
Q507H	3.80	0.32	0.70	2.39	17.16	3.13
H583R	1.53	0.30	0.61	1.19	4.73	1.51
D586V	0.43	--	--	0.39	3.39	0.44
S587Y	1.76	0.25	0.59	1.13	6.46	1.09
S587P	~0.03	--	--	<0.1	--	--
S588P	~0.03	--	--	<0.1	--	--

[a]Rates are in sec^{-1}. (Qk_1 and Qk_2), fast (k_1) and slow (k_2) phases of mRNA quenching; (RBR) reverse intersubunit (30S body) rotation; (FHR) forward 30S head rotation; (RHR), reverse

30S head rotation; (WT), wild-type EF-G. (fk_1), fractional contribution of the k_1 phase to mRNA quenching rate.

Table II. Stimulation of -1 frameshifting by mutations in domain IV of EF-G[a]

Mutant	FS (+WT) % FS	FS (+WT) FS/0-F	FS (+WT) FS/0-F (normalized)	FS (-WT) % FS	FS (-WT) FS/0-F	FS (-WT) FS/0-F (normalized)
WT	23.1 ± 1.7	0.30	1.00	24.8 ± 1.4	0.33	1.00
Q507D	54.3 ±1.7	1.19	3.97	70.3 ± 0.3	2.37	7.18
Q507H	55.3 ± 3.1	1.25	4.17	55.2 ± 0.9	1.23	3.72
H583R	60.5 ± 1.3	1.54	5.13	67.9 ± 0.3	2.11	6.39
D586V	56.3 ± 1.6	1.29	4.30	66.3 ± 1.0	1.97	5.97
S587Y	61.8 ± 2.3	1.64	5.47	64.8 ± 0.2	1.84	5.58
S587P	50.0 ± 1.4	1.01	3.37	N/A	N/A	N/A
S588P	67.1 ± 1.5	2.05	6.83	N/A	N/A	N/A

[a]Efficiencies of -1 frameshifting (FS) for each mutant EF-G in the presence of S100 extract containing (+WT) or lacking (-WT) wild-type EF-G (Fig. 4). (WT), wild-type EF-G; (0-F), 0-frame EF-G product. (FS/0-F), Ratio of frameshifted product to 0-frame product. (N/A), Not available, due to incomplete synthesis of full-length product.

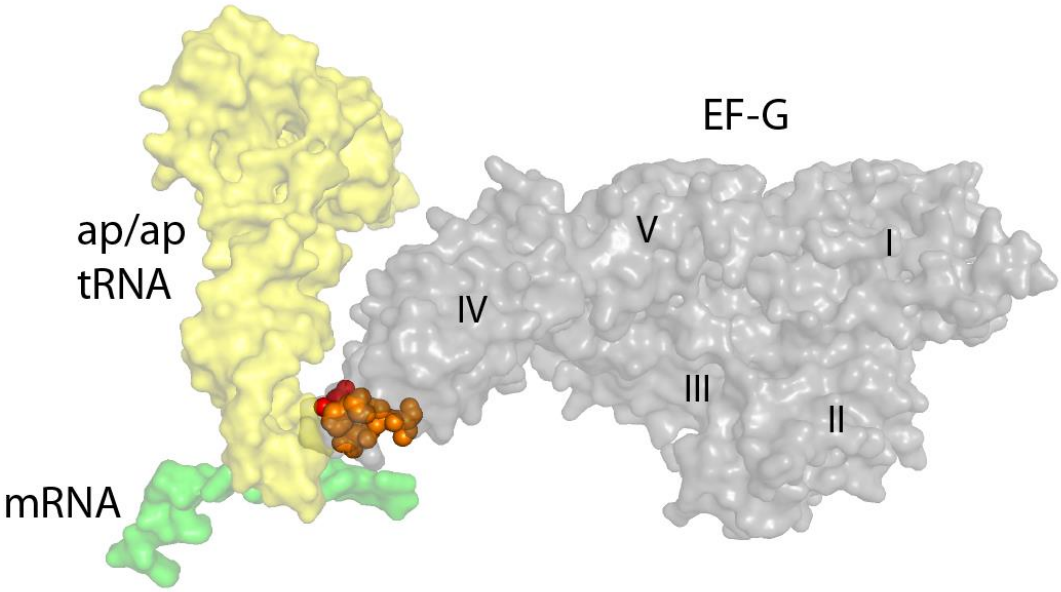

Figure 1. Domain IV of EF-G contacts the codon–anticodon duplex during translocation. In the crystal structure of a trapped chimeric hybrid-state translocation intermediate (Zhou et al. 2014), the tip of domain IV of EF-G contacts the RNA backbones of the anticodon loop of the ap/ap tRNA (yellow) and the codon of the mRNA (green) at their point of convergence. The positions of dominant-lethal mutations in loop I (red) and loop II (orange) of domain IV are indicated.

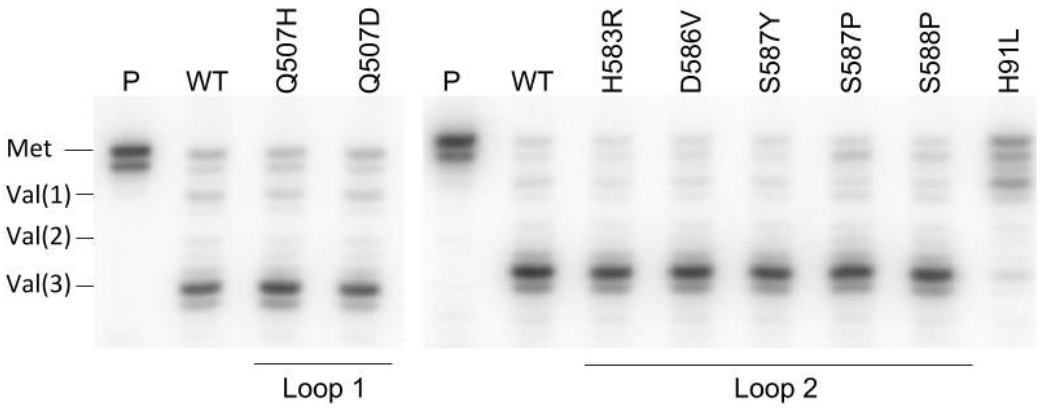

Figure 2. All domain IV mutants catalyze multiple rounds of translocation. Toeprint analysis of translocation by domain IV mutant EF-Gs. (P) Pretranslocation complex; (WT) wild-type EF-G. Positions of reverse transcriptase stops indicate register of mRNA with (Met), P site occupied by N-Ac-Met-tRNAMet; [Val(1), Val(2), (Val(3)], translocation through 1, 2, or 3 consecutive Val codons. The domain I EF-G mutant H91L, which is defective in GTPase activity (Cunha et al. 2013; Holtkamp et al. 2014; Salsi et al. 2014a) is included as a negative control.

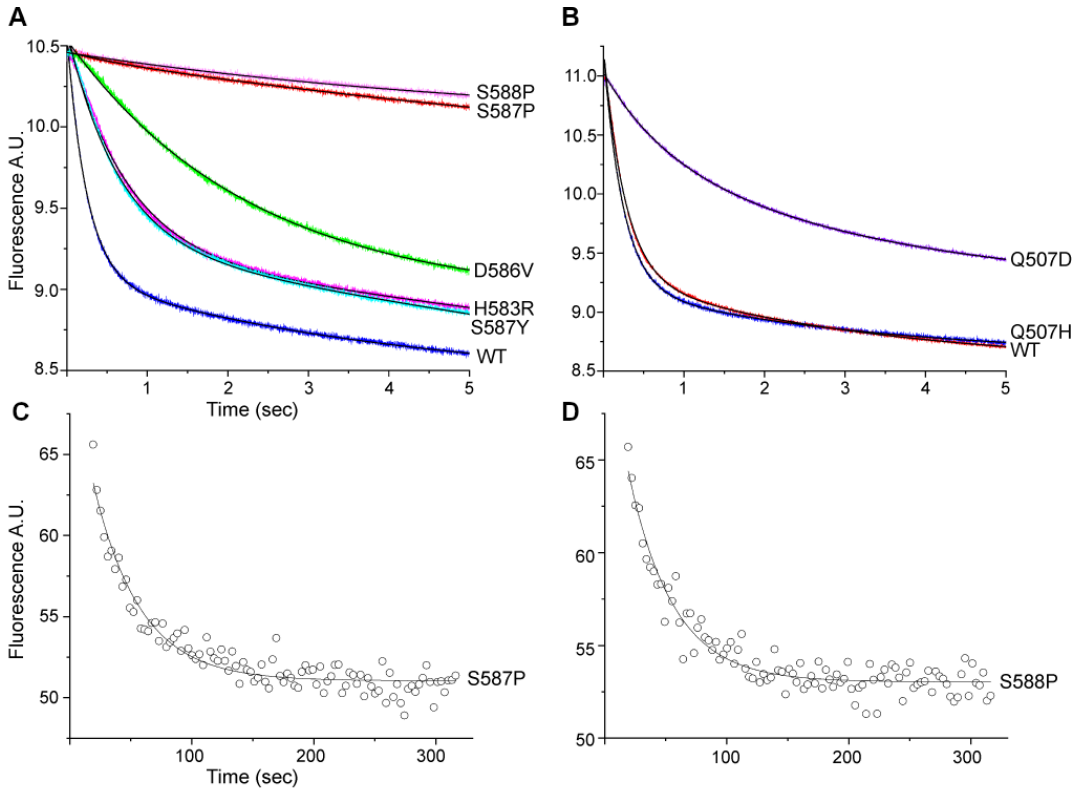

Figure 3. Domain IV mutations cause mRNA translocation defects. A fluorescence quenching assay (Studer et al. 2003) was used to measure mRNA translocation complex containing a 3′ -pyrene-labeled mRNA. (A,B) A pretranslocation complex was rapidly mixed with mutant forms of EF-G·GTP and quenching of fluorescence of the pyrene label was measured in a stopped-flow fluorimeter. Data were fit to double-exponential curves (Table 1). (C,D) Rates of mRNA quenching for EF-G mutants (C) S587P and (D) S588P were measured manually, due to their low translocation rates. Data could be fit to single-exponential curves.

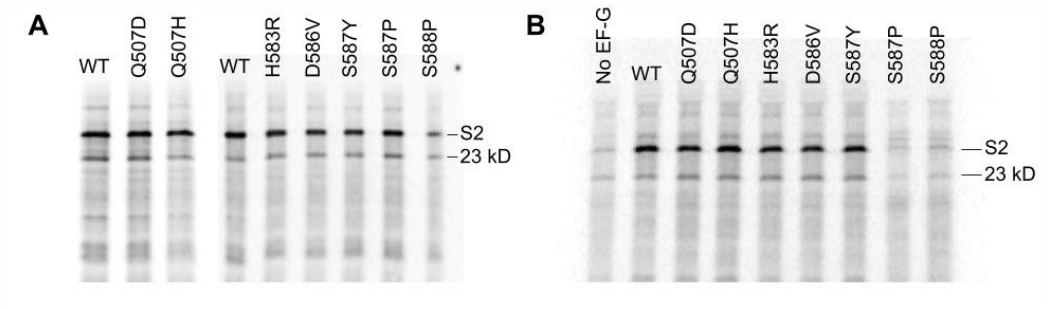

Figure 4. In vitro translation of a full-length protein by domain IV mutant EF-Gs. A mRNA coding for ribosomal protein S2 was translated in vitro by 70S ribosomes in an E. coli system (Ali et al. 2006) using mutant forms of EF-G with S100 extract (A) containing or (B) lacking endogenous wild-type EF-G. (WT) Addition of wild-type EF-G; (No EF-G) wild-type EF-G not added; (S2) position of full-length protein S2; (23 kD) a translation product likely made from a 3'- truncated mRNA. All mutant EF-Gs except S587P and S588P are capable of catalyzing **s**ynthesis of full-length protein.

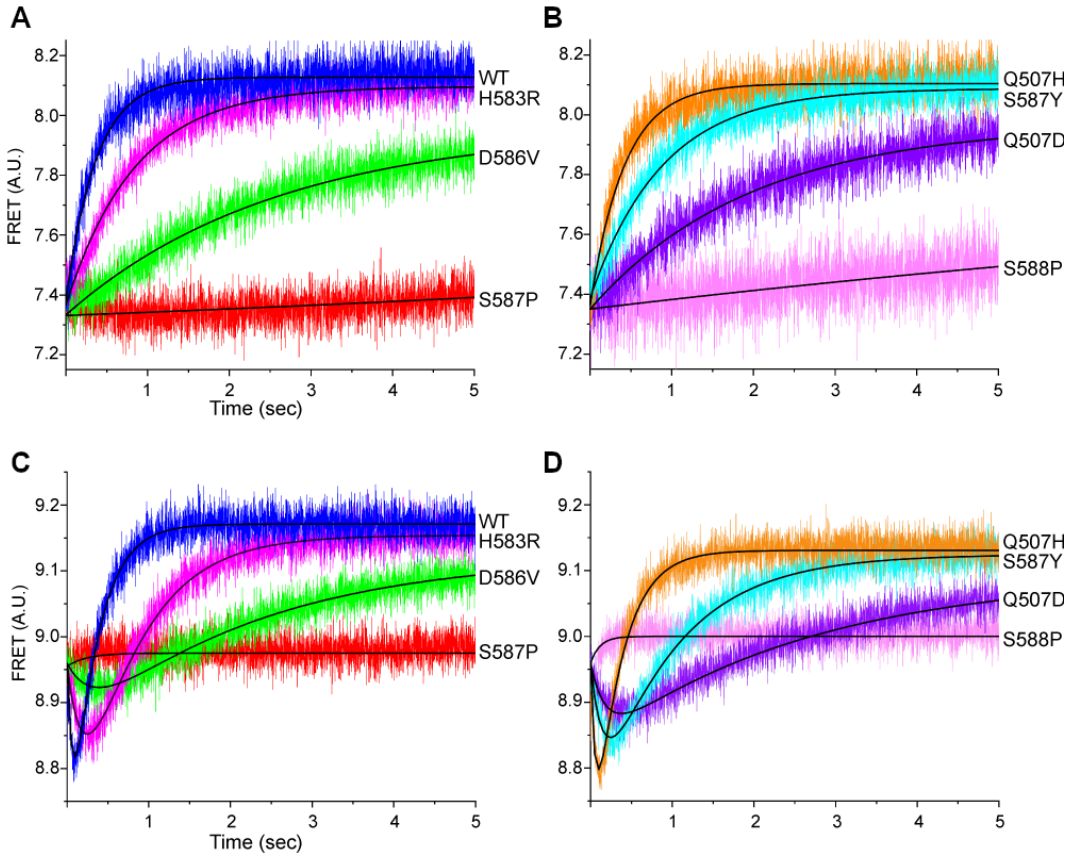

Figure 5. Domain IV mutations affect rates of intersubunit and 30S head rotation. (A,B) Reverse intersubunit rotation during translocation was measured by FRET using doubly labeled 70S ribosomes containing a Cy3 donor on 50S protein L9 and a Cy5 acceptor on 30S protein S6 in a stopped-flow fluorimeter (Ermolenko and Noller 2011). Data were fit to single-exponential curves. (C,D) Forward and reverse rotation of the head domain of the 30S subunit during translocation was measured by FRET using 70S ribosomes formed from doubly labeled 30S subunits containing an Alexa488 donor on protein S12 in the 30S body domain and an Alexa568 acceptor on protein S19 in the 30S domain (Guo and Noller 2012), in a stopped-flow fluorimeter. Data were fit to double-exponential curves corresponding to initial forward head rotation (downward curves) followed by reverse head rotation (upward curves). (WT) Wild-type EF-G.

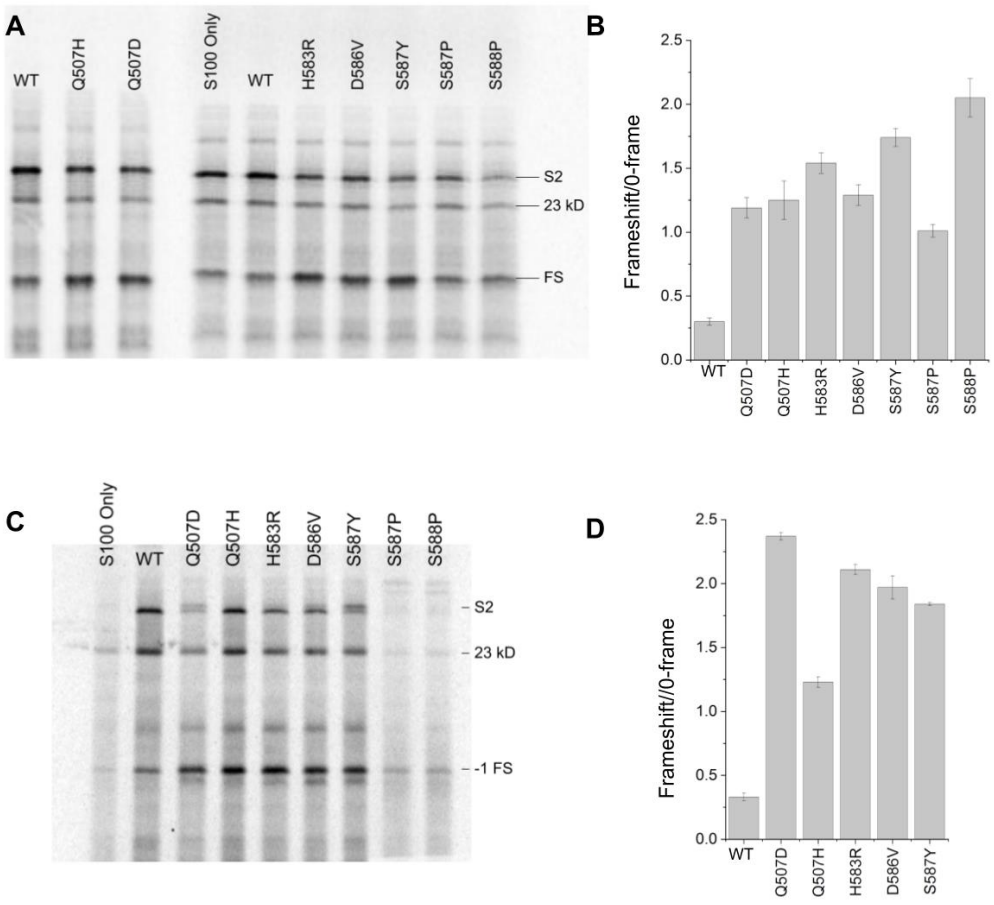

Figure 6. Stimulation of −1 frameshifting by domain IV mutants. SDS gels showing in vitro translation of [35S]-labeled ribosomal protein S2 from a mRNA containing a “slippery sequence” with domain IV mutants using S100 extract (A) containing wild-type EF-G and (C) lacking wild-type EFG. (B,D) Histograms showing frameshifting efficiencies for A and C, respectively, plotted as the ratio of frameshifted product to 0-frame product. (S2) Full-length S2; (23 kDa) carboxy-terminal truncated S2 product; (FS) −1 frameshift product; (WT) wild-type EF-G. Error bars represent standard errors of the mean.

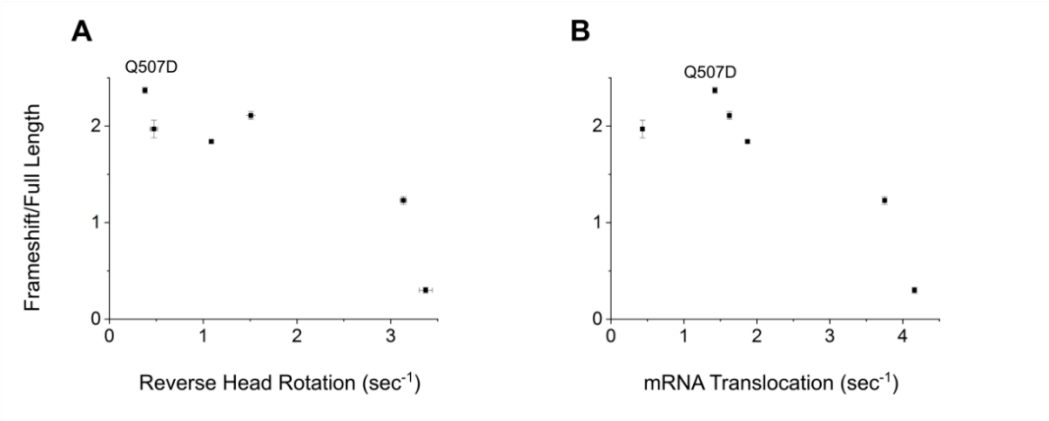

Figure 7. Rates of translocation events versus frameshifting efficiencies. The rates of (A) reverse 30S head rotation and (B) mRNA quenching are roughly correlated inversely with frameshifting efficiencies. The outlier in (B) Q507D, whose rate of reverse head rotation is unusually slow compared to its rate of mRNA quenching (Table 1), suggests that reverse head rotation is more closely correlated with frameshifting than intersubunit rotation or mRNA quenching. Error bars indicate standard errors of the mean.

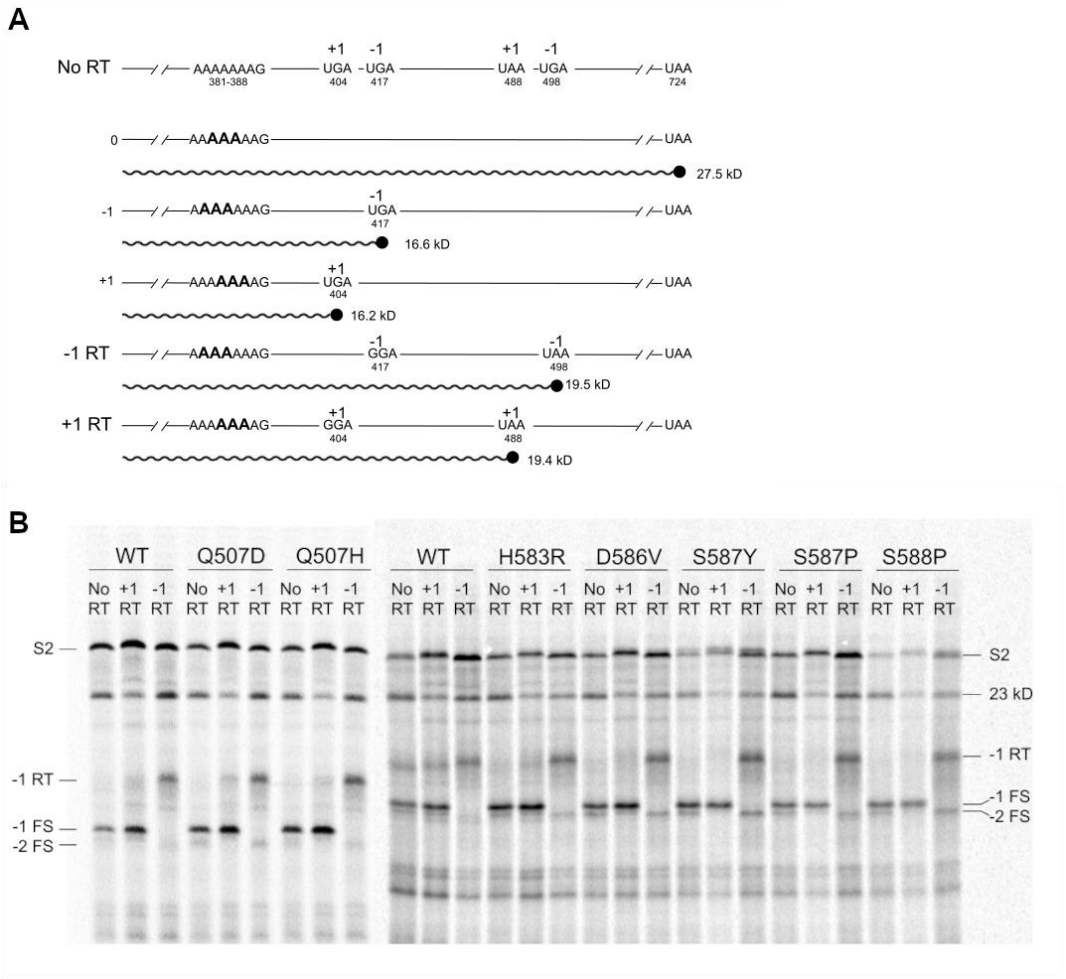

Figure 8. **Domain IV mutants stimulate frameshifting into the −1 reading frame.** (A) Schematic showing (no RT) the S2 mRNA containing a slippery sequence at positions 381–388 showing the positions of +1 and −1 out-of-frame stop codons. (−1 RT) A mRNA designed to create read-through of the −1 frame UGA stop codon at position 417, which was replaced by a GGA sense codon. (+1 RT) A +1 read-through mRNA in which the out-of-frame +1 UGA stop codon at position 404 was replaced by a GGA sense codon. Frameshifting events can be assigned to the −1 or +1 reading frames according to whether a frameshift product of increased size appears when translating the −1 RT or +1 RT mRNA. (B) SDS gel showing results of translation through the +1 read-through (+1 RT), −1 read-through (−1 RT), and no-read-through (No RT) mRNAs. Products indicated are (S2), full-length S2 protein; (23 kD) 23

kD carboxy-terminal truncated EF-G product; (−1 RT) read-through product in the −1 frame; (−1 FS) frameshift product in the −1 frame; (−2 FS) product of 2 −1 frameshifting events. Appearance of the 16.6 kDa product with the −1 RT mRNA confirms that the 19.5 kDa band is indeed the product of −1 frameshifting.

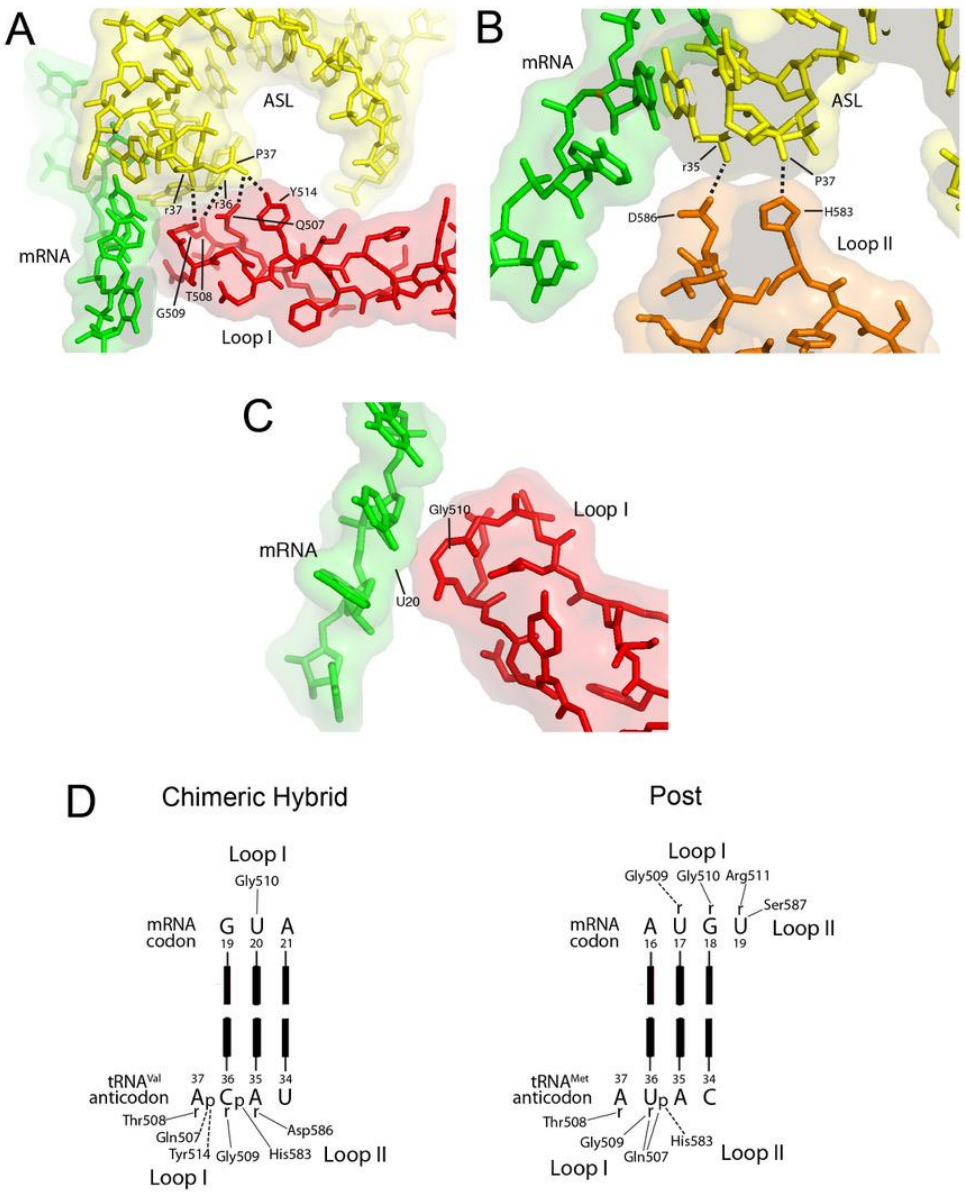

Figure 9. Contacts between the tip of domain IV of EF-G and the RNA backbones of the codon–anticodon duplex. The crystal structure of a trapped chimeric hybrid-state

translocation intermediate (Zhou et al. 2014) shows that (A) Gln507 and Tyr514 in loop I (red) form H-bonds with phosphate 37 in the anticodon loop; Gly 509 and Thr 508 are within Van der Waals contact distance of riboses 36 and 37. (B) His583 and Asp586 at the tip of loop II form H-bonds with the 2′ -OH of ribose 35 and phosphate 37 in the anticodon loop. (C) Gly510 in loop I makes the sole Van der Waals contact between domain IV and the mRNA backbone, at U20 of the GUA Val codon. (D) Schematic representations of domain IV interactions with the codon–anticodon duplex in the chimeric hybrid state complex (Zhou et al. 2014) and posttranslocation complex (Gao et al. 2009). Mutations at Gln507, His583, and Asp586 were found to confer severe frameshifting and translocation phenotypes (Tables 1, 2). In both crystal structures, all contacts with domain IV are with ribose and phosphate backbone moieties of the tRNA and mRNA. Contacts observed in the two structures are overlapping, but not identical; interactions with Thr508, Gly509, His583 are preserved between the two translocational states. Most of the contacts are with the backbone of the anticodon loop, centered around nucleotides that interact with the first and second codon positions. Note that both crystal structures were obtained from T. thermophilus, although we use E. coli numbering here; all residues are identical between the two species, except for Thr508, which is replaced by Ser508 in E. coli EF-G. Supplemental Materials

SUPPLEMENTAL MATERIALS

Table SI. Fraction of full-length S2 in translation products.†

	WT	Q507D	Q507H	H583R	D586V	S587Y	S587P	S588P
S100 (+EF-G)	0.75± 0.01	0.75± 0.01	0.75± 0.02	0.76± 0.02	0.74± 0.02	0.71± 0.05	0.67± 0.04	0.63± 0.05
S100 (-EF-G)	0.55± 0.02	0.37± 0.02	0.50± 0.01	0.46± 0.02	0.45± 0.03	0.47± 0.07	0.43± 0.03	0.37± 0.05

†Fraction of full-length S2 of combined (full-length S2 + 23 kD C-terminal truncated) product.

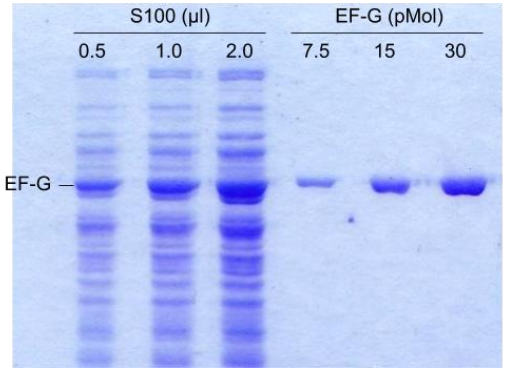

Figure S1. Levels of EF-G in S100 extract. The concentration of EF-G present in the S100 extract was estimated from the Coomassie Blue staining intensity of the EF-G SDS gel bands relative to those of standard amounts of purified EF-G.

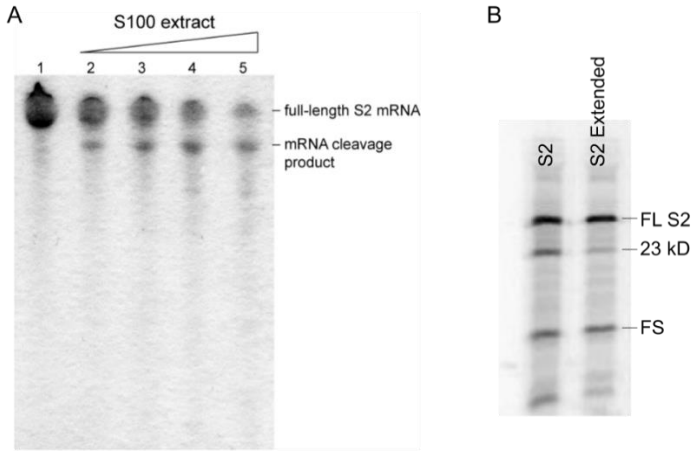

Figure S2. (A) Cleavage of S2 mRNA by incubation with S100 extract. Incubation of S2 mRNA with S100 cell extract results in a cleaved mRNA product. 10 pmol of S2 mRNA (lane 1) was incubated with an increasing amount of S100 extract (lanes 2-5; 0.4, 0.8, 1.7, and 3.3 □l of S100 per pmol of mRNA respectively) for 30 minutes at 37°C in buffer containing 25 mM Tris-Cl (pH 7.5), 60 mM NH_4Cl, 10 mM $MgCl_2$ and 1 mM DTT. Reactions were phenol-

chloroform extracted, ethanol precipitated, and run on a 4% polyacrylamide gel and stained with methylene blue. **(B) Extension of the 3' end of S2 mRNA reduces the amount of 23 kD product.** The level of frameshift product **(FS)** is unaffected by extension of the 3' end of the mRNA by ~100 nucleotides, although the 23 kD product is greatly reduced, consistent with the likelihood that this product is the result of 3' truncation of the mRNA during incubation with S100 extract.

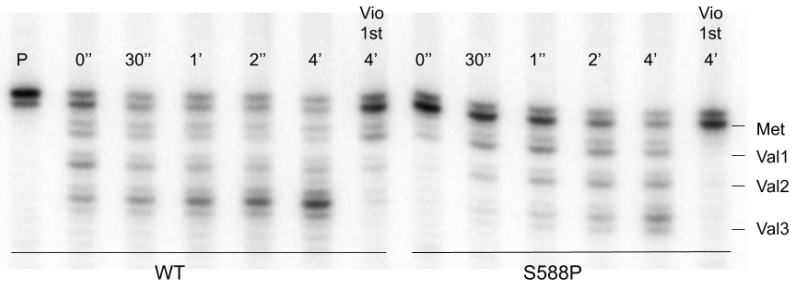

Figure S3. Time course of translocation with S589P. Translocation at room temperature was monitored by toeprinting and terminated by addition of viomycin to a final concentration of 1 mM at the indicated time points, ranging from 0" (0 sec), which was as fast as could be mixed by hand, to 4' (4 min). **(Vio 1st),** Addition of viomycin to the reaction prior to addition of EF-G.

REFERENCES

Ali, I.K., Lancaster, L., Feinberg, J., Joseph, S., and Noller, H.F. (2006). Deletion of a conserved, central ribosomal intersubunit RNA bridge. Mol Cell *23*, 865-874.

Atkins, J.F., Loughran, G., Bhatt, P.R., Firth, A.E., and Baranov, P.V. (2016). Ribosomal frameshifting and transcriptional slippage: From genetic steganography and cryptography to adventitious use. Nucleic Acids Res *44*, 7007-7078.

Brilot, A.F., Korostelev, A.A., Ermolenko, D.N., and Grigorieff, N. (2013). Structure of the ribosome with elongation factor G trapped in the pretranslocation state. Proc Natl Acad Sci U S A *110*, 20994-20999.

Cadwell, R.C., and Joyce, G.F. (1992). Randomization of genes by PCR mutagenesis. PCR Methods Appl *2*, 28-33.

Caliskan, N., Katunin, V.I., Belardinelli, R., Peske, F., and Rodnina, M.V. (2014). Programmed -1 frameshifting by kinetic partitioning during impeded translocation. Cell *157*, 1619-1631.

Chen, J., Petrov, A., Johansson, M., Tsai, A., O'Leary, S.E., and Puglisi, J.D. (2014). Dynamic pathways of -1 translational frameshifting. Nature *512*, 328-332.

Choi, J., O'Loughlin, S., Atkins, J.F., and Puglisi, J.D. (2020). The energy landscape of -1 ribosomal frameshifting. Sci Adv *6*, eaax6969.

Cornish, P.V., Ermolenko, D.N., Noller, H.F., and Ha, T. (2008). Spontaneous intersubunit rotation in single ribosomes. Mol Cell *30*, 578-588.

Culver, G.M., and Noller, H.F. (1999). Efficient reconstitution of functional Escherichia coli 30S ribosomal subunits from a complete set of recombinant small subunit ribosomal proteins. Rna *5*, 832-843.

Cunha, C.E., Belardinelli, R., Peske, F., Holtkamp, W., Wintermeyer, W., and Rodnina, M.V. (2013). Dual use of GTP hydrolysis by elongation factor G on the ribosome. Translation (Austin) *1*, e24315.

Dahlfors, A.A., and Kurland, C.G. (1990). Stoichiometry of elongation factor G function in translation. J Mol Biol *216*, 311-314.

Drummond, D.A., and Wilke, C.O. (2008). Mistranslation-induced protein misfolding as a dominant constraint on coding-sequence evolution. Cell *134*, 341-352.

Ermolenko, D.N., Majumdar, Z.K., Hickerson, R.P., Spiegel, P.C., Clegg, R.M., and Noller, H.F. (2007). Observation of intersubunit movement of the ribosome in solution using FRET. J Mol Biol *370*, 530-540.

Ermolenko, D.N., and Noller, H.F. (2011). mRNA translocation occurs during the second step of ribosomal intersubunit rotation. Nat Struct Mol Biol *18*, 457-462.

Farabaugh, P.J. (1996). Programmed translational frameshifting. Annu Rev Genet *30*, 507-528.

Fredrick, K., and Noller, H.F. (2003). Catalysis of ribosomal translocation by sparsomycin. Science *300*, 1159-1162.

Gao, Y.G., Selmer, M., Dunham, C.M., Weixlbaumer, A., Kelley, A.C., and Ramakrishnan, V. (2009). The structure of the ribosome with elongation factor G trapped in the posttranslocational state. Science *326*, 694-699.

Guo, Z., and Noller, H.F. (2012). Rotation of the head of the 30S ribosomal subunit during mRNA translocation. Proc Natl Acad Sci U S A *109*, 20391-20394.

Guzman, L.M., Belin, D., Carson, M.J., and Beckwith, J. (1995). Tight regulation, modulation, and high-level expression by vectors containing the arabinose PBAD promoter. J Bacteriol *177*, 4121-4130.

Hartz, D., McPheeters, D.S., Traut, R., and Gold, L. (1988). Extension inhibition analysis of translation initiation complexes. Methods Enzymol *164*, 419-425.

Hickerson, R., Majumdar, Z.K., Baucom, A., Clegg, R.M., and Noller, H.F. (2005). Measurement of internal movements within the 30 S ribosomal subunit using Forster resonance energy transfer. J Mol Biol *354*, 459-472.

Holtkamp, W., Cunha, C.E., Peske, F., Konevega, A.L., Wintermeyer, W., and Rodnina, M.V. (2014). GTP hydrolysis by EF-G synchronizes tRNA movement on small and large ribosomal subunits. EMBO J *33*, 1073-1085.

Hou, Y., Yaskowiak, E.S., and March, P.E. (1994). Carboxyl-terminal amino acid residues in elongation factor G essential for ribosome association and translocation. J Bacteriol *176*, 7038-7044.

Khade, P.K., and Joseph, S. (2011). Messenger RNA interactions in the decoding center control the rate of translocation. Nat Struct Mol Biol *18*, 1300-1302.

Kim, H.K., and Tinoco, I., Jr. (2017). EF-G catalyzed translocation dynamics in the presence of ribosomal frameshifting stimulatory signals. Nucleic Acids Res *45*, 2865-2874.

Kunkel, T.A. (1985). Rapid and efficient site-specific mutagenesis without phenotypic selection. Proc Natl Acad Sci USA *82*, 488-492.

Kurland, C.G. (1992). Translational accuracy and the fitness of bacteria. Annu Rev Genet *26*, 29-50.

Lancaster, L., Kiel, M., Kaji, A., and Noller, H. (2002). Orientation of Ribosome Recycling Factor in the Ribosome from Directed Hydroxyl Radical Probing. Cell *111*, 129-140.

Lancaster, L., and Noller, H.F. (2005). Involvement of 16S rRNA nucleotides G1338 and A1339 in discrimination of initiator tRNA. Mol Cell *20*, 623-632.

Larsen, B., Gesteland, R.F., and Atkins, J.F. (1997). Structural probing and mutagenic analysis of the stem-loop required for Escherichia coli dnaX ribosomal frameshifting: programmed efficiency of 50%. J Mol Biol *271*, 47-60.

Larsen, B., Wills, N.M., Gesteland, R.F., and Atkins, J.F. (1994). rRNA-mRNA base pairing stimulates a programmed -1 ribosomal frameshift. J Bacteriol *176*, 6842-6851.

Lieberman, K.R., Firpo, M.A., Herr, A.J., Nguyenle, T., Atkins, J.F., Gesteland, R.F., and Noller, H.F. (2000). The 23S rRNA environment of ribosomal protein L9 in the 50S ribosomal subunit. J Mol Biol *297*, 1129-1143.

Link, A.J., Phillips, D., and Church, G.M. (1997). Methods for generating precise deletions and insertions in the genome of wild-type Escherichia coli: application to open reading frame characterization. J Bacteriol *179*, 6228-6237.

Liu, G., Song, G., Zhang, D., Li, Z., Lyu, Z., Dong, J., Achenbach, J., Gong, W., Zhao, X.S., Nierhaus, K.H.*, et al.* (2014). EF-G catalyzes tRNA translocation by disrupting interactions between decoding center and codon-anticodon duplex. Nat Struct Mol Biol *21*, 817-824.

Martemyanov, K.A., and Gudkov, A.T. (1999). Domain IV of elongation factor G from Thermus thermophilus is strictly required for translocation. FEBS Lett *452*, 155-159.

Moazed, D., and Noller, H.F. (1989). Interaction of tRNA with 23S rRNA in the ribosomal A, P, and E sites. Cell *57*, 585-597.

Munro, J.B., Altman, R.B., Tung, C.S., Cate, J.H., Sanbonmatsu, K.Y., and Blanchard, S.C. (2010). Spontaneous formation of the unlocked state of the ribosome is a multistep process. Proc Natl Acad Sci U S A *107*, 709-714.

O' Connor, M., Thomas, C.L., Zimmermann, R.A., and Dahlberg, A.E. (1997). Decoding fidelity at the ribosomal A and P sites: influence of mutations in three different regions of the decoding domain in 16S rRNA. Nucl Acids Res *25*, 1185-1193.

O'Connor, M., Goringer, H.U., and Dahlberg, A.E. (1992). A ribosomal ambiguity mutation in the 530 loop of E. coli 16S rRNA. Nucl Acids Res *20*, 4221-4227.

Peng, B.Z., Bock, L.V., Belardinelli, R., Peske, F., Grubmuller, H., and Rodnina, M.V. (2019). Active role of elongation factor G in maintaining the mRNA reading frame during translation. Sci Adv *5*, eaax8030.

Peske, F., Savelsbergh, A., Katunin, V.I., Rodnina, M.V., and Wintermeyer, W. (2004). Conformational changes of the small ribosomal subunit during elongation factor G-dependent tRNA-mRNA translocation. J Mol Biol *343*, 1183-1194.

Ramrath, D.J., Lancaster, L., Sprink, T., Mielke, T., Loerke, J., Noller, H.F., and Spahn, C.M. (2013). Visualization of two transfer RNAs trapped in transit during elongation factor G-mediated translocation. Proc Natl Acad Sci U S A *110*, 20964-20969.

Rodnina, M.V., Savelsbergh, A., Katunin, V.I., and Wintermeyer, W. (1997). Hydrolysis of GTP by elongation factor G drives tRNA movement on the ribosome. Nature *385*, 37-41.

Salsi, E., Farah, E., Dann, J., and Ermolenko, D.N. (2014a). Following movement of domain IV of elongation factor G during ribosomal translocation. Proc Natl Acad Sci U S A *111*, 15060-15065.

Salsi, E., Farah, E., Netter, Z., Dann, J., and Ermolenko, D.N. (2014b). Movement of elongation factor G between compact and extended conformations. J Mol Biol *427*, 454-467.

Santer, U.V., Cekleniak, J., Kansil, S., Santer, M., O'Connor, M., and Dahlberg, A.E. (1995). A mutation at the universally conserved position 529 in Escherichia coli 16S rRNA creates a functional but highly error prone ribosome. RNA *1*, 89-94.

Savelsbergh, A., Matassova, N.B., Rodnina, M.V., and Wintermeyer, W. (2000). Role of domains 4 and 5 in elongation factor G functions on the ribosome. J Mol Biol *300*, 951-961.

Schurer, H., Lang, K., Schuster, J., and Morl, M. (2002). A universal method to produce in vitro transcripts with homogeneous 3' ends. Nucleic Acids Res *30*, e56.

Shi, X., Chiu, K., Ghosh, S., and Joseph, S. (2009). Bases in 16S rRNA important for subunit association, tRNA binding, and translocation. Biochemistry *48*, 6772-6782.

Studer, S.M., Feinberg, J.S., and Joseph, S. (2003). Rapid kinetic analysis of EF-G-dependent mRNA translocation in the ribosome. J Mol Biol *327*, 369-381.

Tinoco, I., Jr., Kim, H.K., and Yan, S. (2013). Frameshifting dynamics. Biopolymers *99*, 1147-1166.

Tnalina, G., Belitsina, N.V., and Spirin, A.S. (1982). [Template-free polypeptide synthesis from aminoacyl-tRNA in Escherichia coli ribosomes]. Dokl Akad Nauk SSSR *266*, 741-745.

Traub, P., Mizushima, S., Lowry, C.V., and Nomura, M. (1981). Reconstitution of ribosomes from subribosomal components. In RNA and protein synthesis, K. Moldave, ed. (New York: Academic Press), p. 521.

Tsuchihashi, Z., and Brown, P.O. (1992). Sequence requirements for efficient translational frameshifting in the Escherichia coli dnaX gene and the role of an unstable interaction between tRNA(Lys) and an AAG lysine codon. Genes Dev *6*, 511-519.

Tsuchihashi, Z., and Kornberg, A. (1990). Translational frameshifting generates the gamma subunit of DNA polymerase III holoenzyme. Proc Natl Acad Sci U S A *87*, 2516-2520.

Varshney, U., Lee, C.P., and RajBhandary, U.L. (1991). Direct analysis of aminoacylation levels of tRNAs in vivo. Application to studying recognition of Escherichia coli initiator tRNA mutants by glutaminyl-tRNA synthetase. J Biol Chem *266*, 24712-24718.

Walker, S.C., Avis, J.M., and Conn, G.L. (2003). General plasmids for producing RNA in vitro transcripts with homogeneous ends. Nucleic Acids Res *31*, e82.

Yan, S., Wen, J.D., Bustamante, C., and Tinoco, I., Jr. (2015). Ribosome excursions during mRNA translocation mediate broad branching of frameshift pathways. Cell *160*, 870-881.

Yusupova, G.Z., Belitsina, N.V., and Spirin, A.S. (1986). Template-free ribosomal synthesis of polypeptides from aminoacyl-tRNA. Polyphenylalanine synthesis from phenylalanyl-tRNALys. FEBS Lett *206*, 142-146.

Zhou, J., Lancaster, L., Donohue, J.P., and Noller, H.F. (2014). How the ribosome hands the A-site tRNA to the P site during EF-G-catalyzed translocation. Science *345*, 1188-1191.

Zhou, J., Lancaster, L., Donohue, J.P., and Noller, H.F. (2019). Spontaneous ribosomal translocation of mRNA and tRNAs into a chimeric hybrid state. Proc Natl Acad Sci U S A *116*, 7813-7818.

Chapter 3. Implications of nucleotides near the 3’ end of 16S rRNA in guarding the translational reading frame

ABSTRACT

Loss of the translational reading frame leads to misincorporation and premature termination, which can have lethal consequences. Based on structural evidence that A1503 of 16S rRNA intercalates between specific mRNA bases, we tested the possibility that it plays a role in maintenance of the reading frame by constructing ribosomes with an abasic nucleotide at position 1503. This was done by specific cleavage of 16S rRNA at position 1493 using the colicin E3 endonuclease and replacing the resulting 3'-terminal 49mer fragment with a synthetic oligonucleotide containing the abasic site using a novel splinted RNA ligation method. Ribosomes reconstituted from the abasic 1503 16S rRNA were highly active in protein synthesis but showed elevated levels of spontaneous frameshifting into the -1 reading frame. We then asked whether the residual frameshifting persisting in control ribosomes containing an intact A1503 is due to the absence of the N6-dimethyladenosine modifications at positions 1518 and 1519. Indeed, this frameshifting was rescued by site-specific methylation in vitro by the ksgA methylase. These findings thus implicate two different sites near the 3' end of 16S rRNA in maintenance of the translational reading frame, providing yet another example of a functional role for ribosomal RNA in protein synthesis.

INTRODUCTION

Accurate maintenance of the translational reading frame is a crucial cellular function; shifting to the +1 or –1 frame leads to miscoding and premature termination of the polypeptide chain (Kurland, 1992), which can have lethal consequences. During translocation of mRNA and tRNA through the ribosome, tRNA movement is coupled to rotation of the head domain of the small ribosomal subunit (Ramrath et al, 2013; Zhou et al, 2013; Zhou et al, 2014). However, mRNA movement is presumably passive, dependent on its connections to tRNA through the inherently weak base pairing between codon and anticodon. During

translocation, these codon-anticodon duplexes must leave the stabilizing environments of the ribosomal A and P sites and thus become vulnerable to frameshifting. During movement from the A site to the P site, codon-anticodon pairing is stabilized by contact between the tip of domain 4 of elongation factor EF-G with the minor groove surface of the duplex (Lancaster and Noller, 2005; Ramrath et al, 2013; Zhou et al, 2014; Peng et al, 2019). Accordingly, in the absence of EF-G, spontaneous translocation leads to a stalled intermediate state showing a shift to the –1 reading frame (Zhou et al, 2019). However, little is known about the potential contributions of the ribosome itself to maintenance of the reading frame during translocation. Here, we present evidence for the participation of 16S ribosomal RNA in this function.

The crystal structure of a ribosome translocation complex trapped in an intermediate chimeric-hybrid state (Zhou et al, 2013) revealed the unexpected intercalation of 16S rRNA base A1503 between bases –1 and –2 of the mRNA (where the first base of the P-site codon is defined as position +1; Fig. 1). Inspection of subsequently published high-resolution structures shows that this phenomenon is widespread among certain translocation complexes, as described below. This observation raised the possibility that intercalation of A1503 might serve the purpose of preventing uncoupled movement of the mRNA and consequent shifting of the translational reading frame.

Since all four bases are capable of intercalation, we reasoned that base substitution mutations of A1503 would present an inadequate test of this possibility, we sought to eliminate intercalation of A1503 entirely by creating an abasic nucleotide at this position. Because of the infeasibility of chemical synthesis of full-length 16S rRNA, we introduced the abasic nucleotide by replacing the 3′-terminal 49-mer fragment (containing nucleotides 1494–1542) obtained by cleavage with the colicin E3 endonuclease (Bowman et al, 1971) with a synthetic 49-mer, using a novel splinted RNA ligation method. The resulting semi-synthetic 16S rRNA was then reconstituted *in vitro* with ribosomal proteins and natural 50S subunits to produce 70S ribosomes. Using an *in vitro* assay, we tested the abasic ribosomes for activity

in protein synthesis and for their ability to maintain the translational reading frame. Since these ribosomes also lacked the universally conserved N^6,N^6-dimethyladenosine modifications at positions 1518 and 1519 we also tested their effect on frameshifting. We found that both the abasic ribosomes and non-methylated ribosomes showed elevated levels of frameshifting, implicating two different sites near the 3′ end of 16S rRNA in maintenance of the translational reading frame.

RESULTS

Structural evidence for intercalation of A1503

Intercalation of A1503 of 16S rRNA was first reported for the crystal structure of a ribosomal translocation intermediate complex trapped in the chimeric-hybrid state (Zhou et al, 2013). A1503 was intercalated between bases –1 and –2 of the mRNA (where the first base of the P-site codon is defined as +1) (Figure 1). We asked whether this phenomenon was merely anecdotal, or more widespread among published x-ray and cryo-EM structures of ribosome complexes. We screened 672 deposited structures by calculating the distances between the respective centroids of the A1503 base and proximal mRNA bases, followed by visual inspection to identify 209 structures in which the relative positions of A1503 and nearby mRNA bases could be placed with reasonable confidence. This procedure identified 73 structures in which A1503 was intercalated, and an additional 89 where it was stacked on a single mRNA base; in 47 structures, A1503 was retracted out of range of intercalation or stacking.

We then asked whether intercalation of A1503 might be correlated with specific conformational states of the ribosome, assigned by their intersubunit and 30S head rotation values into classical (non-rotated), hybrid (~6°–10° intersubunit rotation) or chimeric hybrid (~15°–21° 30S head rotation) states (Mohan et al, 2014). Measurement of the rotation angles of the 30S head and body domains for all of the above structures shows that those where

A1503 is intercalated form two clusters, corresponding to the classical and chimeric-hybrid states (Figure 2). In all chimeric-hybrid structures, A1503 is intercalated. No intercalation was found in any hybrid-state complex. Examples of intercalation in chimeric-hybrid and classical state structures are shown in Figures 3 and 4.

In chimeric-hybrid state complexes, A1503 intercalates between bases –1 and –2, and in the classical-state structures between bases –3 and –4. This difference between the respective sites of intercalation can be explained by a 2-nucleotide shift of the mRNA relative to the 30S body domain in the chimeric-hybrid state (Zhou et al, 2013; Zhou et al, 2014). In the classical-state complexes, 55 show intercalation, 89 show stacking on a single mRNA base and 40 are retracted. The incidence of intercalation of A1503 is summarized in Table I; examples are shown in Figure 4.

Constructing ribosomes with an abasic nucleotide at position 1503 of 16S rRNA

Based on the above analysis and the previous proposal that intercalation of A1503 might act to prevent slippage of the translational reading frame during translocation of the mRNA (Zhou et al, 2013), we sought to test this possibility by eliminating its intercalation. Since all four bases are capable of intercalation, we devised a scheme to abolish intercalation by creating ribosomes with an abasic nucleotide at position 1503 of 16S rRNA. This was done by replacing the 3′ 49-nucleotide section of the 1542-nucleotide 16S rRNA with a synthetic 49-mer containing an abasic nucleotide at position 1503. We took advantage of the ability of the colicin E3 endonuclease to make a single specific cut at position 1493, and ligated the resulting large 5′ 1493-mer fragment to a synthetic abasic 49-mer. This was accomplished by splinted ligation (Moore and Sharp, 1992; Moore and Query, 2000) using a novel strategy employing a tailed DNA splint which permits removal of the splint under mild conditions that preserve the native structure of the rRNA (Methods; Smart et al., unpublished). Abasic 70S ribosomes were then constructed from the semi-synthetic 16S

rRNA by *in vitro* reconstitution with total 30S ribosomal proteins followed by association with natural 50S subunits (Figure 5; Materials and methods).

Activity and frameshifting levels of abasic ribosomes

We tested the activity of the reconstituted ribosomes in an *in vitro* assay that measures synthesis of a full-length 27 kD protein (Lancaster and Noller, 2005). Ribosomes reconstituted from natural 16S rRNA were 83% active compared to natural tight-couple ribosomes in translating a full-length protein; those constructed from ligated semi-synthetic wild-type 16S rRNA were 76% active, while ribosomes reconstituted from semi-synthetic 16S rRNA containing an abasic nucleotide at position 1503 were 71% active (Figure 6). We conclude that a base at position 1503 is not essential for protein synthesis activity *per se*, and that ribosomes reconstituted using 16S rRNA constructed by ligation to the synthetic 49mer have only modestly reduced activity relative to those reconstituted from natural 16S rRNA. Ribosomes reconstituted from colicin-cut 16S rRNA were inactive in protein synthesis.

To measure frameshifting, we used an mRNA encoding ribosomal protein S2 that was previously designed to include a programmed frameshifting sequence based on the dnaX gene of *E. coli* (Lancaster and Noller, 2005) (Supplementary Figure S1). This sequence consisted of an internal Shine-Dalgarno-like sequence and a slippery A AAA AAG heptamer located 10 nucleotides downstream (Tsuchihashi and Kornberg, 1990; Flower and McHenry, 1990; Blinkowa and Walker, 1990). Frameshifting into the -1 reading frame was measured by the magnitude of the [^{35}S]-labeled 16kD premature termination product caused by the introduced programmed frameshifting sequence (Lancaster and Noller, 2005) (Figure 7A). Ribosomes reconstituted from natural 16S rRNA or mock-ligation procedures showed frameshifting levels similar to that of natural 70S ribosomes. However, semi-synthetic ribosomes containing an abasic nucleotide at position 1503 had a ratio of –1 to 0-frame product (–1/0 frame ratio) double that of wild-type ribosomes. Interestingly, ribosomes

reconstituted from 16S rRNA constructed from ligation with a wild-type synthetic 49mer showed a small but significant increase in –1 frameshifting ('wt lig', Figure 7A; Table 2).

The wild-type dnaX-programmed frameshifting sequence includes a stimulatory hairpin element located 6 nucleotides downstream from the slippery heptamer (Tsuchihashi and Kornberg, 1990), which is absent in our construct. We simulated the effect of this downstream secondary structure by hybridizing a complementary 20mer DNA oligonucleotide to a sequence 6 residues downstream from the mRNA slippery sequence (Kim and Tinoco, 2017). As expected, the downstream structure stimulated the levels of frameshifting for all ribosome constructs, and the abasic ribosomes showed frameshifting levels about double that of wild-type (Figure 7B). Again, the semi-synthetic wild-type ribosomes had a modestly elevated level of frameshifting relative to that reconstituted from natural 16S rRNA.

Dimethylation of A1518 and A1519 confers a modest effect on maintaining the translational reading frame

As noted above, a modest but reproducible increase in frameshifting was observed for semi-synthetic ribosomes constructed with the wild-type synthetic 49mer RNA (Figure 7). In natural 16S rRNA, this 49mer sequence contains the modified base N^6,N^6-dimethyladenine at positions 1518 and 1519, representing two of the most highly conserved post-transcriptional modifications in ribosomal RNA (McCloskey and Rozenski, 2005; Woese et al, 1975). We asked whether the absence of these modifications in the synthetic 49mer might contribute to the observed elevated level of frameshifting for the semi-synthetic wild-type ribosomes. To test this possibility, ribosomes with non-methylated 16S rRNA at positions A1518 and A1519 were purified from ribosomes from a *ksgA* deletion strain (ΔKsgA) (Connolly et al, 2008), which lacks the dimethyl-A methylase. The absence of modifications at positions 1518 and 1519 was confirmed by primer extension of the 16S rRNA (Figure 8A).

Using the same assay as in Figure 7A, ribosomes isolated from the *ksgA* strain showed an increase in -1 frameshifting equivalent to that observed for the semi-synthetic ribosomes containing an intact A1503 (Figure 8B). Upon treatment of these ribosomes *in vitro* with purified KsgA methyltransferase, the level of frameshifting was rescued to a level that was indistinguishable from that of natural tight-couple ribosomes (Figure 8B). We conclude that the conserved methylations of A1518 and A1519 confer a modest but significant effect on preserving the translational reading frame. Thus, at least two elements in the 3′ 49 nucleotides of 16S rRNA contribute to reading frame accuracy.

DISCUSSION

Shifting of the translational reading frame generally leads to premature termination of an error-riddled polypeptide that is often toxic to the cell (Kurland, 1992; Wills and Atkins, 2006; Drummond and Wilke, 2008; Stochmanski et al, 2012). Accordingly, it is not surprising that frameshifting error rates are typically about two orders of magnitude smaller than that for miscoding (Kurland et al, 1992). Our understanding of how the translational machinery maintains the reading frame at such high accuracy in spite of the relative weakness of codon-anticodon base pairing (Labuda et al, 1982; Turner, 1996) is still incomplete. Recent studies have implicated elongation factor EF-G in this process. During movement of the codon-anticodon duplex from the A site to the P site of the small subunit, pairing is no longer stabilized by the structure of the A site; during this vulnerable moment, structural studies have shown that the tip of domain IV of EF-G remains in contact with the minor groove of the duplex, apparently replacing the missing A-site contacts (Ramrath et al, 2013; Zhou et al, 2013). Mutation of residues in the tip of domain IV causes frameshifting into –1 reading frame (Lancaster and Noller, 2005; Peng et al, 2019). Here, we ask whether the ribosome itself, and specifically its 16S ribosomal RNA, might play a role in maintaining the reading frame. This possibility was suggested by our previous structural observation that the highly conserved A1503 was intercalated between bases of the mRNA (Zhou et al, 2013).

Our analysis of published structures of ribosome complexes shows that intercalation of the conserved A1503 into the mRNA is indeed widespread, and specific to certain conformational states of the ribosome (Figure 2). In some cases, A1503 stacks against one of the two mRNA bases at the intercalation site instead of full intercalation. A1503 intercalates between positions –1 and –2 in all examples of chimeric hybrid-state complexes, and between positions –3 and –4 in many classical-state structures (Table 1). We also note that intercalation or stacking of the conserved C1397 on the 5′ side of downstream base +10 in chimeric-hybrid complexes (or on +8 in classical-state complexes) is strongly correlated with intercalation of A1503. Both bases project from the tips of conserved, compact, tertiary hairpin-like structures (Figure 4). Moreover, the two hairpins are connected by a conserved, tertiary Watson-Crick base pair between C1399 and G1504, consistent with coupling of their movements during translocation. Both interactions would be expected to block slippage of the mRNA in either the forward or reverse direction.

The position of nucleotide A1503 within the colicin E3 fragment near the 3′ end of 16S rRNA (Bowman et al, 1971) suggested an experimental strategy to test the latter possibility. Using a novel splinted ligation technique, we replaced the 3′-terminal 49mer colicin fragment of 16S rRNA with a synthetic oligomer containing an abasic nucleotide at position 1503. Ribosomes reconstituted with the abasic rRNA show an increase in frameshifting into the –1 frame (Figure 7), providing support for a role for A1503 in maintaining the translational reading frame. We were unable to address the potential effects of stacking of base C1397 on the downstream mRNA, since C1397 lies outside the boundaries of the 49-nucleotide colicin E3 fragment.

We previously proposed that intercalation of A1503 could reversibly lock the register of the mRNA, preventing slippage of the translational reading frame at critical states during translocation, and retract to allow movement of the mRNA (Zhou et al, 2013). A further possibility is suggested by our previous observation of -1 frameshifting during spontaneous

translocation into the chimeric-hybrid state in the absence of EF-G (Zhou et al, 2019). Intercalation of A1503 between positions –1 and –2 would interfere with base pairing of the P-tRNA anticodon with the adjacent base at position -1, preventing a shift into the –1 reading frame. In this way, A1503 could help establish a boundary for how far the P-tRNA can move during transition to the chimeric hybrid state simply by preventing the next two bases from pairing with tRNA.

Finally, in order for the mRNA to be translocated, A1503 must retract from its intercalated or stacked position. At what point in the series of rotational movements of the ribosome does this occur? The majority of classical-state and all chimeric-hybrid state ribosome structures in our analysis show intercalation of A1503, while no intercalation of A1503 was found in any hybrid-state complex (Figure 2). Since the first major rotational event in translocation involves forward rotation of the body of the 30S subunit to transition from the classical state to the hybrid state (Ermolenko and Noller, 2011; Guo and Noller, 2012; Belardinelli et al, 2016; Noller et al, 2017) we infer that retraction of A1503 must happen during this step. This conclusion is consistent with the observation that A1503 is intercalated at two different positions of the mRNA in the classical and chimeric-hybrid states (Figure 4). It is also compatible with the observation that no net translocational movement of the mRNA occurs during forward rotation of the small subunit body domain (Noller et al, 2017; Rexroad et al, 2022). Intercalation of A1503 in all chimeric-hybrid state structures in our analysis is in keeping with the apparent vulnerability of the ribosome to frameshifting during 30S head rotation (Lancaster and Noller 2005; Peng et al, 2019; Zhou et al, 2019).

We also observed a modest but significantly increased rlevel of frameshifting for ribosomes containing a wild-type synthetic 3′ 49mer (Figure 7). We tested the possibility that this could be due to the absence of the conserved methylations of A1519 and A1519 in the synthetic 49mer. Indeed, non-methylated ribosomes isolated from a methylase-deficient *ksgA* strain showed a similar increased level of frameshifting, which was reduced to

wild-type levels by methylation *in vitro* using the ksgA methylase (Figure 8). Inspection of the interactions of nucleotides 1518 and 1519 with the surrounding ribosome structure does not suggest any obvious explanation for how their methylation could affect frameshifting; both bases are >8 Å from the nearest mRNA nucleotides and 20 Å from A1503. The effects of their methylation, albeit subtle, must therefore be indirect.

It is difficult to say how conserved our proposed mechanism would be, since there are relatively few structures available at sufficiently high resolution from diverse species. A1503 itself is highly conserved, although not universal (99.1%; *C* value of 1.926), according to our current alignment containing 1961 diverse sequences from bacteria, archaea and eukaryotes (Noller et al, 2021), suggesting that its intercalation is widespread.

The machinery of protein synthesis has evolved to stringently guard the accuracy of the translational reading frame (Kurland, 1992). Previous studies have shown that elongation factor EF-G is an important player in this process (Lancaster and Noller, 2005; Ramrath et al 2013; Zhou et al, 2013; Zhou et al, 201; Peng et al, 2019; Zhou et al, 2019; Rexroad et al, 2022). Our finding that elements of 16S rRNA also help to maintain the accuracy of the translational reading frame now reveal yet another functional role for ribosomal RNA in protein synthesis.

MATERIALS AND METHODS

Structural Analysis

Analysis of potential intercalation of 16S rRNA nucleotide A1503 was carried out on high-resolution X-ray and cryo-EM structures of 70S ribosome complexes that contain mRNA and one or more tRNAs, from the PDB and EMDB databases. Screening of 672 deposited ribosome structures identified a total of 209 in which the relative positions of A1503 and nearby mRNA bases could be placed with reasonable confidence, based on local resolution and/or map quality. We first used a computational approach to measure the positions of base

A1503 relative to bases in the mRNA according to the distance between the centroids of the A1503 base and the nearest proximal mRNA bases. This was followed by visual inspection to identify structures in which A1503 is intercalated between two mRNA bases or stacked on a single mRNA base. Our screen identified 73 structures in which A1503 was intercalated, an additional 89 where it was stacked, and 47 structures where it was retracted out of range of intercalation or stacking.

Ribosome structures were assigned to specific conformational states according to the magnitudes of their intersubunit or 30S head rotation angles, as classical state (non-rotated), hybrid state (6°–10° 30S body rotation) or chimeric-hybrid state (15°–21° 30S head rotation) using the Euler-Rodrigues method, as previously described (Mohan et al, 2014).

Preparation of ribosomes and translation components

Tight-couple 70S ribosomes were isolated from *Escherichia coli* MRE600 as described (Moazed and Noller, 1989; Powers and Noller, 1991; Lancaster et al, 2002). S100 extract was prepared from *E. coli* MRE600 cells and purified over DEAE resin as previously described (Traub et al, 1971). Total tRNA from *E. coli* was obtained from Sigma. Initiation factors IF1, IF2 and IF3 were overexpressed and purified as described (Lancaster and Noller, 2005). Initiator fMet-tRNA was prepared by *in vitro* transcription and cleavage with a *cis* HDV ribozyme present downstream from the tRNA sequence; the tRNA product was treated with T4 polynucleotide kinase to remove the resulting 2′,3′-cyclic phosphate, charged with methionine and acetylated, as described by Lancaster *et al.* (Lancaster and Noller, 2005).

Construction of ribosomes containing an abasic nucleotide at position 1503 of 16S rRNA

Colicin E3 endonuclease was expressed from plasmid pDW1 (Walker et al, 2003), which encodes 6His-tagged Colicin E3 immunity protein and Colicin E3 endonuclease in tandem, and was purified essentially as described (Walker et al, 2003). The endonuclease

was used to cleave the 16S rRNA in *E. coli* MRE600 70S ribosomes (Lancaster et al, 2008). The resulting long 16S rRNA fragment obtained from specific cleavage at position 1493 was purified by phenol extraction and sucrose gradient sedimentation. It was then ligated to a synthetic 49mer containing an abasic nucleotide at the position corresponding to A1503 of 16S rRNA (Dharmacon) with the following sequence (where the abasic nucleotide is shown in boldface and underlined):

5′-GUCGUAACA**A**GGUAACCGUAGGGGAACCUGCGGUUGGAUCACCUCCUUA-3′

Ligation was carried out with T4 RNA ligase 2 (Ho and Shuman, 2002) using a tailed DNA splint that could be removed by annealing a complementary DNA oligonucleotide under conditions that preserve the higher-order structure of the rRNA. The DNA splint contained a core sequence complementary to the ends of the 1493mer and 49mer RNAs, flanked by non-complementary 5′ and 3′ tails. It could be removed efficiently at 46° by annealing to a competing DNA oligonucleotide with full complementarity to the entire tailed splint. A full description of the ligation procedure will be described elsewhere (Smart *et al.*, in preparation). For reconstitution of 30S subunits, 20 μM 16S rRNA was incubated with 25 μM total 30S proteins in a buffer containing 25 mM Tris–HCl (pH 7.5), 400 mM NH_4Cl, 20 mM $MgCl_2$ and 5 mM β-mercaptoethanol at 42° for 1 h. For reconstitution of complete 70S ribosomes, we added an equimolar amount of natural 50S subunits from *E. coli* MRE600 in a buffer containing 25 mM Tris–HCl (pH 7.5), 100 mM NH_4Cl, 20 mM $MgCl_2$ and 5 mM β-mercaptoethanol at 37° for 15 min. The resulting abasic ribosomes were purified by sedimentation over a 10–35% sucrose gradient in 25 mM Tris·HCl (pH 7.5), 100 mM NH_4Cl, 15 mM $MgCl_2$ and 5 mM β-mercaptoethanol (Figure 5).

Assays for *in vitro* protein synthesis and frameshifting

Frameshifting assays were based on *in vitro* protein synthesis using an mRNA coding for the 27 kD ribosomal protein S2 that was modified to mimic the –1 frameshifting observed

for the dnaX system (Supplementary Figure S1) (Tsuchihashi and Brown, 1992, Larsen et al, 1997). It used an S2 mRNA modified to carry an internal Shine-Dalgarno sequence (AGGGAG) at positions 365–370 and the slippery sequence GAAAAAAG at positions 381–388 of the coding sequence, as described (Lancaster and Noller, 2005), with the modifications that the slippery sequence was changed from AAAAAAAG to GAAAAAAG to eliminate low levels of a –2 frameshift product, and that no excess EF-G or EF-Tu were added to reaction mixtures. The effects of downstream mRNA secondary structure were simulated by hybridization of a DNA olgonucleotide with the sequence 5′-GTGCGCATCAGCGCTTCTTT-3′.

Following *in vitro* translation, [^{35}S]-methioine-labeled products were separated and visualized by SDS-PAGE and autoradiography. Frameshifting levels were determined by quantification of bands corresponding to full-length and truncated products. Intensities were normalized based on the number of internal methionines in the predicted polypeptide products. Frameshifting was reported as the ratio of frameshifted product to full-length product.

TABLES AND FIGURES

Table 1. Intercalation of A1503 in mRNA[a]

State	Total	Interc	Positions	%	Stack	%	Retr	%
Classical	184	55	–3|−4	30	89	48	40	22
Hybrid	7	0	−	0	0	0	7	100
Chimeric Hybrid	18	18	−1|−2	100	0	0	0	0

[a]Summary of intercalation states of A1503 from 209 X-ray and cryo-EM structures, giving the numbers of structures in which A1503 is intercalated between two mRNA bases (Interc), stacked on a single mRNA base (Stack), or retracted out of range of intercalation (Retr), for the classical, hybrid and chimeric-hybrid states. PDB codes for all structures are listed in Supplementary Table S1. Positions of intercalation are indicated.

Table 2. Frameshifting levels[a]

70S construct	% –1 Frameshift	–1 Frameshift/0-Frame	Translation activity
Tight couple natural	33.8 ± 1.3	0.51 ± 0.03	1.00 ± 0.04
Natural 16S recon	36.8 ± 2.7	0.58 ± 0.08	0.83 ± 0.10
Mock ligated recon	35.7 ± 2.2	0.56 ± 0.05	0.69 ± 0.13
Abasic 1503 recon	55.4 ± 2.4	1.24 ± 0.11	0.71 ± 0.08
Ligated WT recon	42.1 ± 0.5	0.73 ± 0.01	0.76 ± 0.09
ΔKsgA submethylated	42.3 ± 2.7	0.75 ± 0.12	0.93 ± 0.01
Methylated *in vitro*	34.5 ± 1.7	0.53 ± 0.06	0.89 ± 0.09

[a]Efficiencies of –1 and +1 frameshifting and *in vitro* translation activities for each ribosomal construct (Figures 7 and 8). (% Frameshift) percent of product from –1 frameshift out of total product translated; (Frameshift/0-Frame) ratio of frameshifted product to 0-frame product.

Recon indicates ribosomes constructed by *in vitro* reconstitution. Statistics are presented in the legends to Figures 6–8.

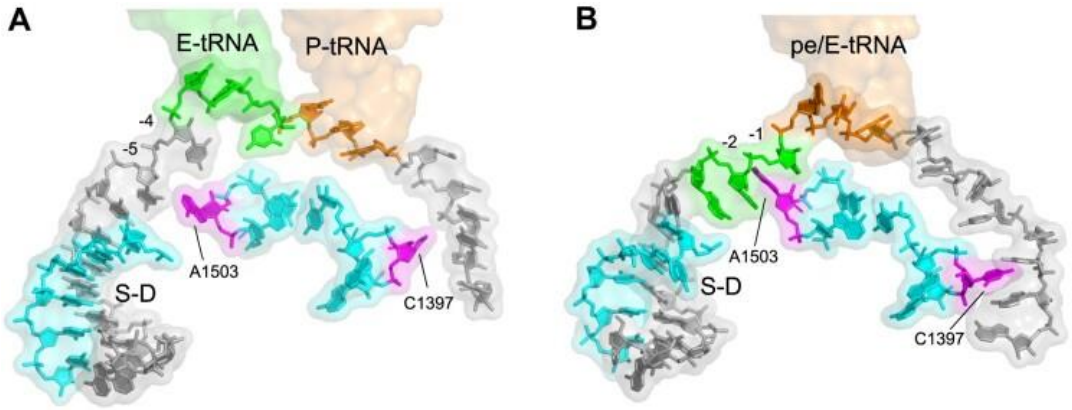

Figure 1. Intercalation of A1503 Between mRNA Bases. (A) A1503 in its retracted position in a classical-state ribosome complex (PDB code 4V6F) (Jenner et al, 2010). (B) Intercalation of A1503 between bases –1 and –2 of the mRNA in ribosomes trapped in a chimeric-hybrid intermediate state of translocation (PDB code 4V9K) (Zhou et al, 2013). Stacking of C1397 on position +10 of mRNA in the chimeric hybrid state is also shown. The positions of E-tRNA, P-tRNA and pe/E-tRNA are shown in transparent surface rendering. SD, Shine-Dalgarno helix.

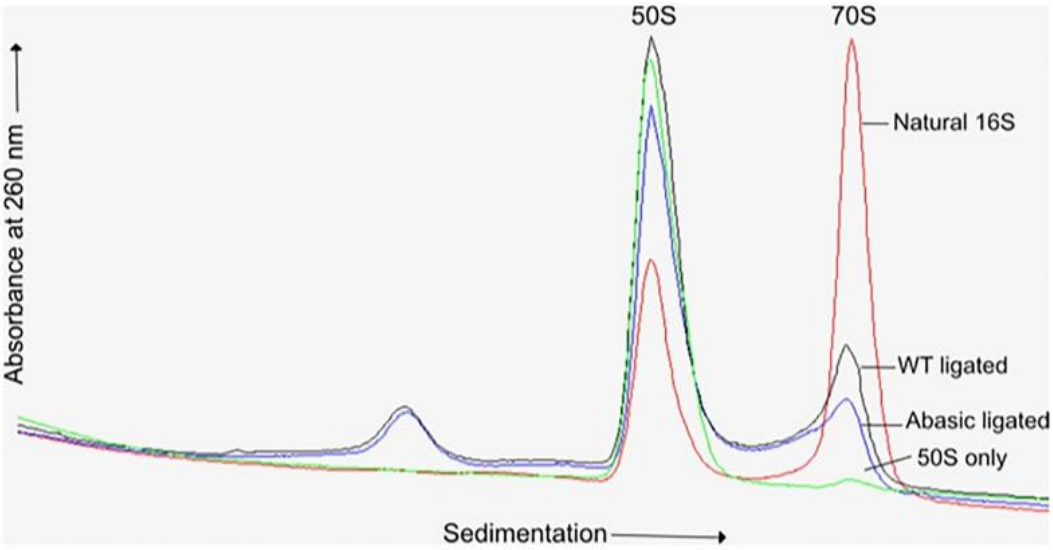

Figure 2. Isolation of reconstituted abasic ribosomes. 30S ribosomal subunits were reconstituted *in vitro* from semi-synthetic 16S rRNA constructed by ligation of the large 1491-nucleotide colicin fragment to a synthetic 49-mer RNA oligomer containing an abasic nucleotide at position 1503 or a wild-type (WT) sequence. Ribosomes were also reconstituted from natural full-length 16S rRNA for comparison. Reconstituted 30S subunits were associated with excess natural 50S subunits and the resulting 70S ribosomes were isolated by sucrose gradient centrifugation (Materials and methods).

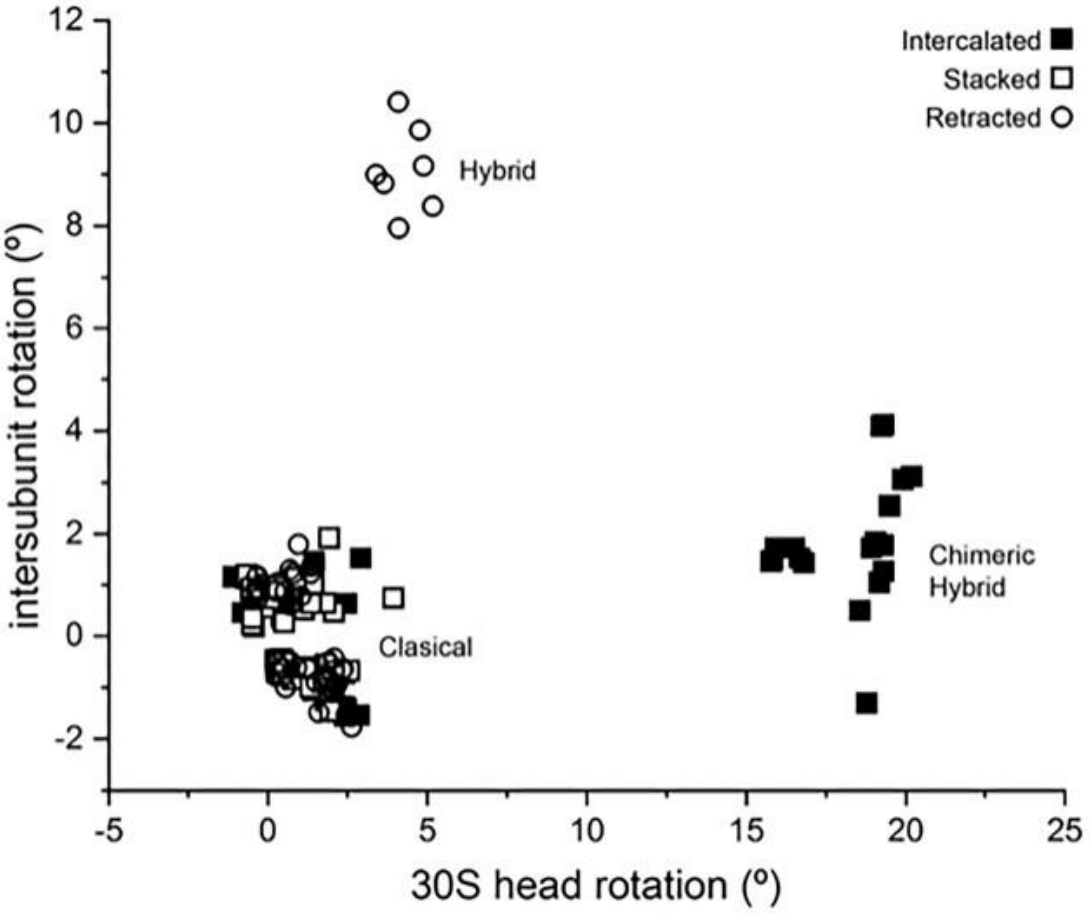

Figure 3. A1503 intercalation and ribosome rotational state. 30S head and body rotation values are plotted for 209 structures of ribosome complexes (Supplementary Table S1), relative to a classical-state reference structure (7K00). Symbols indicate whether A1503 is intercalated (▪), stacked on a single mRNA base (□) or retracted (○). Intercalation of A1503 is observed in all structures with rotation values corresponding to the chimeric-hybrid state, and in a subset of classical-state structures. No intercalation is observed in hybrid-state structures.

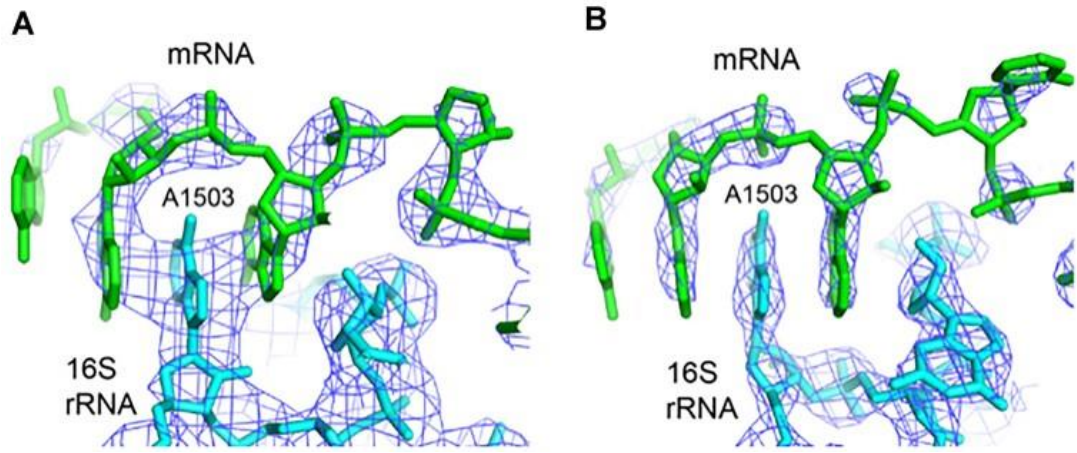

Figure 4. Examples of intercalation of A1503 in chimeric-hybrid and classical state ribosome structures. (A) 3.5Å resolution X-ray structure of a chimeric-hybrid state complex (PDB code 4V9K) (Zhou et al, 2013). (B) 3.1 Å resolution X-ray structure of a classical state complex (PDB code 4V5P) (Schmeing et al, 2011).

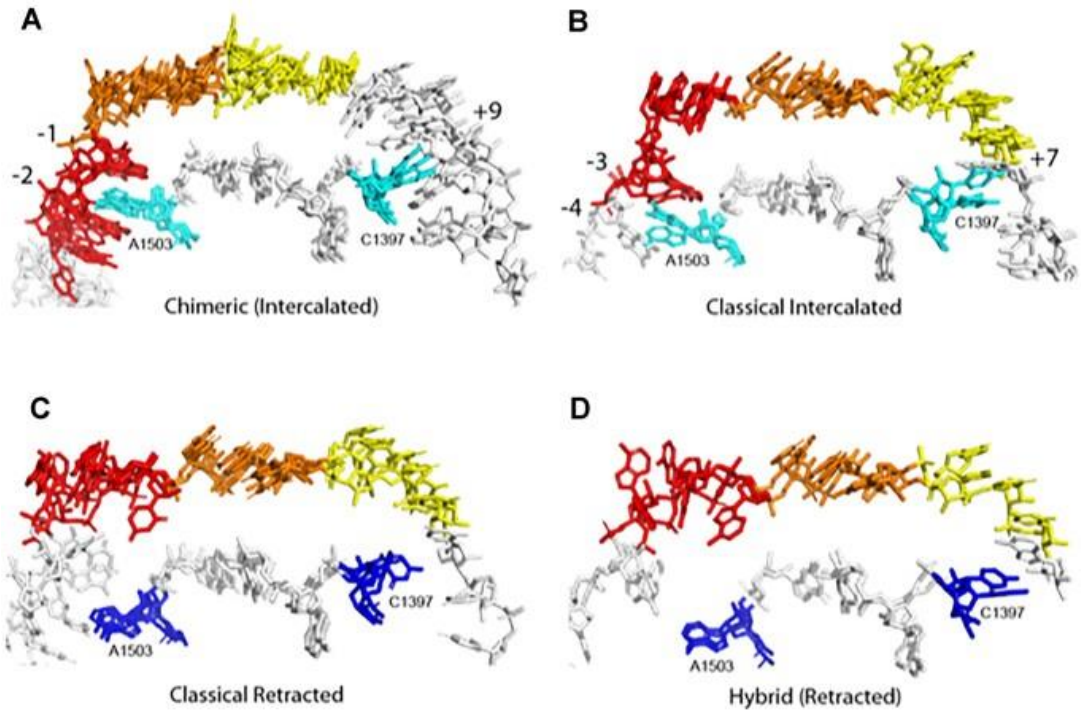

Figure 5. Positions of A1503 in different ribosomal states. Superimposition of multiple examples of ribosome complexes shows that A1503 is (A) intercalated between mRNA

positions –1 and –2 in all chimeric-hybrid state complexes (examples from PDB codes 4W29, 4V9K, 4V9L, 6N1D); (B) intercalated between positions –3 and –4 (PDB codes 4WZD, 4WQ1, 4WZO) or (C) retracted (PDB codes 4V6F, 4V9D, 4V5F) in classical-state complexes and (D) retracted in all hybrid-state complexes (PDB codes 4V9D and 6WDG). The mRNA codons are colored according to A site (yellow), P site (orange) and E site (red). Note that stacking of C1397 on positions +7 or +9 is strongly correlated with intercalation of A1503.

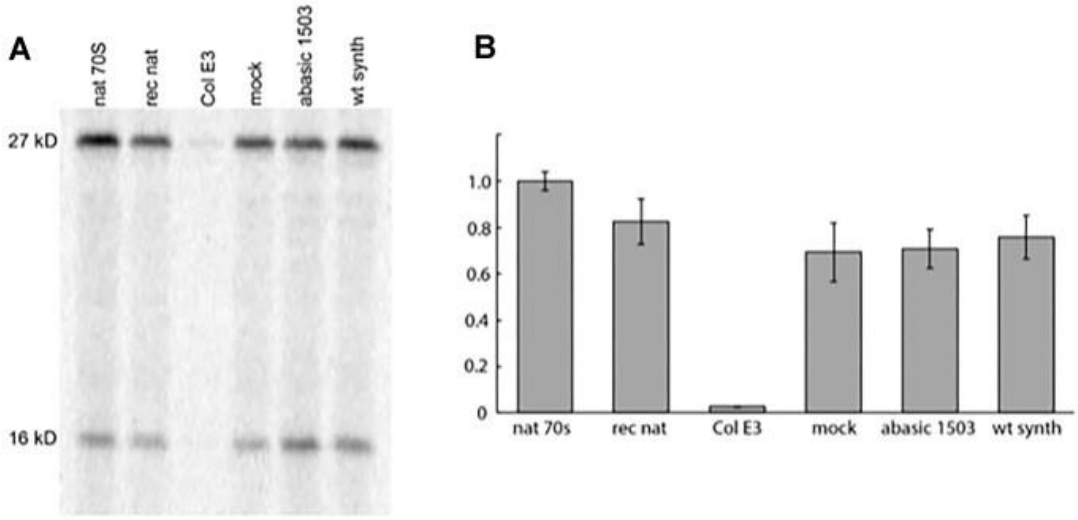

Figure 6. Semi-synthetic abasic ribosomes are active in *in vitro* protein synthesis. (A) Ribosomes reconstituted from semi-synthetic 16S rRNA containing an abasic nucleotide at position 1503 were tested for *in vitro* protein synthesis activity using a mRNA encoding the 27 kDa ribosomal protein S2 by incorporation of [^{35}S]-methionine (Lancaster and Noller, 2005). The 16 kDa band corresponds to a premature termination product caused by a -1 frameshift at an engineered slippery sequence used in the experiments shown in Figures 7 and 8. (B) Protein synthesis activities of reconstituted ribosomes calculated as the sum of full-length and frameshifted products. Activities are presented as the fraction of that of wild-type natural tight-couple 70S ribosomes; standard errors of the mean are shown from N = 8 independent experiments (Table 2; Col E3 = 0.03 ± 0.00). Abbreviations indicate natural 70S ribosomes (nat 70S), and ribosomes reconstituted from natural 16S rRNA (nat

rec), colicin E3 cleaved 16S rRNA (Col E3), natural 16S rRNA subjected to RNA ligation conditions (mock), and 16S rRNA constructed from ligation with the abasic 49mer (abasic 1503) or with a wild-type synthetic 49mer (wt synth).

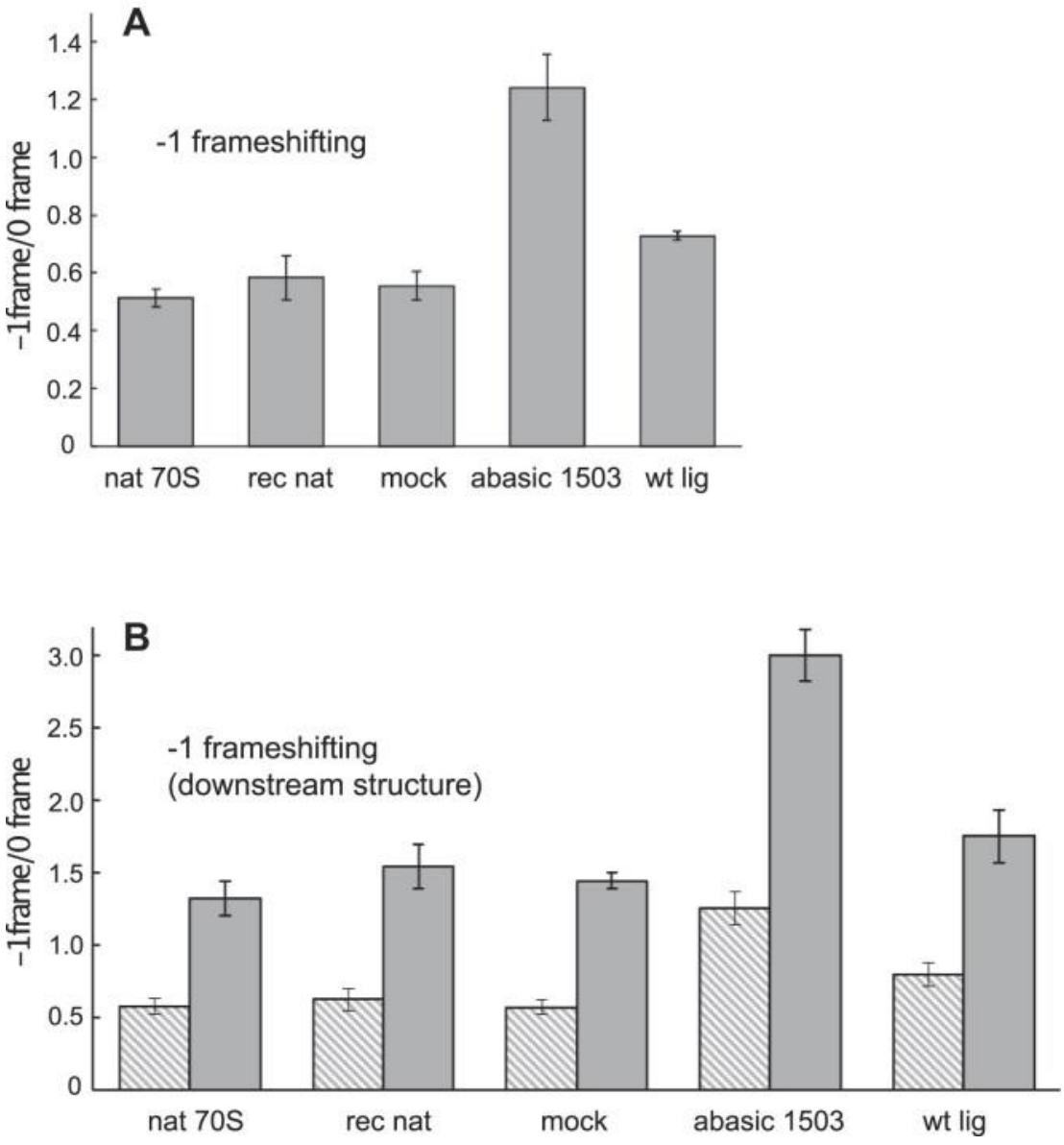

Figure 7. Frequencies of frameshifting *in vitro* (A) Increased –1 frameshifting by semi-synthetic ribosomes containing an abasic nucleotide at position 1503 (presented as the ratio of –1 frame to 0 frame translation) through an S2 mRNA containing a programmed

frameshifting sequence. Frameshifting was quantified by the magnitude of the truncated 16 kDa polypeptide (Figure 6A) relative to that of full-length 27 kDa S2 protein (Lancaster and Noller, 2005). Data are from *N* = 8 independent experiments with mean and standard error values as reported in Table 2 (Lancaster and Noller, 2005). (B) The effects of the dnaX frameshift-stimulating downstream mRNA hairpin on –1 frameshifting was simulated by hybridizing a complementary 20-nucleotide DNA oligonucleotide 6 residues downstream from the slippery sequence (Materials and methods). Data from downstream mRNA hairpin simulating constructs were from *N* = 3 independent experiments (nat 70S = 1.32 ± 0.12, rec nat = 1.54 ± 0.15, mock = 1.44 ± 0.05, abasic 1503 = 3.00 ± 0.18, wt lig = 1.75 ± 0.18. Hatched bars in panel B show the data from panel A for comparison).

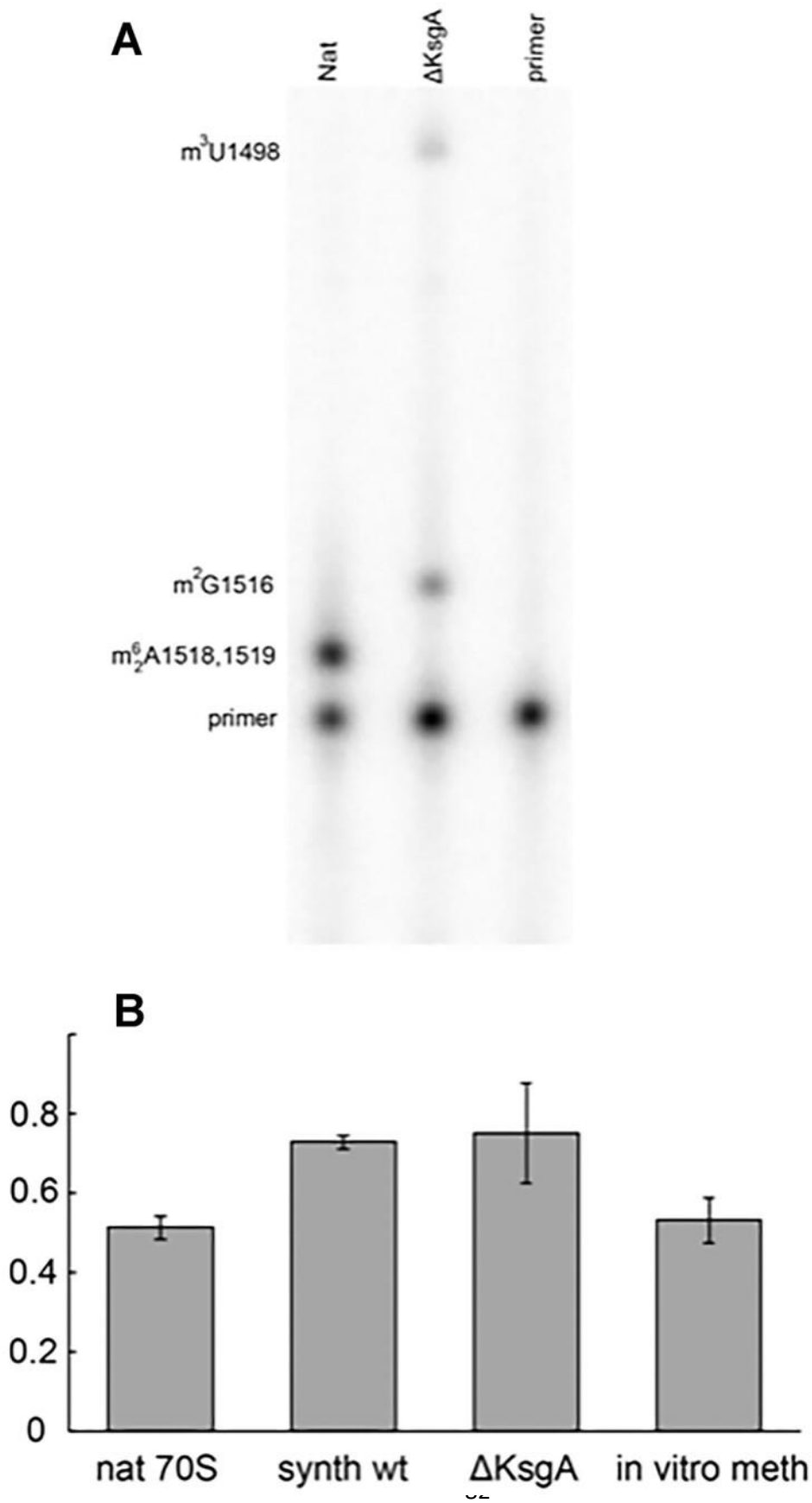
A
Nat
ΔKsgA
primer
m3U1498
m2G1516
m62A1518,1519
primer
B
0.8
0.6
0.4
0.2
0
nat 70S
synth wt
ΔKsgA
in vitro meth

Figure 8. Increased frameshifting in non-methylated A1518-1519 ribosomes. (A) The $N^6{}_2$-dimethyladenosines at positions 1518 and 1519 cause a strong primer extension stop in wild-type natural 16S rRNA (Nat), which is absent in 16S rRNA from a methylase-deficient *KsgA* strain (ΔKsgA). (B) Semi-synthetic ribosomes containing the unmodified wild-type 49mer sequence (synth wt) or ribosomes purified from the methylase-deficient *KsgA* strain (ΔKsgA) have elevated levels of –1 frameshifting relative to natural 70S ribosomes (nat 70S), which are rescued by *in vitro* methylation (*in vitro* meth). Shown are mean values (Table 2) with error bars representing the standard error of the mean from independent experiments (*N* = 8 for nat 70S and synth wt); *N* = 5 for ΔKsgA and *in vitro* meth).

SUPPLEMENTARY MATERIAL

Fig. S1. Complete sequence of the mRNA used for *in vitro* frameshifting experiments.

AUGCACCACCACCACCACCACGCAACUGUUUCCAUGCGCGACAUGCUCAAGGCU
GGUGUUCACUUCGGUCACCAGACCCGUUACUGGAACCCGAAAAUGAAGCCGUU
CAUCUUCGGUGCGCGUAACAAAGUUCACAUCAUCAACCUUGAGAAAACUGUACC
GAUGUUCAACGAAGCUCUGGCUGAACUGAACAAGAUUGCUUCUCGCAAAGGUAA
AAUCCUUUUCGUUGGUACUAAACGCGCUGCAAGCGAAGCGGUGAAAGACGCUG
CUCUGAGCUGCGACCAGUUCUUCGUGAACCAUCGCUGGCUGGGCGGUAUGCUG
ACUAACUGGAAAACCGUUCGUCAGUCCAUCAAACGUCUGAAAGACCUGGAAACU
CAGUCUCAGGGAGGUACUUUCGGAAAAAAGACCAAGAAAGAAGCGCUGAUGCGC
ACUCGUGAGCUGGAGAAACUGGAAAACAGCCUGGGCGGUAUCAAAGACAUGGG
CGGUCUGCCGGACGCUCUGUUUGUAAUCGAUGCUGACCACGAACACAUUGCUA
UCAAAGAAGCAAACAACCUGGGUAUUCCGGUAUUUGCUAUCGUUGAUACCAACU
CUGAUCCGGACGGUGUUGACUUCGUUAUCCCGGGUAACGACGACGCAAUCCGU

Fig. S1. Complete sequence of the mRNA used for in vitro frameshifting experiments. Highlight colors indicate Internal Shine-Dalgarno squence; Slippery sequence; -1 stop codon; 3' stem loop to create resistance to 3' exonucleases. AAAGAAGCGCUGAUGCGCAC

indicates the sequence used to anneal the DNA oligonucleotide

GTGCGCATCAGCGCTTCTTT to simulate downstream secondary structure.

Table S1. PDB Codes and 30S Subunit Head and Body Rotation Angles for Structures Identified in Figure 2.

A. Structures with A1503 Intercalated Into mRNA

4V5D-2	0.48	0.32	3.5	X-RAY
4V5L-1	-0.43	0.17	3.1	X-RAY
4V5P-1	1.01	0.94	3.1	X-RAY
4V5P-2	0.61	0.54	3.1	X-RAY
4V5Q-1	0.81	0.85	3.1	X-RAY
4V5Q-2	0.47	0.49	3.1	X-RAY
4V5R-1	0.4	0.55	3.1	X-RAY
4V5R-2	0.6	0.82	3.1	X-RAY
4V5S-1	0.69	0.75	3.1	X-RAY
4V5S-2	0.44	0.38	3.1	X-RAY
4V9J-1	19.31	4.11	3.86	X-RAY
4V9J-2	19.23	4.09	3.86	X-RAY
4V9K-1	16.51	1.72	3.5	X-RAY
4V9K-2	15.93	1.72	3.5	X-RAY
4V9L-1	16.68	1.52	3.5	X-RAY
4V9L-2	15.83	1.48	3.5	X-RAY
4V9M-1	16.82	1.43	4	X-RAY
4V9M-2	15.78	1.46	4	X-RAY
4W29-1	19.92	3.05	3.8	X-RAY
4W29-2	20.19	3.11	3.8	X-RAY
4W2E-1	2.87	-1.54	2.9	X-RAY
4W2F-1	-0.39	0.87	2.4	X-RAY
4W2F-2	0.24	-0.47	2.4	X-RAY
4W2G-1	-0.43	0.93	2.54	X-RAY
4W2G-2	0.32	-0.53	2.54	X-RAY
4W4G-2	2.42	-1.56	3.3	X-RAY
4WPO-1	0.3	0.65	2.8	X-RAY
4WQ1-2	-0.53	0.94	3.1	X-RAY
4WQF-1	1.46	1.46	2.8	X-RAY
4WQU-1	1.23	0.83	2.8	X-RAY
4WQY-1	1.01	0.83	2.8	X-RAY

4WU1-2	0.4	0.98	3.2	X-RAY
4WZD-1	1.94	-1.1	3.1	X-RAY
4WZD-2	0.47	0.95	3.1	X-RAY
4YPB-1	2.48	0.63	3.4	X-RAY
4YPB-2	2.24	-1.36	3.4	X-RAY
4YZV-2	2.46	-1.41	3.1	X-RAY
4Z3S-1	0.41	0.88	2.65	X-RAY
4Z3S-2	0.46	-0.52	2.65	X-RAY
4ZSN-2	2.39	-1.38	3.6	X-RAY
5DOY-1	-0.42	0.86	2.6	X-RAY
5DOY-2	0.74	-0.61	2.6	X-RAY
5E7K-2	0.38	0.99	3.2	X-RAY
5E81-2	-0.41	0.9	2.95	X-RAY
5EL4-2	0.6	1.04	3.15	X-RAY
5EL7-2	0.41	0.96	3.15	X-RAY
5J4B-1	-0.34	0.98	2.6	X-RAY
5J4C-1	0.32	0.96	2.8	X-RAY
5VPP-1	18.94	1.72	3.9	X-RAY
5VPP-2	19.18	1.05	3.9	X-RAY
5WIS-2	0.64	-0.59	2.7	X-RAY
5WIT-1	0.2	0.76	2.6	X-RAY
6GSK-2	0.58	0.99	3.36	X-RAY
6N1D-1	19.05	1.84	3.2	X-RAY
6N1D-2	19.5	2.54	3.2	X-RAY
6NWY-1	19.3	1.78	3.5	X-RAY
6NWY-2	19.31	1.26	3.5	X-RAY
6OF6-1	0.59	-0.7	3.2	X-RAY
6OJ2-2	0.27	0.77	3.2	X-RAY
6OPE-2	0.36	0.72	3.1	X-RAY
6OSI-1	18.78	-1.3	4.13	X-RAY
6OTR-2	2.17	-1.47	3.12	X-RAY
6OXI-2	1.82	-1.26	3.49	X-RAY
6QNQ-2	0.39	0.92	3.5	X-RAY
6UCQ-1	2.92	1.52	3.5	X-RAY

B. Structures with A1503 Stacked on mRNA

PDB Code	Head Rotation	Body Rotation	Resolution (Å)	Method
6OTR-1	2.09	0.47	3.12	X-RAY

6ORD-1	0.6	-0.54	3.1	X-RAY
6ORD-2	0.5	0.87	3.1	X-RAY
6OF6-2	0.22	0.9	3.2	X-RAY
6OJ2-1	1.2	-0.8	3.2	X-RAY
6O97-2	0.42	-0.45	2.75	X-RAY
6OF1-2	0.67	-0.67	2.8	X-RAY
6OXA-1	1.83	-0.55	3.25	X-RAY
6OXI-1	1.82	0.64	3.49	X-RAY
6UCQ-2	3.94	0.74	3.5	X-RAY
7JQM-2	1.95	-0.84	3.05	X-RAY
5W4K-2	0.48	-0.55	2.7	X-RAY
6CFJ-2	0.45	-0.57	2.8	X-RAY
6ND5-1	0.3	0.78	2.6	X-RAY
6ND5-2	1.05	-0.78	2.6	X-RAY
6ND6-2	0.75	-0.67	2.85	X-RAY
5J4B-2	0.49	-0.48	2.6	X-RAY
5J4C-2	0.43	-0.48	2.8	X-RAY
5VP2-2	0.62	-0.55	2.8	X-RAY
5EL5-2	-0.33	1	3.15	X-RAY
5EL6-2	0.59	1.03	3.1	X-RAY

5EL7-1	0.31	-0.72	3.15	X-RAY
4Y4P-2	0.79	-0.65	2.5	X-RAY
4YZV-1	2.41	-0.72	3.1	X-RAY
4ZSN-1	2.41	-0.73	3.6	X-RAY
4W2I-1	0.47	0.97	2.7	X-RAY
4W4G-1	2.56	-0.68	3.3	X-RAY
4V6G-2	0.27	0.87	3.5	X-RAY
4V5G-1	-0.1	0.54	3.6	X-RAY
4V5G-2	-0.48	0.22	3.6	X-RAY
1VY4-1	-0.26	0.85	2.6	X-RAY
1VY5-1	-0.37	0.78	2.54	X-RAY
1VY6-1	-0.45	0.83	2.9	X-RAY
1VY7-1	-0.42	0.78	2.8	X-RAY
4V63-1	1.44	-1.06	3.2	X-RAY
4V63-2	1.44	1.02	3.2	X-RAY
4V97-1	0.53	0.26	3.51	X-RAY
4W2I-2	0.26	-0.56	2.7	X-RAY

4WQR-1	0.76	-0.76	3.15	X-RAY
4WQR-2	-0.41	0.9	3.15	X-RAY
4WR6-1	0.79	-0.84	3.05	X-RAY
4WRA-2	-0.51	0.89	3.05	X-RAY
4WSD-1	0.96	-0.69	2.95	X-RAY
4WSD-2	0.54	0.93	2.95	X-RAY
4WT1-1	0.85	-0.74	3.05	X-RAY
4WT1-2	-0.5	0.95	3.05	X-RAY
4WU1-1	2.02	-0.97	3.2	X-RAY
4WZO-1	1.92	-0.94	3.3	X-RAY
4WZO-2	0.48	1.02	3.3	X-RAY
4Y4P-1	-0.3	0.84	2.5	X-RAY
5AFI-1	-0.47	0.34	2.9	CRYOEM
5E7K-1	0.42	-0.72	3.2	X-RAY
5E81-1	0.45	-0.77	2.95	X-RAY
5EL4-1	1.79	-0.99	3.15	X-RAY
5EL5-1	1.03	-0.85	3.15	X-RAY
5EL6-1	0.41	-0.72	3.1	X-RAY
5IB7-1	0.9	-0.85	2.99	X-RAY
5IB8-1	1.68	-1.06	3.13	X-RAY
5IB8-2	0.49	0.91	3.13	X-RAY
5IBB-1	0.48	-0.75	2.96	X-RAY
5IBB-2	-0.43	0.87	2.96	X-RAY
5W4K-1	-0.34	0.89	2.7	X-RAY
5WIS-1	-0.29	0.81	2.7	X-RAY
5WIT-2	0.39	-0.53	2.6	X-RAY
6BUW-2	-0.66	1.12	3.5	X-RAY
6BZ6-2	-0.65	1.19	3.18	X-RAY
6CAE-1	0.54	0.84	2.6	X-RAY
6CAE-2	1.23	-0.61	2.6	X-RAY
6CFJ-1	-0.3	0.83	2.8	X-RAY
6GSK-1	1.34	-1	3.36	X-RAY
6GSL-2	-0.53	0.9	3.16	X-RAY
6N9F-1	0.68	0.93	3.7	X-RAY
6ND6-1	0.34	0.86	2.85	X-RAY
6NSH-2	0.9	1.12	3.39	X-RAY
6NUO-1	2.07	-0.76	3.2	X-RAY
6NUO-2	1.14	0.51	3.2	X-RAY

6O3M-1	2.09	-0.69	3.97	X-RAY
6O3M-2	1.37	0.63	3.97	X-RAY
6O97-1	-0.49	0.92	2.75	X-RAY
6OF1-1	0.33	0.9	2.8	X-RAY
6OXA-2	1.97	-1.46	3.25	X-RAY
6QNQ-1	1.76	-0.91	3.5	X-RAY
6UO1-1	0.42	0.85	2.95	X-RAY
6XQD-1	0.09	0.72	2.8	X-RAY
6XQE-1	0.34	0.94	3	X-RAY
7JQM-1	-0.49	0.93	3.05	X-RAY
7QV1-1	1.94	1.92	3.5	CRYOEM
7QV3-1	1.94	1.92	5.14	CRYOEM
7RQ9-2	0.52	-0.53	2.6	X-RAY

C. Structures with A1503 Retracted

PDB Code	Head Rotation	Body Rotation	Resolution (Å)	Method
7RQ8-1	-0.37	0.91	2.5	X-RAY
7RQ8-2	0.91	-0.62	2.5	X-RAY
7RQ9-1	-0.33	0.89	2.6	X-RAY
7JQL-1	-0.34	0.82	3	X-RAY
7JQL-2	1.9	-0.81	3	X-RAY
6XHV-1	-0.26	0.92	2.4	X-RAY
6XHV-2	0.44	-0.61	2.4	X-RAY
6XHW-1	0.25	0.87	2.5	X-RAY
6XHW-2	0.3	-0.53	2.5	X-RAY
6XHY-1	-0.29	0.84	2.6	X-RAY
6XHY-2	0.46	-0.65	2.6	X-RAY
7K53-1	2.17	-0.95	3.2	CRYOEM
7LH5-1	0.29	-0.71	3.27	X-RAY
4V6G-1	1.85	-0.86	3.5	X-RAY
4V9D-2	1.34	1.22	3	X-RAY
5IB7-2	0.56	0.87	2.99	X-RAY
5VP2-1	-0.29	0.91	2.8	X-RAY

6NSH-1	2.34	-0.66	3.39	X-RAY
6OFX-1	0.96	1.8	3.3	CRYOEM
6QNR-1	0.74	0.6	3.1	X-RAY
3JA1-1	5.18	8.38	3.6	CRYOEM
4V4Z-1	2.63	-1.77	4.51	X-RAY
4V4J-1	1.61	-1.49	3.83	X-RAY
4V4Y-1	2.47	-1.53	5.5	X-RAY
4V5F-1	1.37	1.36	3.6	X-RAY
4V5F-2	1.04	0.78	3.6	X-RAY
4V5K-1	1.86	-0.99	3.2	X-RAY
4V6F-1	0.7	0.6	3.1	X-RAY
4V6F-2	-0.35	1.15	3.1	X-RAY
4V90-1	4.11	7.96	2.95	X-RAY
4V9D-1	3.4	8.99	3	X-RAY
5UQ7-1	1.91	-0.5	3.5	CRYOEM
5UQ8-1	2.09	-0.43	3.2	CRYOEM
6BUW-1	1.53	-0.9	3.5	X-RAY
6BY1-2	0.7	1.29	3.94	X-RAY
6BZ6-1	1.27	-0.65	3.18	X-RAY
6GSL-1	0.57	-1	3.16	X-RAY
6NTA-1	2.37	-0.64	3.1	X-RAY
6NTA-2	0.8	1.21	3.1	X-RAY
6QNR-2	-0.32	1.17	3.1	X-RAY
6YEF-1	2.08	-1.07	3.2	CRYOEM
7N1P-1	-0.31	0.72	2.33	CRYOEM
7SSL-1	4.76	9.86	3.8	CRYOEM
7SSN-1	4.89	9.16	3.2	CRYOEM
7SSO-1	3.65	8.82	3.2	CRYOEM
7ST2-1	2.12	-0.93	2.9	CRYOEM

7ST7-1	4.09	10.41	3.2	CRYOEM

REFERENCES

Belardinelli R., Sharma H., Caliskan N., Cunha C.E., Peske F., Wintermeyer W., Rodnina M.V. Choreography of molecular movements during ribosome progression along mRNA. Nat. Struct. Mol. Biol. 2016; 23:342–348.

Blinkowa A.L., Walker J.R. Programmed ribosomal frameshifting generates the Escherichia coli DNA polymerase III gamma subunit from within. Nucleic Acids Res. 1990; 18:1725–1729.

Bowman C.M., Dahlberg J.E., Ikemura T., Konisky J., Nomura M. Specific inactivation of 16S ribosomal RNA induced by colicin E3 In vivo. Proc. Natl. Acad. Sci. U.S.A. 1971; 68:964–968.

Connolly K., Rife J.P., Culver G. Mechanistic insight into the ribosome biogenesis functions of the ancient protein KsgA. Mol. Microbiol. 2008; 70:1062–1075.

Drummond D.A., Wilke C.O. Mistranslation-induced protein misfolding as a dominant constraint on coding-sequence evolution. Cell. 2008; 134:341–352.

Ermolenko D.N., Noller H.F. mRNA translocation occurs during the second step of ribosomal intersubunit rotation. Nat. Struct. Mol. Biol. 2011; 18:457–462

Flower A.M., Mchenry C.S. The y subunit of DNA polymerase III holoenzyme of Escherichia coli is produced by ribosomal frameshifting. Proc. Natl. Acad. Sci. U.S.A. 1990; 87:3713–3717.

Guo Z., Noller H.F. Rotation of the head of the 30S ribosomal subunit during mRNA translocation. Proc. Natl. Acad. Sci. U.S.A. 2012; 109:20391–20394.

Ho C.K., Shuman S. Bacteriophage T4 RNA ligase 2 (gp24.1) exemplifies a family of RNA ligases found in all phylogenetic domains. Proc. Natl. Acad. Sci. U.S.A. 2002; 99:12709–12714.

Jenner L.B., Demeshkina N., Yusupova G., Yusupov M. Structural aspects of messenger RNA reading frame maintenance by the ribosome. Nat. Struct. Mol. Biol. 2010; 17:555–560.

Kim H.-K., Tinoco I. Jr EF-G catalyzed translocation dynamics in the presence of ribosomal frameshifting stimulatory signals. Nucleic Acids Res. 2017; 45:2865–2874.

Kurland C.G. Translational accuracy and the fitness of bacteria. Annu. Rev. Genet. 1992; 26:29–50

Labuda D., Grosjean H., Striker G., Pörschke D. Codon:anticodon and anticodon:anticodon interaction. Evaluation of equilibrium and kinetic parameters of complexes involving a G:u wobble. Biochim. Biophys. Acta BBA - Gene Struct. Expr. 1982; 698:230–236.

Lancaster L., Kiel M.C., Kaji A., Noller H.F. Orientation of ribosome recycling factor in the ribosome from directed hydroxyl radical probing. Cell. 2002; 111:129–140.

Lancaster L., Noller H.F. 'Involvement of 16S rRNA nucleotides G1338 and A1339 in discrimination of initiator tRNA'. Mol. Cell. 2005; 20:623–632.

Lancaster L., Noller H.F. Involvement of 16S rRNA nucleotides G1338 and A1339 in discrimination of initiator tRNA. Mol. Cell. 2005; 20:623–632.

Lancaster L.E., Savelsbergh A., Kleanthous C., Wintermeyer W., Rodnina M.V. Colicin E3 cleavage of 16S rRNA impairs decoding and accelerates tRNA translocation on Escherichia coli ribosomes. Mol. Microbiol. 2008; 69:390–401.

Larsen B., Gesteland R.F., Atkins J.F. Structural probing and mutagenic analysis of the stem-loop required for Escherichia coli dnaX ribosomal frameshifting: programmed efficiency of 50%11Edited by D. E. Draper. J. Mol. Biol. 1997; 271:47–60.

McCloskey J.A., Rozenski J. The small subunit rRNA modification Database. Nucleic Acids Res. 2005; 33:D135–D138.

Moazed D., Noller H.F. Intermediate states in the movement of transfer RNA in the ribosome. Nature. 1989; 342:142–148.

Mohan S., Donohue J.P., Noller H.F. Molecular mechanics of 30S subunit head rotation. Proc. Natl. Acad. Sci. U.S.A. 2014; 111:13325–13330.

Moore M.J., Sharp P.A. Site-specific modification of pre-mRNA: the 2'-hydroxyl groups at the splice sites. Science. 1992; 256:992–997.

Moore M.J., Query C.C. [7]Joining of RNAs by splinted ligation. Methods in Enzymology. 2000; 317:RNA - Ligand Interactions, Part A. Academic Press; 109–123.

Noller H.F., Lancaster L., Zhou J., Mohan S. The ribosome moves: RNA mechanics and translocation. Nat. Struct. Mol. Biol. 2017; 24:1021–1027

Noller H.F., Donohue J.P., Gutell R.R. The universally conserved nucleotides of the small subunit ribosomal RNAs. RNA. 2021; 28:623–644.

Peng B.-Z., Bock L.V., Belardinelli R., Peske F., Grubmüller H., Rodnina M.V. Active role of elongation factor G in maintaining the mRNA reading frame during translation. Sci. Adv. 2019; 5:eaax8030.

Powers T., Noller H.f. A functional pseudoknot in 16S ribosomal RNA. EMBO J. 1991; 10:2203–2214.

Ramrath D.J.F., Lancaster L., Sprink T., Mielke T., Loerke J., Noller H.F., Spahn C.M.T. Visualization of two transfer RNAs trapped in transit during elongation factor G-mediated translocation. Proc. Natl. Acad. Sci. U.S.A. 2013; 110:20964–20969.

Rexroad G., Donohue J.P., Lancaster L., Noller H.F. The role of GTP hydrolysis by EF-G in ribosomal translocation. Proc. Natl. Acad. Sci. U.S.A. 2022; 119:e2212502119.

Schmeing T.M., Voorhees R.M., Kelley A.C., Ramakrishnan V. How mutations in tRNA distant from the anticodon affect the fidelity of decoding. Nat. Struct. Mol. Biol. 2011; 18:432–436.

Stochmanski S.J., Therrien M., Laganière J., Rochefort D., Laurent S., Karemera L., Gaudet R., Vyboh K., Van Meyel D.J., Di Cristo G. et al. Expanded ATXN3 frameshifting events are toxic in Drosophila and mammalian neuron models. Hum. Mol. Genet. 2012; 21:2211–2218.

Tsuchihashi Z., Brown P.O. Sequence requirements for efficient translational frameshifting in the Escherichia coli dnaX gene and the role of an unstable interaction between tRNA(Lys) and an AAG lysine codon. Genes Dev. 1992; 6:511–519.

Tsuchihashi Z., Kornberg A. Translational frameshifting generates the gamma subunit of DNA polymerase III holoenzyme. Proc. Natl. Acad. Sci. U.S.A. 1990; 87:2516–2520.

Traub P., Mizushima S., Lowry C.V., Nomura M. [41]Reconstitution of ribosomes from subribosomal components. Methods in Enzymology. 1971; 20:Academic Press; 391–407.Part C: Nucleic Acids and Protein Synthesis.

Turner D.H. Thermodynamics of base pairing. Curr. Opin. Struct. Biol. 1996; 6:299–304.

Walker D., Moore G.R., James R., Kleanthous C. Thermodynamic consequences of bipartite immunity protein binding to the ribosomal ribonuclease colicin E3. Biochemistry. 2003; 42:4161–4171.

Wills N.M., Atkins J.F. The potential role of ribosomal frameshifting in generating aberrant proteins implicated in neurodegenerative diseases. RNA. 2006; 12:1149–1153.

Woese C.R., Fox G.E., Zablen L., Uchida T., Bonen L., Pechman K., Lewis B.J., Stahl D. Conservation of primary structure in 16S ribosomal RNA. Nature. 1975; 254:83–86.

Zhou J., Lancaster L., Donohue J.P., Noller H.F. Crystal structures of EF-G-ribosome complexes trapped in intermediate states of translocation. Science. 2013; 340:1236086.

Zhou J., Lancaster L., Donohue J.P., Noller H.F. How the ribosome hands the A-site tRNA to the P site during EF-G-catalyzed translocation. Science. 2014; 345:1188–1191.

Zhou J., Lancaster L., Donohue J.P., Noller H.F. Spontaneous ribosomal translocation of mRNA and tRNAs into a chimeric hybrid state. Proc. Natl. Acad. Sci. U.S.A. 2019; 116:7813–7818.

Chapter 4. Translational reading frame maintenance by a universally conserved nucleotide in 16S rRNA

ABSTRACT

Recent studies have revealed a role for ribosomal RNA in preservation of the translational reading frame. Here, we focus on G926, the universally conserved bulged base

in helix h28 of 16S rRNA that forms part of the P site of the small ribosomal subunit and has been localized to one of the two hinge points that enable rotation of its head domain. G926 makes two of the rare interactions between the ribosome and the mRNA, projecting into the mRNA channel where it H-bonds with the +1 phosphate of the mRNA and stacks on the -1 base. We tested the possibility that G926 plays a role in reading frame maintenance by measuring the effects of deletion and substitution mutations on frameshifting levels during *in vitro* translation of mRNAs containing the sequences of the prfB and dnaX genes, which stimulate programmed frameshifting into the +1 and -1 reading frames, respectively. We find that deletion of G926 doubles the incidence of frameshifting into both the +1 and -1 frames, while the substitution mutations had minimal effect. We additionally provide direct evidence that prfB and dnaX frameshifting occur at different steps of the elongation cycle through independent pathways. We conclude that interactions between G926 and the mRNA help to preserve the translational reading frame by providing a steric barrier to uncoupled movement of the mRNA.

INTRODUCTION

During the elongation phase of protein synthesis, the mRNA and tRNA must undergo many rounds of coupled translocation in precise three-nucleotide increments. Uncoupled movement of the tRNA and mRNA results in loss of the correct translational reading frame. Frameshifting errors are the most serious class of translational error, resulting in incorporation of a series of incorrect amino acids followed by premature termination at an out-of-frame stop codon. The resulting truncated polypeptide can confer a dominant-lethal effect (Drummond and Wilke, 2008), explaining why frameshifting errors are observed to occur at a frequency of less than 10^{-5} per codon (Kurland, 1992).

Nevertheless, certain regulatory mechanisms have evolved to exploit translational frameshifting. These sequences, known as programmed ribosomal frameshifting (PRF) sequences, or "slippery sequences", contain elements that increase frameshifting efficiencies

by orders of magnitude above background levels. PRF sequences generally fall into two different sets of motifs, which stimulate ether -1 frameshifting or +1 frameshifting (Farabaugh, 1996a). Cases of -1 PRF have been described by a 'simultaneous slippage' model, where a ribosome with two tRNAs bound slips on a heptameric 'slippery' sequence upon encountering a barrier such as secondary structure. Early models presumed that frameshifting of this type occurred either prior to peptidyl transfer (Jacks et al, 1988), or just after peptidyl transfer but before translocation (Weiss et al, 1989). More recently, it has become evident that -1 frameshifting can occur during translocation. The three base-pair codon-anticodon duplex, which is inherently unstable, appears to be held most tightly by the ribosome in the small subunit A site, where it is surrounded by a network of universally conserved nucleotides from 16S rRNA. Thus, the reading frame becomes particularly vulnerable during translocation, when the codon-anticodon duplexes are no longer stabilized by contact with the ribosome. But cryo-EM and X-ray structures of translocation complexes showed that the tip of domain IV of elongation factor EF-G appears to mimic the 16S rRNA A-site contacts with the codon-anticodon duplex and maintains contact throughout its translocational trajectory (Gao et al, 2009; Zhou et al, 2014; Brilot et al, 2013; Carbone et al 2021; Petrychenko et al 2021; Rundlet et al; 2021). Increased -1 frameshifting upon mutation of the contacting residues in the tip of domain IV has shown that these contacts with EF-G indeed help to guard against shifting into the -1 frame (Peng et al, 2019; Niblett et al, 2021) and that slippage does indeed occur during translocation.

While cases of +1 PRF are far fewer, known examples are consistent with a 'hungry frameshifting' model (Temperley et al, 2010; Atkins et al, 2016; Poulis et al, 2023), in which a 4-nucleotide slippery P-site sequence adjoins a slowly decoded A-site codon. The +1 frameshifting event is likely induced on ribosomes containing a single peptidyl-tRNA in the P site and a vacant A site (Craigen et al, 1985; Matsufuji et al, 1995; Farabaugh, 1996a). Frameshifting of this type can be induced when there are limiting amounts of an amino acid,

tRNA, or release factor RF2, hence the term ‘hungry frameshifting’ (Curran and Yarus, 1989; Donly et al, 1990; Caliskan et al, 2017). While hungry frameshifting can also stimulate -1 frameshifting during starvation conditions (Gallant and Lindsley, 1992; Lindsley and Gallant, 1993; Caliskan et al, 2017), programmed examples appear to be used predominantly, if not exclusively, for +1 frameshifting (Farabaugh et al, 1996a).

How does the translation machinery protect the cell against the dangers of frameshifting events? In addition to the established role of EF-G, there is emerging evidence that the ribosome itself may also employ strategies to avoid uncoupled slippage of the mRNA. Although its tRNA binding sites constrain the movement of the tRNAs, contacts between the ribosome and the mRNA are comparatively sparse, apart from those found in the decoding center, where a network of universally conserved nucleotides from 16S rRNA clamps down on the A-site codon-anticodon duplex (Ogle et al, 2001). One such contact is the intercalation of A1503 of 16S rRNA between nucleotides -1 and -2 of the mRNA (Zhou et al, 2013). Recently, it was found that replacement of A1503 by an abasic nucleotide results in doubling of the frequency of frameshifting during *in vitro* protein synthesis, providing evidence that A1503 helps to prevent translational frameshifting (Smart et al, 2024). Here, we note that the universally conserved G926, which forms a single-base bulge in helix h28 of 16S rRNA, intercalates between G1505 of 16S rRNA and the -1 base of the mRNA. In an effort to investigate its possible role in maintaining the translational reading frame, we constructed ribosomes containing both deletion and substitution mutations of G926. *In vitro* protein synthesis shows that deletion of G926 doubles the incidence of both +1 and -1 frameshifting errors. Although its guanine base forms H-bonds with the +1 phosphate of the mRNA, base substitutions confer only modest increases in frameshifting, indicating that the main effects of G926 are due to stacking on mRNA bases, rather than H-bonding with mRNA phosphates. Separately, we revisited the effects of the EF-G mutant, Q507D, which we previously showed to stimulate -1 frameshifting (Niblett et al, 2021), on +1 frameshifting. We find that Q507D has

no effect on +1 frameshifting, consistent with the idea that frameshifting during translocation is caused by uncoupled forward movement of the tRNA (Zhou et al., 2019).

RESULTS

MS2-tagged Δ926 ribosomes show robust translational activity in *in vitro* translation

In an effort to characterize the function of G926 in detail, we constructed a 926-deletion mutant on a plasmid encoded 16S rRNA gene containing an MS2-tag located in helix 6 (the 30S spur), allowing for purification of mutant ribosomes from wild-type using an MS2-glutathione affinity chromatography system (Lancaster and Noller, 2005). Due to G926 being positioned as a single nucleotide bulge within helix 28, we reasoned its deletion should not perturb the local secondary structure. MS2-tagged Δ926 30S subunits were then associated with natural 50S subunits and tested for their ability to synthesize a full-length protein using an *in vitro* protein synthesis assay supplemented with [^{35}S]-methionine to label the polypeptide products (Ali et al, 2006). 70S ribosomes were programmed with an mRNA encoding the 240 amino acid ribosomal protein S2, which contains 7 internal methionines, and time points were taken from 0 to 48 minutes and visualized by SDS-PAGE and autoradiography. To our surprise, MS2-tagged Δ926 ribosomes showed no defect in translation, with both the rate and activity being indistinguishable from MS2-tagged wild-type ribosomes (Fig. 1). These results raised a question: if G926 is unnecessary for efficient translation, what is its function and why has it evolved to be invariably conserved across the entire phylogenetic tree?

Deletion of G926 results in elevated levels of -1 frameshifting

While the previously described *in vitro* protein synthesis assay tasks the ribosomes with initiation and many rounds of elongation, one function that it is not well-suited to test for is reading frame maintenance. Background levels of frameshifting are estimated to be on the order of once per 10^5 codons (Kurland, 1992) and even a large increase to frameshifting

would be difficult to observe at these levels using SDS-PAGE. To measure the effect of G926 mutations on frameshifting efficiency, we turned to an *in vitro* protein synthesis assay that we had previously developed which utilizes an mRNA containing a frameshift-prone sequence partway through the transcript (Niblett et al, 2021; Smart et al, 2024). This frameshift-prone sequence was based on the -1 programmed frameshifting sequence from the dnaX gene of *E. coli*, which is one of the most extensively studied programmed frameshifting sequences in bacteria (Tsuchihashi and Kornberg, 1990; Larsen et al, 1994, 1997; Chen et al, 2014; Kim and Tinoco 2017; Bao et al, 2020). The native version of this sequence relies on 3 sequence elements to stimulate frameshifting (Fig. 3): (1) a 'slippery' A AAA AAG heptamer, which allows for cognate A- and P-site pairing in both the 0 and -1 frame; (2) a downstream stem-loop starting at position +13, near the entrance to the downstream mRNA tunnel; (3) an internal Shine-Dalgarno sequence positioned 11 nucleotides upstream of the P-site codon. The combination of all 3 elements results in an unusually high frameshifting efficiency of 50-80%, or greater than 4 orders of magnitude above background levels.

The -1 mRNA constructed for our assay omits the downstream stem-loop, resulting in a lower frameshifting efficiency of ~20% (Niblett et al, 2021). This decision allows for a broader range of possible frameshifting efficiencies upon stimulation, resulting in a more sensitive assay. We translated the -1 mRNA using 70S ribosomes formed from the association of MS2-tagged G926 30S mutants with natural 50S subunits (Fig. 2.). Deletion of G926 resulted in an increase in frameshifting efficiency from ~22.5% to ~40.3%. Interestingly, the G926A substitution mutation failed to produce a statistically significant effect on frameshifting levels ($p=0.47$), while G926U had a modest 5.2% increase ($p=0.037$).

+1 frameshifting on prfB mRNA is unaffected by frameshift-stimulating EF-G mutants

Due to the diversity of frameshift stimulatory elements found in natural programmed frameshifting sequences (Farabaugh, 1996a,b), particularly between -1 and +1 stimulatory sequences, we chose to design an additional reporter based on the +1 frameshifting sequence of the *E. coli* prfB gene encoding the ribosomal release factor RF2 (Craigen et al, 1985; Craigen and Caskey, 1986; Weiss et al, 1987). While we previously showed that dnaX -1 frameshifting occurs during translocation (Niblett et al, 2021), the +1 prfB reporter differs from the -1 reporter in two fundamental ways that suggest a different frameshifting pathway: First, the prfB slippery sequence is only 4 nucleotides in contrast to the 7 nucleotide slippery sequence in dnaX, being able to accommodate the +1 slippage of only 1 tRNA while dnaX can accommodate the -1 slippage of 2 tRNAs (Curran, 1993). Second, the +1 reporter contains a slowly-decoded in-frame UGA stop codon in the A site, serving a similar role to the downstream stem-loop found in dnaX by promoting ribosomal stalling at the slippery sequence (Craigen and Caskey, 1985; Donly et al, 1990; Adamski et al, 1993). This results in a negative feedback loop, where sufficient concentrations of RF2 result in a truncated product due to early in-frame termination, while low concentrations of RF2 promote stalling followed by a +1 frameshift and subsequent synthesis of the complete polypeptide product. The 4-nucleotide slippery sequence and the requirement for slowly decoded A-site codon taken together suggest a mechanism where frameshifting on prfB occurs on ribosomes stalled at the slippery sequence with a vacant A-site while awaiting an incoming release factor.

To clarify the difference in mechanisms between the dnaX and prfB sequences, we measured the effect of a frameshift-prone EF-G mutant, Q507D (Peng et al, 2019; Niblett et al, 2021), on prfB +1 frameshifting efficiency. We reasoned that since EF-G is active on the ribosome during translocation, an mRNA sequence that stimulates frameshifting at a different step in the elongation cycle should be unaffected by the mutant. Starting from a previously described *E. coli* strain containing an amino-terminal 6-his tag on the genomic EF-G copy, we used homologous recombination to add a second 6-his tag to the carboxy-terminus of RF2,

allowing us to generate S100 extract depleted of endogenous EF-G and RF2 over a Ni^{++} column (Materials and Methods). We used *in vitro* translation to compare the frameshifting efficiency of ribosomes supplemented with wild-type EF-G versus ribosomes supplemented with Q507D EF-G at 5 different concentrations of RF2, covering a broad range of frameshifting efficiencies. While we previously showed that Q507D stimulated -1 frameshifting ~3-fold (24.8% to 70.3%), the same mutation had virtually no effect on the levels of +1 frameshifting at each RF2 concentration (Fig. 4). These results confirm that the +1 prfB frameshifting stimulation is mechanistically distinct from that of the -1 dnaX frameshifting stimulation, likely occurring at different steps of the elongation cycle.

Deletion of G926 results in elevated levels of +1 frameshifting

Next, we tested the G926 mutants for their effect on +1 frameshifting. 70S ribosomes reconstituted from MS2-tagged 30S ribosomes bearing G926 mutations were tasked with the *in vitro* translation of the +1 prfB mRNA, utilizing the S100 extract depleted of endogenous RF2 described above (Fig. 5). For each mutant, the *in vitro* translation was performed at 3 different RF2 concentrations which represented the most dynamic region of the wild-type concentration vs frameshifting curve – 250, 500, or 1000 nM. The percentage of frameshifted product synthesized by the deletion mutant ranged from ~1.8-2.3-fold over the percentage synthesized by MS2-tagged wild-type ribosomes across the 3 RF2 concentrations. The G926A and U substitution mutants failed to produce a statistically significant effect on +1 frameshifting efficiency.

DISCUSSION

G926 is one of relatively few residues in 16S rRNA that makes direct contact with the mRNA and the only rRNA residue contacting the mRNA at the P site. Notably, G926 constitutes one of two 16S rRNA nucleotides determined by rigid body analysis to function as a hinge for 30S head domain rotation (Mohan et al, 2014). Although there is variability from

structure to structure, contacts between G926 and the mRNA are present at all stages of the elongation cycle. In nearly all structures, G926 stacks on G1505, makes Van der Waals contact with the mRNA backbone, and forms hydrogen bonds to phosphates in the P-site. In classical and hybrid state ribosomes, G926 typically interacts with the mRNA at position -1 either through stacking on the base or H-bonding to the phosphate depending on the orientation of the nucleotide (Fig. 6A). The position of G926 within the mRNA channel presents a steric barrier to unregulated mRNA movement, especially in chimeric-hybrid state complexes where the mRNA wraps around G926, which in conjunction with A1503 intercalation creates a clear boundary between the P- and E-site codons (Fig. 6B). Unexpectedly, despite universal conservation across all organisms, G926 appears to be completely dispensable for efficient *in vitro* protein synthesis, raising questions regarding its function and extreme conservation. Here, we show that G926 plays an important role in maintenance of the translational reading frame and guards against both +1 and -1 programmed ribosomal frameshifting.

How does G926 contribute to translational reading frame maintenance? Ribosomal frameshifting on a slippery sequence requires a tRNA to un-pair with its 0-frame codon and then re-pair with an overlapping out-of-frame codon. tRNA-mRNA un-pairing, and thus frameshifting, can be inhibited by contacts that stabilize the codon-anticodon duplex such as those made by residues at the tip of domain IV of elongation factor EF-G during translocation (Peng et al, 2019; Niblett et al, 2021). In the window between un-pairing and re-pairing, the tRNA and mRNA must then undergo uncoupled movement relative to each other by at least one nucleotide. While the movement of tRNAs is heavily restricted by their three-dimensional binding sites, the mRNA makes very few interactions with the ribosome and is presumably significantly more mobile. Accordingly, the few 16S rRNA residues that do restrict mRNA movement are good candidates for reading frame maintenance functions. Consistent with this idea, previous work focused on A1503, which intermittently intercalates and retracts between

mRNA bases during the elongation cycle, also found an effect on the level of -1 frameshifting (Smart et al, 2024). Intercalation of A1503 likely constrains lateral mRNA movement in accordance with the idea that unregulated mRNA movement results in elevated frameshifting.

The elongation cycle begins with a classical state ribosome containing a single tRNA bound to the P-site. In this configuration, the reading frame is determined by the position of a single tRNA. Similarly, the movement of the mRNA is arguably the least restricted compared to other steps of the elongation cycle, owing to an absence of E- and A- site interactions. Consequently, G926, which is the only mRNA-rRNA P-site contact, likely has a disproportionate contribution to reading frame maintenance at this stage relative to other stages of the elongation cycle. In our analysis, all classical-state complexes contain at least one hydrogen bond between G926 and the +1 phosphate, with two or three hydrogen bonds also being common. These H-bonds contribute to the energy barrier of mRNA movement and position the codon for base-pairing with its anticodon. Additionally, G926 is usually seen stacking between the -1 base and G1505 in classical state structures. When not stacking on G926, the -1 base is flipped around to face the tRNA, placing the -1 phosphate within H-bonding distance of G926 instead and resulting in G926 H-bonding to both the +1 and -1 phosphates. When G926 stacks on the -1 base, it must be physically displaced for the mRNA to successfully realign in the +1 direction (Fig. 6).

Upon A-site tRNA binding, the mRNA is additionally restricted by the A-site anticodon and the decoding center. The decoding center consists of a network of 5 nucleotides, facilitated by ribosomal protein S12 and a Mg^{2+} ion, that clamps down on the A-site codon-anticodon, stabilizing the duplex and imposing conformational restrictions on the mRNA. Ribosomes at this stage may undergo spontaneous and reversible inter-subunit rotation, readily inter-converting between the classical and hybrid states. G926-mRNA interactions are similar between classical and hybrid state structures, although their contribution is relatively less significant in the presence of newly formed A-site interactions. Next, the ribosome

undergoes EF-G-catalyzed translocation, where the A- and P-site tRNAs leave the stability of their binding sites and make their way to the next site. While the A-site interactions are completely lost, the resulting loss of codon-anticodon stability is at least partially supplemented by newly formed interactions made by residues within loops I and II at the tip of domain IV of EF-G. While stacking between G926 and the -1 base is completely lost at this step, one to four H-bonds to one of several mRNA phosphates remain.

The +1 PrfB programmed frameshifting sequence consists of an internal Shine-Dalgarno sequence, a four-nucleotide slippery sequence, and a slowly-decoded in-frame stop codon. Studies have shown that the in-frame stop codon can be substituted for a sense codon with frameshifting efficiency being inversely proportional to the rate at which that sense codon is decoded (Curran and Yarus, 1989; Sipley and Goldman, 1993; Gao et al, 1995). Frameshift stimulation by this element resembles the so-called 'hungry frameshifting' pathway, which has been used *in vitro* to stimulate -1 and -2 frameshifting by deliberately leaving certain cognate aminoacyl-tRNAs from the translation reaction (Caliskan et al, 2017; Poulis et al, 2023). This would suggest that ribosomes undergoing frameshifting on the prfB mRNA are stalled with a vacant A site while awaiting RF2 binding and UGA stop codon recognition. Consistent with this idea is prfB's 4-nucleotide slippery sequence, which can accommodate the slippage of only a single tRNA by 1 nucleotide while still allowing near-cognate codon-anticodon interactions. Similarly, investigations into the effect of E-site tRNA on +1 prfB frameshifting found an inverse correlation between the strength of the E-site codon-anticodon interactions and frameshifting efficiency (Sanders and Curran, 2007). Data from the Nierhaus group additionally indicated that the internal Shine-Dalgarno sequence, with its unusually short spacing to the P site on the prfB sequence, promoted premature release of E-site tRNA via displacement upon 16S anti-SD binding (Márquez et al, 2004). Thus, ribosomes undergoing frameshifting on the prfB sequence appear to contain a single tRNA bound to the P-site, where G926 is one of the few residues stabilizing the proper mRNA

register. This vulnerable state is particularly susceptible to reading frame defects from G926 deletion, which is made more pronounced at lower RF2 concentrations due to the increased time spent in this state. Since EF-G does not bind at this stage in the elongation cycle, the frameshift-stimulating EF-G mutants have no effect here.

In contrast to prfB, dnaX requires a 7-nucleotide slippery sequence for efficient frameshifting, suggesting that it proceeds via simultaneous slippage of two tRNAs. Previous work has shown that EF-G domain IV tip mutants can greatly stimulate -1 frameshifting on dnaX. This indicates that -1 dnaX frameshifting can occur during translocation, although we cannot rule out the possibility that it also occurs in between rounds of translocation to some degree. During translocation, the ribosome undergoes 30S head domain rotation and enters a chimeric hybrid-state conformation as the A- and P-site tRNAs are moved partway to their next binding site. In this state, maintenance of the A-site codon-anticodon is transferred from the ribosomal decoding center to loops I and II at the tip of domain IV of EF-G. At the P-site, G926 forms a constriction of the mRNA tunnel where the mRNA makes a sharp turn, contacting the mRNA through Van der Waals interactions and hydrogen bonds to one or two mRNA phosphates (**Fig. 6**). Finally, the boundary between the P- and E-sites is demarcated by intercalation of A1503 between the -1 and -2 bases, preventing the -1 base from inadvertently pairing with the P-site tRNA.

Notably, the effect of G926A/U substitution on both -1 and +1 frameshifting was subtle or negligible in comparison to the 926 deletion mutant, with only G926U achieving statistical significance on -1 frameshift stimulation. Both substitutions are predicted to result in a loss of the aforementioned H-bonds to the +1 mRNA phosphate, either by a loss of the appropriate hydrogen bond donors in the case of adenosine, or as a result of insufficient reach in the case of uridine. The ability to stack between the -1 base and G1505 is present in all nucleotides, with uridine having the weakest stacking propensity. This could explain the slight defect caused by G926U on -1 frameshifting. Alternatively, these results may indicate

that the steric effect of a nucleotide placed at position 926 is more important for reading frame maintenance than the hydrogen bonds, with uridine occupying less space in the mRNA channel than guanosine or adenosine. A significant amount of free energy may be required for the mRNA to displace or move around any nucleotide at position 926, which protrudes into the mRNA channel. Nonetheless, a guanosine at this position has clearly been favored by natural selection due to some significant advantage. One possible explanation for this is that while the hydrogen bonds formed from guanosine were dispensable for efficient *in vitro* translation of our mRNA, their role may be more significant for translation initiation *in vivo,* particularly in the case of mRNAs that interact more weakly with the ribosome.

MATERIALS AND METHODS

Materials

Tight-coupled ribosomes were purified as described (Lancaster et al, 2002). Natural 30S and 50S subunits were obtained by dissociating 70S into 30S and 50S subunits and purifying them over a sucrose gradient (Moazed et al, 1986). S100 extract was prepared from wild-type *E. coli* MRE600 or from CSH142 containing genomic 6-his tagged EF-G and RF2 (Traub et al, 1971) and separated from endogenous EF-G and RF2 by purification over a Ni^{++} column as previously described (Niblett et al, 2021). Total tRNA and initiator $tRNA^{fMet}$ from *E coli* were purchased from Roche and Sigma respectively. $tRNA^{fMet}$ was aminoacylated and formylated as described (Lancaster and Noller, 2005). Complete aminoacylation of tRNA was confirmed via acid gel electrophoresis (Varshney et al, 1991)

Mutagenesis

All site-directed mutagenesis was performed using the Kunkel method (Kunkel, 1985). Site directed mutagenesis of pKF207.MS2 16S rDNA (Lancaster and Noller, 2005) was used to either delete G926 or to substitute it with an A or a T. The following changes were made to pET24b-encoded ribosomal protein S2 (Culver and Noller, 1999): First, S2_SL

and S2_dnaX_SL mRNA were created by the addition of an 11-base-pair GC-rich stem-loop to the 3' end of either the wild-type S2 sequence, or the previously described S2_dnaX sequence to protect the mRNA from degradation by 3' exonucleases, which had previously resulted in synthesis of a truncated protein product during *in vitro* translation (Niblett et al, 2021). S2_prfB_SL was then created by replacing the 25-nucleotide stretch from 362-386 of S2_SL with the 20-nucleotide sequence 5'-CAGGGGGTTT**CTTT**GACTAC-3'. [The Shine-Dalgarno sequence and the in-frame stop codon are both underlined, while the CTTT slippery sequence is in bold.] The CTA following the stop codon creates a poor termination context, allowing frameshifting to compete efficiently with termination (Major et al, 1996; Poole et al, 1998). The final cytosine substitutes a native guanine to prevent the creation of an in-frame stop codon following the +1 frameshift. Note that this programmed frameshift sequence differs by 1 nucleotide from the native *E. coli* RF2 sequence shown in **Figure 4,** but results in a comparable level of frameshifting (Sanders and Curran, 2007). All mutagenesis was confirmed by sequencing.

3' helix added to S2 to create S2-SL: 5'-GGACTCCGGAGGAGACTCCGGAGTCC-3'

Purification of MS2-tagged 30S subunits

Purification of MS2(V75E, A81G)-GST fusion protein and expression and purification of MS2-affinity-tagged 30S subunits was performed essentially as described (Lancaster and Noller, 2005), with the exception that the expression vector for the rrnB operon was changed from pLK35 to pBAD18. This allows for expression to be carried out at 37℃ by addition of arabinose instead of 42℃. The rrnB operon containing an MS2-tag that replaced nucleotides 79-91 of 16S rDNA was cloned into pBAD18 using KpnI and XhoI restriction sites. Site-directed mutagenesis was used to generate Δ926, G926A, and G926U mutants. The vector was then transformed into the *E. coli* expression strain KLF9 (CSH142 srl::Tn10 recA1). To express 16S rRNA, 50-ml cultures of LB plus 100 μg/ml of ampicillin were grown to an A_{550} > 0.5, at which point the cells were induced by addition of 5 ml of culture to 1 L of LB plus 100

μg/ml of ampicillin and 2 mM arabinose pre-warmed to 37℃. Cell lysis and affinity chromatography were then carried out as before (Lancaster and Noller, 2005).

In vitro translation and quantification of frameshifting

Prior to *in vitro* translation, natural or MS2-tagged 30S subunits were heat-activated and associated with natural 50S subunits (Ali et al, 2006). *In vitro* translation was then carried out as previously described (Niblett et al, 2021), using either S2_SL, S2_dnaX_SL, or S2_prfB_SL mRNA. Quantification of frameshifting was performed using ImageLab (BioRad) as previously described (Niblett et al, 2019), calculated using 5 Met in -1 product, 5 Met in the prfB 0-frame early termination product, and 7 Met in the full-length product, as predicted from the mRNA sequence.

FIGURES

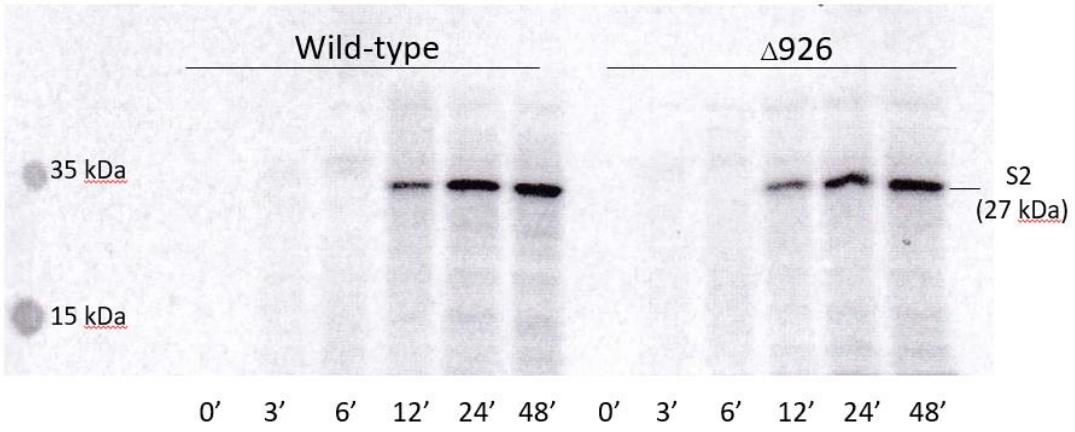

Figure 1. *In vitro* translation time course. The 27 kD ribosomal protein S2 was synthesized using either MS2-tagged wildtype ribosomes (left) or MS2-tagged Δ926 ribosomes (right). Δ926 ribosomes showed no defect in either the rate of translation or the amount of product synthesized.

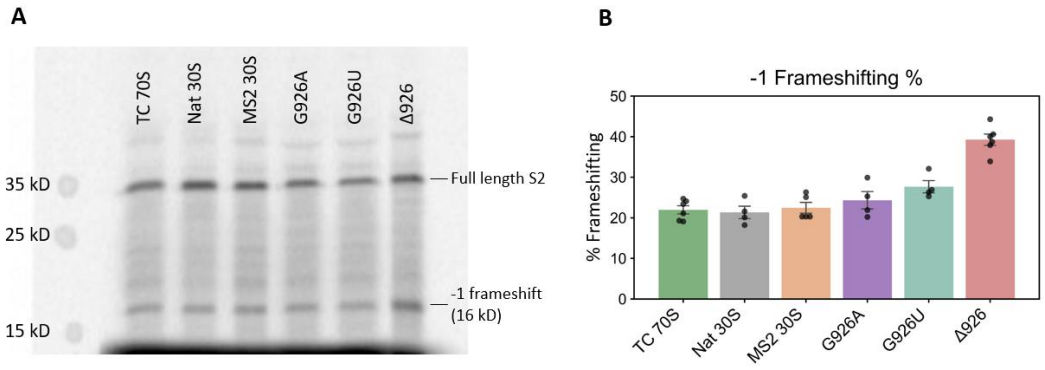

Figure 2. Stimulation of -1 frameshifting by MS2-tagged Δ926 ribosomes. (A) SDS gel showing the products of the translation reaction. (B) Histogram showing frameshifting efficiencies for corresponding lanes in A. (TC 70S) Tight-coupled ribosomes purified as natural 70S subunits; (Nat 30S) 70S subunits formed from the *in vitro* association of purified natural 30S and 50S subunits. (MS2 30S) 70S subunits formed from MS2-tagged 30S and natural 50S subunits; (G926A, G926U, Δ926) MS2-tagged ribosomes containing a G to A substitution, a G to U substitution, or a deletion at position 926. Labeled translation products include the full-length 27 kD ribosomal protein S2 (Full length S2), or the 16 kD truncated product resulting from a -1 frameshift and termination at an out of frame stop codon (-1 frameshift). Error bars represent standard error of the mean.

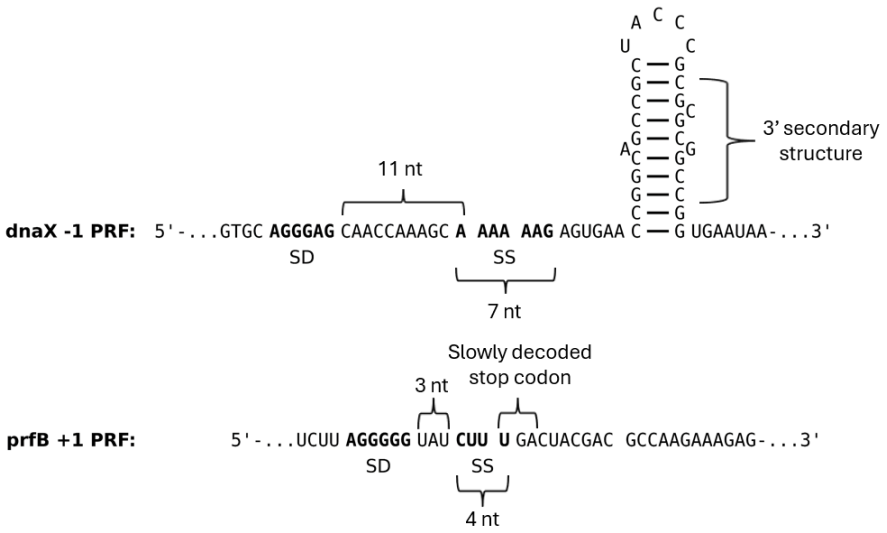

Figure 3. Differences between -1 dnaX and +1 prfB programmed frameshifting sequences. Sequence elements that promote frameshifting for dnaX (top) and prfB (bottom) are shown. (SD): Internal Shine-Dalgarno sequence, which pairs with the anti-SD on 16S rRNA while tRNAs are paired with the slippery sequence (Larsen et al, 1994; Weiss et al, 1998). The spacing between the SD and the first nucleotide of the P-site is shown. Note that the optimal SD spacing for translation initiation is roughly the half-way point between the optimal SD spacing for +1 and -1 frameshifting. (SS) Slippery sequence: an RNA sequence that allows for tRNAs to form favorable interactions in both the 0-frame and an alternative frame upon slippage by 1 nucleotide. The dnaX SS can accommodate the slippage of two tRNAs while the prfB SS can only accommodate the slippage of one. (3' secondary structure): A stem-loop that forms just outside the mRNA entry tunnel and provides a kinetic barrier to translocation while tRNAs are paired with the slippery sequence. (Slowly decoded stop codon): A codon that substitutes a downstream secondary structure to stall the ribosome. Can be substituted for rare sense codons as well, with frameshifting efficiency being inversely proportional to the rate of tRNA selection (Curran and Yarus, 1998).

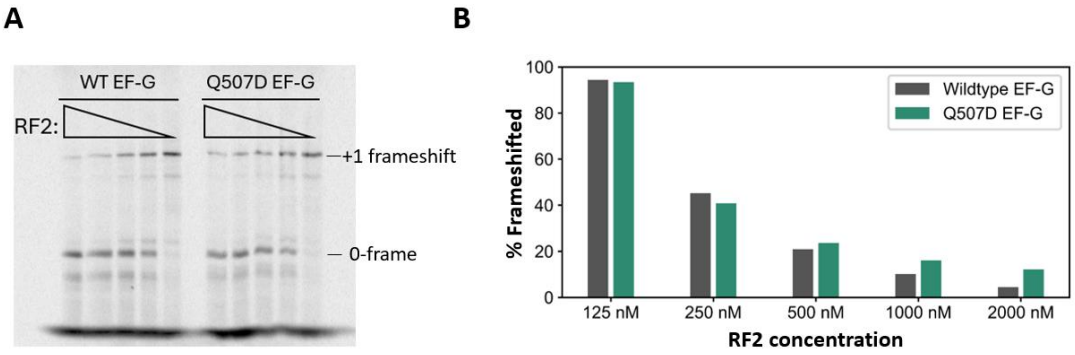

Figure 4. Q507D EF-G has no effect on prfB +1 frameshifting efficiency. (A) SDS gel showing products of *in vitro* translation reactions supplemented with either wild-type EF-G (WT EF-G) or a -1 frameshift stimulating EF-G mutant (Q507D EF-G). Reactions were carried out with RF2 concentrations ranging from 125 nM to 2000 nM. (B) Bands in (A) corresponding to 0-frame and frameshifted product were normalized based on the number of methionines and frameshifting was quantified as the percentage of frameshifted product out of total product.

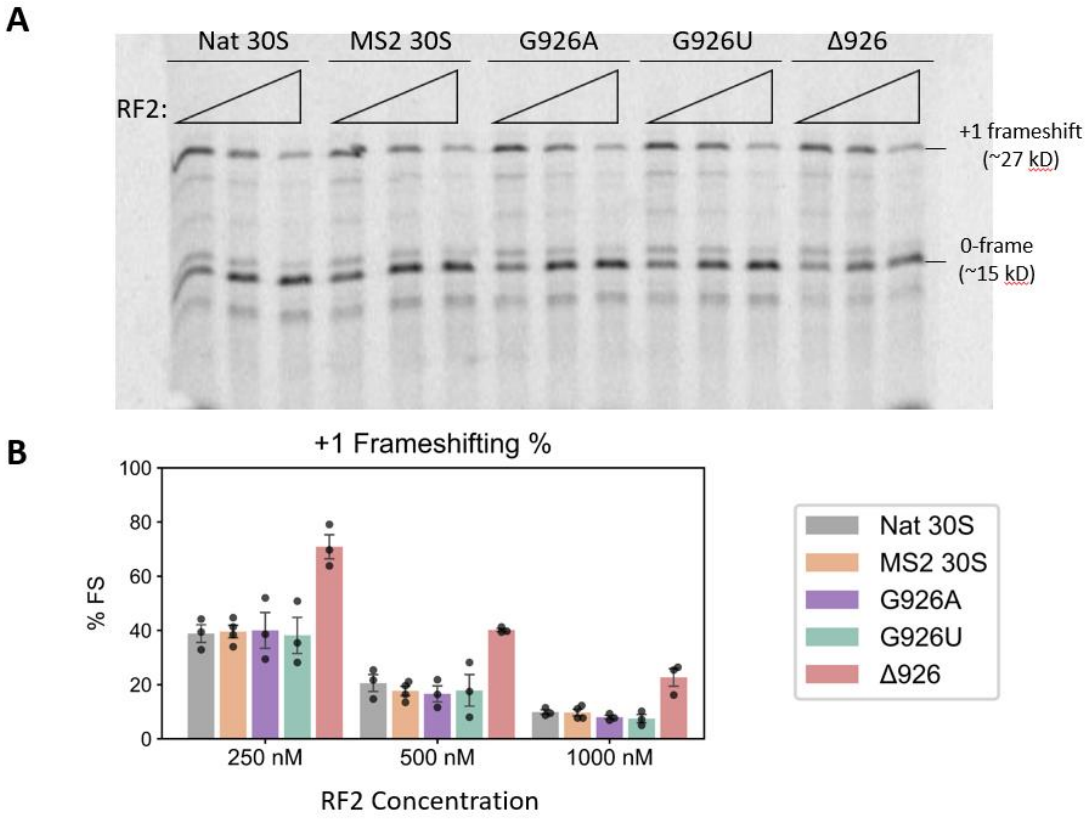

Figure 5. Effect of G926 mutations on +1 frameshifting efficiency. (A): SDS gel showing products of *in vitro* protein synthesis for each G926 mutant and control. Each 70S sample was tested at 250, 500, and 1000 nM RF2. (B) Frameshifting was quantified and reported as the percentage of frameshifted product out of the total product. (Nat 30S) 70S subunits made from the *in vitro* association of purified natural 30S and 50S subunits. (MS2 30S) MS2-tagged wild-type ribosomes; (G926A, G926U, Δ926) MS2-tagged ribosomes containing a G to A substitution, a G to U substitution, or a deletion at position 926. (+1 frameshift) The 27 kD full-length S2 protein, which requires a +1 frameshift to synthesize. (0-frame) The product of translation in the 0-frame, which results in termination at an in-frame stop codon and creates a truncated 15 kD product. Error bars represent standard error of the mean.

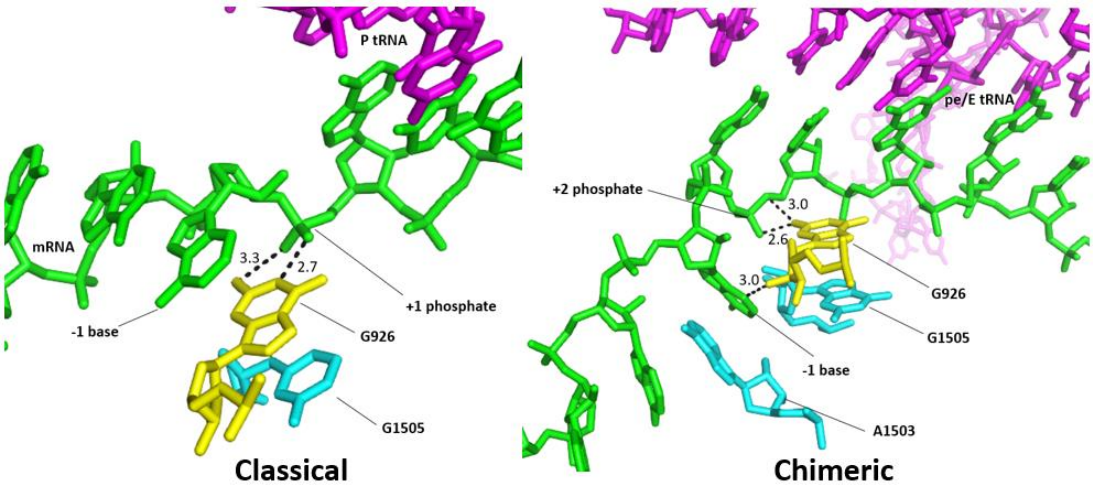

Figure 6. G926-mRNA contacts. (A) A classical-state complex (Watson et al, 2020). G926 protrudes into the mRNA channel where it stacks between the -1 mRNA base and G1505 of 16S rRNA while its N1 and N2 positions form hydrogen bonds to the +1 phosphate. (B) A chimeric-hybrid state complex (Zhou et al, 2014). Upon rotation of the 30S head domain and partial translocation of the mRNA relative to the 30S body, the mRNA forms a tight bend around G926, creating a boundary between the E- and P-site codons. The -1 base is rotated away from the tRNA to stack on the intercalating base A1503 while G926 forms two H-bonds to the +2 phosphate.

REFERENCES

Adamski, F. M., Donly, B. C., & Tate, W. P. (1993). Competition between frameshifting, termination and suppression at the frameshift site in the Escherichia coli release factor-2 mRNA. *Nucleic acids research*, *21*(22), 5074–5078. https://doi.org/10.1093/nar/21.22.5074

Ali IK, Lancaster L, Feinberg J, Joseph S, Noller HF. 2006. Deletion of a conserved, central ribosomal intersubunit RNA bridge. *Mol Cell* **23**: 865–874. 10.1016/j.molcel.2006.08.011

Atkins JF, Loughran G, Bhatt PR, Firth AE, Baranov PV. Ribosomal frameshifting and transcriptional slippage: From genetic steganography and cryptography to adventitious use. Nucleic Acids Res. 2016 Sep 6;44(15):7007-78. doi: 10.1093/nar/gkw530. Epub 2016 Jul 19. PMID: 27436286; PMCID: PMC5009743.

Bao C, Loerch S, Ling C, Korostelev AA, Grigorieff N, Ermolenko DN. mRNA stem-loops can pause the ribosome by hindering A-site tRNA binding. Elife. 2020 May 19;9:e55799. doi: 10.7554/eLife.55799. PMID: 32427100; PMCID: PMC7282821.

Brilot AF, Korostelev AA, Ermolenko DN, Grigorieff N. Structure of the ribosome with elongation factor G trapped in the pretranslocation state. Proc Natl Acad Sci U S A. 2013 Dec 24;110(52):20994-9. doi: 10.1073/pnas.1311423110. Epub 2013 Dec 9. PMID: 24324137; PMCID: PMC3876248.

Caliskan, N., Wohlgemuth, I., Korniy, N., Pearson, M., Peske, F., & Rodnina, M. V. (2017). Conditional Switch between Frameshifting Regimes upon Translation of dnaX mRNA. *Molecular cell*, *66*(4), 558–567.e4. https://doi.org/10.1016/j.molcel.2017.04.023

Carbone, C. E., Loveland, A. B., Gamper, H. B., Jr, Hou, Y. M., Demo, G., & Korostelev, A. A. (2021). Time-resolved cryo-EM visualizes ribosomal translocation with EF-G and GTP. *Nature communications*, *12*(1), 7236.

Chen, J., Petrov, A., Johansson, M., Tsai, A., O'Leary, S. E., & Puglisi, J. D. (2014). Dynamic pathways of -1 translational frameshifting. *Nature*, *512*(7514), 328–332.

Craigen, W. J., Cook, R. G., Tate, W. P., & Caskey, C. T. (1985). Bacterial peptide chain release factors: conserved primary structure and possible frameshift regulation of release factor 2. *Proceedings of the National Academy of Sciences of the United States of America*, *82*(11), 3616–3620.

Craigen, W. J., & Caskey, C. T. (1986). Expression of peptide chain release factor 2 requires high-efficiency frameshift. *Nature*, *322*(6076), 273–275.

Culver, G. M., & Noller, H. F. (1999). Efficient reconstitution of functional Escherichia coli 30S ribosomal subunits from a complete set of recombinant small subunit ribosomal proteins. *RNA (New York, N.Y.)*, *5*(6), 832–843. https://doi.org/10.1017/s1355838299990714

Curran, J. F., & Yarus, M. (1989). Rates of aminoacyl-tRNA selection at 29 sense codons in vivo. *Journal of molecular biology*, *209*(1), 65–77.

Curran JF. Analysis of effects of tRNA:message stability on frameshift frequency at the Escherichia coli RF2 programmed frameshift site. Nucleic Acids Res. 1993 Apr 25;21(8):1837-43. doi: 10.1093/nar/21.8.1837. PMID: 8493101; PMCID: PMC309422.

Donly BC, Edgar CD, Adamski FM, Tate WP. Frameshift autoregulation in the gene for Escherichia coli release factor 2: partly functional mutants result in frameshift enhancement.

Nucleic Acids Res. 1990 Nov 25;18(22):6517-22. doi: 10.1093/nar/18.22.6517. PMID: 2251114; PMCID: PMC332604.

Drummond DA, Wilke CO. Mistranslation-induced protein misfolding as a dominant constraint on coding-sequence evolution. Cell. 2008 Jul 25;134(2):341-52. doi: 10.1016/j.cell.2008.05.042. PMID: 18662548; PMCID: PMC2696314.

Farabaugh P. J. (1996). Programmed translational frameshifting. *Annual review of genetics*, *30*, 507–528. https://doi.org/10.1146/annurev.genet.30.1.507

Farabaugh PJ. Programmed translational frameshifting. Microbiol Rev. 1996 Mar;60(1):103-34. doi: 10.1128/mr.60.1.103-134.1996. PMID: 8852897; PMCID: PMC239420.

Gao W, Jakubowski H, Goldman E. Evidence that uncharged tRNA can inhibit a programmed translational frameshift in Escherichia coli. J Mol Biol. 1995 Aug 11;251(2):210-6. doi: 10.1006/jmbi.1995.0428. PMID: 7643397.

Gao YG, Selmer M, Dunham CM, Weixlbaumer A, Kelley AC, Ramakrishnan V. The structure of the ribosome with elongation factor G trapped in the posttranslocational state. Science. 2009 Oct 30;326(5953):694-9. doi: 10.1126/science.1179709. PMID: 19833919; PMCID: PMC3763468.

Jacks, T., H. D. Madhani, F. R. Masiarz, and H. E. Varmus. 1988. Signals for ribosomal frameshifting in the Rous sarcoma virus gag-pol region. Cell 55:447–458.

Kim HK, Tinoco I Jr. EF-G catalyzed translocation dynamics in the presence of ribosomal frameshifting stimulatory signals. Nucleic Acids Res. 2017 Mar 17;45(5):2865-2874. doi: 10.1093/nar/gkw1020. PMID: 27799473; PMCID: PMC5389563.

Korostelev A, Trakhanov S, Laurberg M, Noller HF. Crystal structure of a 70S ribosome-tRNA complex reveals functional interactions and rearrangements. Cell. 2006 Sep 22;126(6):1065-77. doi: 10.1016/j.cell.2006.08.032. Epub 2006 Sep 7. PMID: 16962654.

Kunkel T. A. (1985). Rapid and efficient site-specific mutagenesis without phenotypic selection. *Proceedings of the National Academy of Sciences of the United States of America*, *82*(2), 488–492.

Kurland C. G. (1992). Translational accuracy and the fitness of bacteria. *Annual review of genetics*, *26*, 29–50.

Lancaster, L., Kiel, M. C., Kaji, A., & Noller, H. F. (2002). Orientation of ribosome recycling factor in the ribosome from directed hydroxyl radical probing. *Cell*, *111*(1), 129–140.

Lancaster, L., & Noller, H. F. (2005). Involvement of 16S rRNA nucleotides G1338 and A1339 in discrimination of initiator tRNA. *Molecular cell*, *20*(4), 623–632.

Larsen, B., Wills, N. M., Gesteland, R. F., & Atkins, J. F. (1994). rRNA-mRNA base pairing stimulates a programmed -1 ribosomal frameshift. *Journal of bacteriology*, *176*(22), 6842–6851.

Larsen, B., Gesteland, R. F., & Atkins, J. F. (1997). Structural probing and mutagenic analysis of the stem-loop required for Escherichia coli dnaX ribosomal frameshifting: programmed efficiency of 50%. *Journal of molecular biology*, *271*(1), 47–60.

Major LL, Poole ES, Dalphin ME, Mannering SA, Tate WP. Is the in-frame termination signal of the Escherichia coli release factor-2 frameshift site weakened by a particularly poor

context? Nucleic Acids Res. 1996 Jul 15;24(14):2673-8. doi: 10.1093/nar/24.14.2673. PMID: 8758994; PMCID: PMC145990.

Márquez, V., Wilson, D. N., Tate, W. P., Triana-Alonso, F., & Nierhaus, K. H. (2004). Maintaining the ribosomal reading frame: the influence of the E site during translational regulation of release factor 2. *Cell*, *118*(1), 45–55.

Matsufuji S, Matsufuji T, Miyazaki Y, Murakami Y, Atkins JF, Gesteland RF, Hayashi S. Autoregulatory frameshifting in decoding mammalian ornithine decarboxylase antizyme. Cell. 1995 Jan 13;80(1):51-60. doi: 10.1016/0092-8674(95)90450-6. PMID: 7813017; PMCID: PMC7133313.

Moazed, D., Van Stolk, B. J., Douthwaite, S., & Noller, H. F. (1986). Interconversion of active and inactive 30 S ribosomal subunits is accompanied by a conformational change in the decoding region of 16 S rRNA. *Journal of molecular biology*, *191*(3), 483–493.

Moazed, D., & Noller, H. F. (1990). Binding of tRNA to the ribosomal A and P sites protects two distinct sets of nucleotides in 16 S rRNA. *Journal of molecular biology*, *211*(1), 135–145.

Mohan, S., Donohue, J. P., & Noller, H. F. (2014). Molecular mechanics of 30S subunit head rotation. *Proceedings of the National Academy of Sciences of the United States of America*, *111*(37), 13325–13330.

Niblett D, Nelson C, Leung CS, Rexroad G, Cozy J, Zhou J, Lancaster L, Noller HF. Mutations in domain IV of elongation factor EF-G confer -1 frameshifting. RNA. 2021 Jan;27(1):40-53. doi: 10.1261/rna.077339.120. Epub 2020 Oct 2. PMID: 33008838; PMCID: PMC7749637.

Noller, H. F., Donohue, J. P., & Gutell, R. R. (2022). The universally conserved nucleotides of the small subunit ribosomal RNAs. *RNA (New York, N.Y.)*, *28*(5), 623–644.

Ogle JM, Brodersen DE, Clemons WM Jr, Tarry MJ, Carter AP, Ramakrishnan V. Recognition of cognate transfer RNA by the 30S ribosomal subunit. Science. 2001 May 4;292(5518):897-902. doi: 10.1126/science.1060612. PMID: 11340196.

Peng BZ, Bock LV, Belardinelli R, Peske F, Grubmüller H, Rodnina MV. Active role of elongation factor G in maintaining the mRNA reading frame during translation. Sci Adv. 2019 Dec 20;5(12):eaax8030. doi: 10.1126/sciadv.aax8030. PMID: 31903418; PMCID: PMC6924986.

Petrychenko V, Peng BZ, de A P Schwarzer AC, Peske F, Rodnina MV, Fischer N. Structural mechanism of GTPase-powered ribosome-tRNA movement. Nat Commun. 2021 Oct 11;12(1):5933. doi: 10.1038/s41467-021-26133-x. PMID: 34635670; PMCID: PMC8505512.

Poole ES, Major LL, Mannering SA, Tate WP. Translational termination in Escherichia coli: three bases following the stop codon crosslink to release factor 2 and affect the decoding efficiency of UGA-containing signals. Nucleic Acids Res. 1998 Feb 15;26(4):954-60. doi: 10.1093/nar/26.4.954. PMID: 9461453; PMCID: PMC147352.

Poulis P, Peske F, Rodnina MV. The many faces of ribosome translocation along the mRNA: reading frame maintenance, ribosome frameshifting and translational bypassing. Biol Chem. 2023 Apr 21;404(8-9):755-767. doi: 10.1515/hsz-2023-0142. PMID: 37077160.

Rundlet EJ, Holm M, Schacherl M, Natchiar SK, Altman RB, Spahn CMT, Myasnikov AG, Blanchard SC. Structural basis of early translocation events on the ribosome. Nature. 2021 Jul;595(7869):741-745. doi: 10.1038/s41586-021-03713-x. Epub 2021 Jul 7. PMID: 34234344; PMCID: PMC8318882.

Sanders CL, Curran JF. Genetic analysis of the E site during RF2 programmed frameshifting. RNA. 2007 Sep;13(9):1483-91. doi: 10.1261/rna.638707. Epub 2007 Jul 27. Erratum in: RNA. 2007 Nov;13(11):2051. PMID: 17660276; PMCID: PMC1950767.

Sipley J, Goldman E. Increased ribosomal accuracy increases a programmed translational frameshift in Escherichia coli. Proc Natl Acad Sci U S A. 1993 Mar 15;90(6):2315-9. doi: 10.1073/pnas.90.6.2315. PMID: 8460140; PMCID: PMC46077.

Smart, A., Lancaster, L., Donohue, J. P., Niblett, D., & Noller, H. F. (2024). Implication of nucleotides near the 3' end of 16S rRNA in guarding the translational reading frame. *Nucleic acids research*, *52*(10), 5950–5958.

Temperley R, Richter R, Dennerlein S, Lightowlers RN, Chrzanowska-Lightowlers ZM. Hungry codons promote frameshifting in human mitochondrial ribosomes. Science. 2010 Jan 15;327(5963):301. doi: 10.1126/science.1180674. PMID: 20075246.

Traub,P., Mizushima,S., Lowry,C.V. and Nomura,M. (1971) [41]Reconstitution of ribosomes from subribosomal components. In: Methods in Enzymology. Part C: Nucleic Acids and Protein Synthesis. Academic Press, Vol. 20, pp. 391–407.

Tsuchihashi, Z., & Kornberg, A. (1990). Translational frameshifting generates the gamma subunit of DNA polymerase III holoenzyme. *Proceedings of the National Academy of Sciences of the United States of America*, *87*(7), 2516–2520.

Watson ZL, Ward FR, Méheust R, Ad O, Schepartz A, Banfield JF, Cate JH. Structure of the bacterial ribosome at 2 Å resolution. Elife. 2020 Sep 14;9:e60482. doi: 10.7554/eLife.60482. PMID: 32924932; PMCID: PMC7550191.

Weiss RB, Dunn DM, Dahlberg AE, Atkins JF, Gesteland RF. Reading frame switch caused by base-pair formation between the 3' end of 16S rRNA and the mRNA during elongation of protein synthesis in Escherichia coli. EMBO J. 1988 May;7(5):1503-7. doi: 10.1002/j.1460-2075.1988.tb02969.x. PMID: 2457498; PMCID: PMC458402.

Weiss, R. B., D. M. Dunn, M. Shuh, J. F. Atkins, and R. F. Gesteland. 1989. E. coli ribosomes re-phase on retroviral frameshift signals at rates ranging from 2 to 50 percent.

Varshney, U., Lee, C. P., & RajBhandary, U. L. (1991). Direct analysis of aminoacylation levels of tRNAs in vivo. Application to studying recognition of Escherichia coli initiator tRNA mutants by glutaminyl-tRNA synthetase. *The Journal of biological chemistry*, *266*(36), 24712–24718.

Zhou J, Lancaster L, Donohue JP, Noller HF. Crystal structures of EF-G-ribosome complexes trapped in intermediate states of translocation. Science. 2013 Jun 28;340(6140):1236086. doi: 10.1126/science.1236086. PMID: 23812722; PMCID: PMC3979973.

Zhou J, Lancaster L, Donohue JP, Noller HF. How the ribosome hands the A-site tRNA to the P site during EF-G-catalyzed translocation. Science. 2014 Sep 5;345(6201):1188-91. doi: 10.1126/science.1255030. PMID: 25190797; PMCID: PMC4242719.

Zhou J, Lancaster L, Donohue JP, Noller HF. Spontaneous ribosomal translocation of mRNA and tRNAs into a chimeric hybrid state. Proc Natl Acad Sci U S A. 2019 Apr 16;116(16):7813-7818. doi: 10.1073/pnas.1901310116. Epub 2019 Apr 1. PMID: 30936299; PMCID: PMC6475402.